Norwegian University
of Life Sciences

Master's Thesis 2023 60 ECTS
Faculty of Chemistry, Biotechnology and Food Science)

Optimization of CRISPR-Cas9 Genome Editing in Human PBMCs

Sigrid Fu Skjelbostad
Master's of Biotechnology

Optimization of CRISPR-Cas9 Genome Editing in Human PBMCs

Haapaniemi Lab,

Centre for Molecular Medicine Norway

And

The Norwegian University of Life Sciences

Faculty of Chemistry, Biotechnology and Food Science

Acknowledgements

The study presented in current thesis was conducted from May 2022 to May 2023 at Centre for Molecular Medicine Norway (NCMM) and the Norwegian University of Life Sciences (NMBU), Faculty of Chemistry, Biotechnology and Food Science under supervision by Dr. Emma Haapaniemi and associate professor Simen Rød Sandve.

First and foremost, I would like to thank Pavel Kopcil for all support and guidance throughout my time at NCMM. I am very grateful you dedicated so much of your time supervising me and for all the scientific discussions and long meetings we had together. I appreciate the good laughs we had in the lab joking about my lack of mathematical skills or if Dori the fish came visiting, but I am also extremely grateful that you were so understanding during my toughest periods.

I would also like to express my gratitude to everyone that has reach out a helping hand when needed: Monika- without you the lab would not have been up and running, thank you for always answering my questions and being patient teaching me how various instruments work and where to find reagents, Britt and Tiril- thank you for introducing me to LaTex and answering my desperate calls for help when I couldn't figure out the coding myself, Aurora- thank you for helping me with the method part, going through the most boring sections of the thesis, sentence by sentence, Pierre- you spent a Friday evening listening to me explaining the basic of CRISPR, Mum, Dad and Ingeborg- looking through the abstract in Norwegian, Johanne and Ragnhild- reading and commenting the entire thesis, and lastly, the CIGENE writing group- receiving constructive feedback from peers has been very much appreciated and I especially want to thank Guro and Simen for hosting these sessions.

Finally, I want to thank my beloved friends for being understandable when arriving late to dinner plans because my lab work did not go as planned, and for my total absent the final months wrapping up my thesis. Especially thanks to Eirik, Inger Marit, and Sarah for mental support and pleasant lunches and dinners, and Martin for all the times you made dinner and the table was set as soon as I entered the kitchen. Thank you, Ragnhild, for keeping me with company during Easter and always sharing your valuable opinions and life hacks. I also want to thank Heidi for accompanying me to Romsdalen going back country skiing as soon as the first draft was handed in.

Abstract

Targeted genomic manipulation by the Clustered regularly interspaced short palindromic repeats (CRISPR)-associated (Cas) nuclease system has the ability to make precise changes in mammalian genomes. Furthermore, the development of mRNA-based delivery has showed great potential in gene editing therapy due to its transient expression, and currently, several clinical trials based on mRNA genetic editing are in progress.

In present thesis, the aim was to produce a more stable and less immunologically triggering Cas9 mRNA to be delivered to human peripheral blood mononuclear cells (PBMCs). We aimed for enhanced precise repair pathway, known as homology-directed repair (HDR), by delivering the single-stranded oligodeoxynucleotide (ssODN) repair template 24 hours post-first-electroporation with single-guide RNA (sgRNA) and Cas9wt mRNA. Cas9 was also coupled to the chromatin modulating fusion HMGB1 to promote HDR outcomes. Gene editing was detected by droplet digital PCR (ddPCR), and western blot was performed to verify Cas9 protein expression. mRNA was synthesized *in vitro* and various approaches were tested to obtain precise editing outcomes in desired locus, such as adding 8M of urea to the mRNA synthesis, extended purification of RNA, and adding 40 units of RNase inhibitors prior to electroporation.

Our results demonstrated that time-controlled two-step transfection of Cas9wt mRNA led to a higher non-homologous end joining (NHEJ) compared to Cas9-HMGB1 mRNA ($\sim$ 10% versus $<$ 1%), while for HDR, the editing results were close to 0% for Cas9wt mRNA and Cas9-HMGB1 mRNA. Ribonucleoproteins (RNPs) of Cas9wt were used as a standard, with an editing outcome between $\sim 20-60\%$. Optimizing the *in vitro* transcription protocol by adding urea to the mRNA synthesis did not improve precise gene editing ($<$ 1% for HDR and $<$ 3% for NHEJ). The extended purification of RNA did not affect the purity significantly, leading to a decrease in obtained mRNA concentration instead. Finally, testing two different RNase inhibitors resulted in $<$ 5% HDR and $<$ 5% NHEJ.

We concluded that optimization of the *in vitro* transcription protocol is needed to obtain a more stable mRNA. The inclusion of RNase inhibitors increased the editing of HDR and NHEJ to some extent compared to the other conditions tested, however, the ratio between mRNA and inhibitor added should be further tested out. Preventing the

degradation of mRNA remains a great challenge, and tackling this is crucial to provide a foundation for the development of mRNA-based CRISPR therapeutics into a safe, stable, and efficient editing platform.

Sammendrag

Presis manipulering av genomet ved hjelp av Clustered regularly interspaced short palindromic repeats (CRISPR)-assosierte (Cas) nuklease system gjør det mulig å presist endre det menneskelige genomet. Utviklingen av mRNA som et terapeutisk verktøy er lovende da mRNA har en kortvarig ekspresjon. Ulike kliniske studier med fokus på mRNA er nå under utprøving.

Formålet med denne oppgaven var å produsere et mer stabilt og mindre immunologisk triggende Cas9 mRNA som ble levert til menneskelige blodceller (PBMCs). Vi leverte enkeltrådet oligondeoksinukleotid (ssODN) reperasjonstemplat til single-guide (sgRNA) og Cas9wt mRNA 24 timer etter første elektroporering for å oppnå nøyaktig DNA-reparasjon, også kjent som homologirettet DNA-reparasjon (HDR). Cas9 ble også koblet til en kromatinmodulerende fusjon (HMGB1) for å øke HDR. Genredigering ble detektert med droplet digital PCR (ddPCR) og western blot ble gjennomført for å verifisere Cas9 proteinekspresjon. mRNA ble syntetisert *in vitro*, og ulike metoder ble testet ut for å øke genredigering. I forbindelse med dette ble det blant annet benyttet metoder som å tilsette 8M av urea til mRNA syntesen, utvidet rensing av RNA, og tilsette 40 enheter av RNase inhibitorer før elektroporering.

Våre resultater viste at en tidskontrollert to-stegs transfeksjonsprotokoll av Cas9wt mRNA førte til en høyere ikke-homolog endebinding (NHEJ) sammenlignet med Cas9-HMGB1 mRNA ($\sim$ 10% versus $<$ 1%), mens HDR var rundt 0% for Cas9wt mRNA og Cas9-HMGB1. Ribonukleoproteiner (RNPs) av Cas9wt ble brukt som standard, med genredigeringsresultater mellom $\sim 20 - 60\%$. En optimalisert *in vitro* transkripsjonsprotokoll – gjennom tilsetning av urea til mRNA syntesen – forbedret ikke nøyaktig genredigering ($<$ 1 % for HDR og $<$ 3% for NHEJ). Ekstra vasking av RNA påvirket ikke renheten signifikant, men bidro derimot til en nedgang i mRNA konsentrasjon. To ulike RNase inhibitorer ble testet ut, noe som resulterte i $<$ 5% HDR og $<$5% NHEJ.

Vi konkluderte med at ytterligere optimalisering av *in vitro* transkripsjonsprotokollen er nødvendig for å oppnå et mer stabilt mRNA. Det å tilsette RNase inhibitorer økte NHEJ noe, men forholdet mellom mRNA og inhibitor bør videre testes ut. Forhindring av degradering av mRNA gjenstår som en utfordring. Løsningen på dette er viktig for å kunne videreutvikle trygge, stabile og effektive mRNA-baserte terapeutiske metoder.

List of Abbreviations

AAV	Adeno-associated virus
ARCA	Anti-reverse cap analog
BCA assay	Bicinchoninic acid assay
Cas	CRISPR-associated
CRISPR	Clustered regularly interspaced short palindromic repeats
crRNA	CRISPR RNA
ddPCR	Droplet digital PCR
DNA	Deoxyribonucleic acid
dsDNA	Double-stranded DNA
dsODN	Double-stranded oligodeoxynucleotide
dsRNA	Double-stranded RNA
ECL	Enhanced chemiluminescence
ELISA	Enzyme-linked immunosorbent assay
gRNA	guide RNA
GTP	Guanosine triphosphate
HDR	Homology-directed repair
HEK cell line	Human embryonic kidney cell line
HMGB1	High mobility group box 1
HSPCs	Hematopoietic stem and progenitor cells
ICE	Inference of CRISPR edits
KLD treatment	Kinase, ligase and Dpnl
LNPs	Lipid nanoparticles
m7G	7-methyl guanosine
MDA5	Melanoma differentiation associated factor gene 5
mRNA	messenger RNA
nCas9	nickase Cas9
NGS	Next-generation sequencing
NHEJ	Non-homologous end joining
ODN	Oligodeoxynucleotid

ORFs	Open reading frames
PAM	Protospacer adjacent motif
PBMCs	Peripheral blood mononuclear cells
PBS	Primer binding site
pegRNA	Prime editing guide RNA
pre-crRNA	Precursor CRISPR RNA
pre-mRNA	Precursor messenger RNA
PVDF membrane	Polyvinylidene difluoride
RIG-I	Retinoic-acid inducible gene I
RNA	Ribonucleic acid
RNase	Ribonuclease
RNPs	Ribonucleoproteins
RP-HPLC	Reverse-phase high-performance liquid chromatography
SARS-CoV-2	Severe acute respiratory syndrome coronavirus 2
SCD	Sickle cell disease
sgRNA	Single-guide RNA
ssDNA	Single-stranded DNA
ssODN	Single-stranded oligodeoxynucleotid
TALENs	Transcription activator-like effector nucleases
TLRs	Toll-like receptors
tracrRNA	Trans-activating CRISPR RNA
tRNA	transfer RNA
UTRs	Untranslated regions
ZFNs	Zinc finger nucleases

Table of Contents

List of Tables

List of Figures

1 Introduction

1.1 Genome Editing

Over the past years, the development of gene editing technologies has accelerated, and with an immense speed paved the path to modify the genome of various cell types. Specific gene manipulations in tissue culture cells, also known as genome editing, has the potential to efficiently and precisely manipulate genome sequences. These novel approaches involve the use of designer nucleases [1], including base editors [2]. Various designer nucleases, such as zinc finger nucleases (ZFNs) [3], transcription activator-like effector nucleases (TALENs) [4], and clustered regularly interspaced short palindromic repeats (CRISPR) nucleases [5], were engineered to create a double-stranded break in specific genomic target sequences (Figure 1.1 and Figure 1.2). The advance of programmable nucleases has opened up vast possibilities in terms of gene editing in clinical practice, and has unprecedentedly enabled scientific community with a powerful tool to manipulate DNA or RNA sequences in a wide variety of cell types and species.

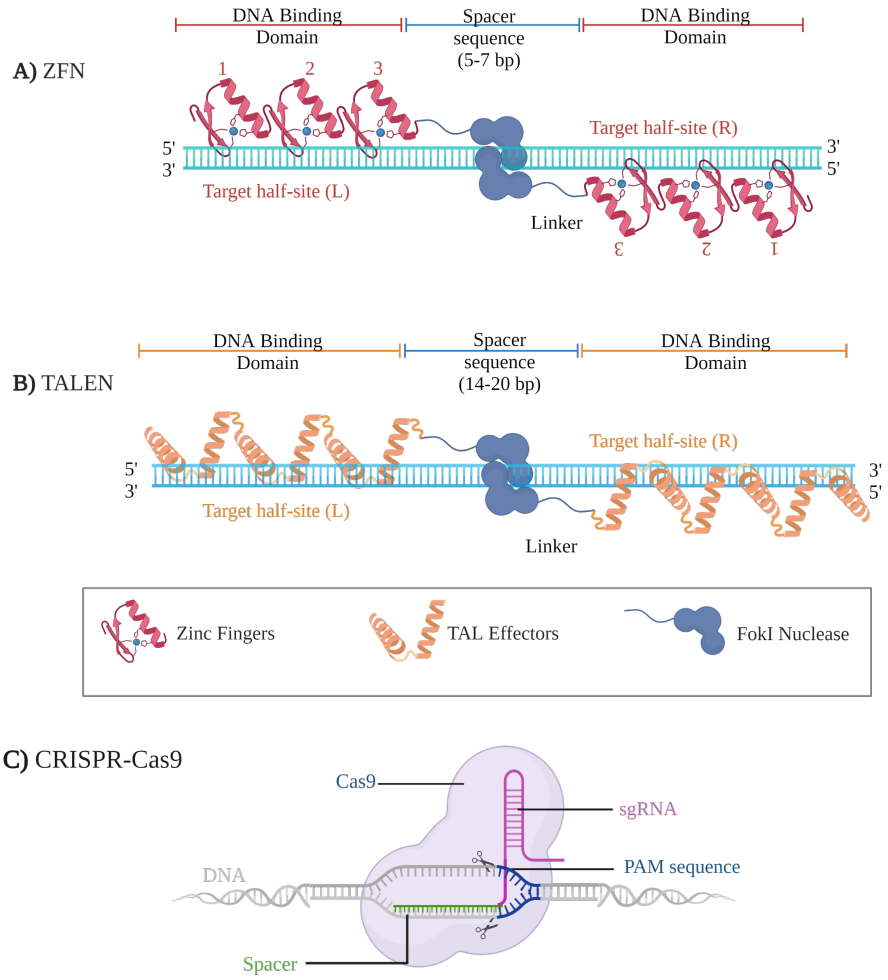

Figure 1.1: **An overview of the three major designer nucleases: zinc-finger nuclease (ZFN), transcription activator-like (TAL) effecor nuclease (TALEN), and clustered regularly interspaced short palindromic repeats (CRISPR)-associated (Cas) nuclease (CRISPR-Cas).**
A) ZFNs link two different zinc finger subunits to the cleavage domain of *Fok I* endonuclease. Each subunit contains a cluster of three zinc finger domains (labelled 1-2-3) arranged in tandem arrays. A short linker (blue) connects the two domains which activates the nuclease after dimerization [6] leading to a double-stranded cut in the DNA spacer sequence, and separating the two target half-sites (L) and (R). **B)** The natural TAL effector protein consists of two distinct domains; an effector domain and a specific DNA-binding domain. The structure of the DNA-binding domain contains a variable number of amino acid repeats that is made up by 18-35 amino acids recognizing a single DNA base pair [7]. A double-stranded break at a targeted genomic loci is initiated by fusing the DNA-binding domain to the *Fok I* nuclease [8]. **C)** CRISPR, together with its associated proteins (Cas), consists of Cas9 nuclease and a single-guide RNA (sgRNA) which is located upstream to the protospacer adjacent motif (PAM). sgRNA guides Cas9 to select DNA sequences that are complementary to the target site, making a precise double-stranded cut within the protospacer, 3 nucelotides upstream of the PAM sequence [9]. Created with BioRender (`https://www.biorender.com/`) and adapted from the original submission in BioRender by Esmeé Dragt, Louis Ngai, Karim Shalaby, and Niima Vaezzadeh.

1.1.1 Repairing Lethal Double-Stranded DNA Breaks

Double-stranded breaks are deleterious to the cells and are repaired by endogenous cellular mechanisms. The two major pathways to repair double-stranded DNA breaks in mammalian cells are non-homologous end joining (NHEJ) and homology-directed repair (HDR) (Figure 1.2) [10]. NHEJ repair is the error prone repair pathway that rejoins the broken DNA ends using little or no sequence homology [11]. This leads to the formation of unintended indels, also known as insertions or deletions of nucleotides. In contrast, HDR requires substantial lengths of sequence homology to prime repair synthesis [12]. The repair template can be delivered by viral vectors such as adeno-associated viruses (AAVs) [13, 14], which is both time-consuming and costly. Hence, increasing amount of effort is being made to deliver DNA repair templates using nonviral strategies [15, 16]. However, one challenge with these strategies is the formation of double-stranded DNA (dsDNA) causing cytotoxicity, especially in primary cells [17].

In terms of delivering the repair template to perform precise gene editing, various methods have been investigated, including the incorporation of chemical modifications into the DNA repair templates to prolong half-life [18], the use of long circular single-stranded (ssDNA) donors [19], increasing homology arm length [20], and manipulation of cell cycle [21]. In addition, several Cas9 fusions have been reported to increase HDR editing, including Cas9-HMGB1 [22, 23].

Delivering naked DNA as repair template is therefore attractive due to the ease of manufacturing. In order to incorporate an exogenous sequence at a double-stranded break site, the repair template must harbor DNA sequence homology to the 5' and 3' flanking sequence at the cut sites. Single- and double-stranded oligodeoxynuclotides (ssODN and dsODN) can be used when introducing sequences into the genome for precise gene editing. Oligodeoxynucleotides (ODNs) are short synthetic DNA molecules harboring the desired point mutation [24]. Compared to dsODN, ssODN repair template is less toxic and is less likely to insert randomly into the genome [19, 25].

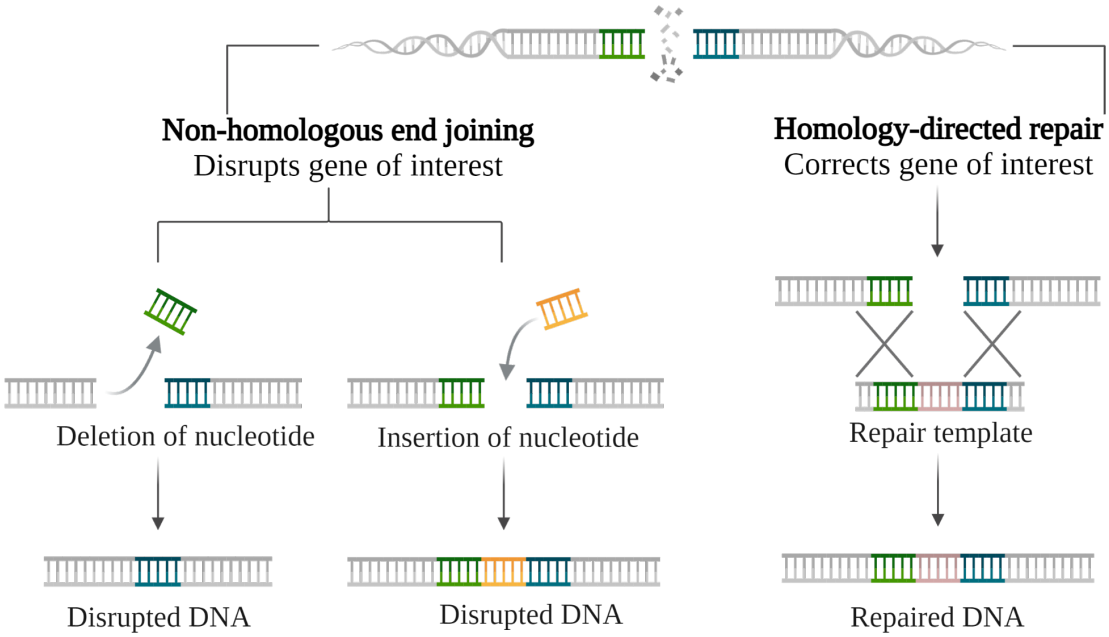

Figure 1.2: **An overview of the two major repair mechanisms in mammalian cells: Non-homologous end joining (NHEJ) and homology-directed repair (HDR).** NHEJ is the primary repair pathway in mammalian cells generally resulting in small deletions or insertions at the break site prior to ligation. This can potentially create mutations and disruptions to the locus. On the other hand, HDR may reconstruct the cleaved DNA in a precise manner by introducing a repair template harboring the desired mutation directly into the targeted cells. Created with BioRender (`https://www.biorender.com/`) and adapted from the original submission in BioRender by Esmeé Dragt and Louis Ngai.

1.2 Programmable Nucleases and Its Advantages

In the early development stage of genome editing, zinc finger nucleases (ZFNs) [3] or meganucleases [26] were engineered to induce the desired double-stranded break at the particular DNA target site. These nuclease systems made it possible to perform genetic manipulations.

ZFNs are artificial restriction enzymes consisting of a nonspecific cleavage domain fused to a site-specific DNA-binding domain that is attached on the zinc finger proteins [3]. Because each zinc finger unit selectively recognizes three base pairs of DNA sequences, a subunit will therefore bind a nine base pairs long target site [3]. Efficient double-stranded cleavage requires two chimeric nucleases, thus, the recognition of 18 base pairs of DNA provides the degree of specificity [27]. Assembling the DNA-binding zinc finger proteins to the cleavage domain of *FokI* restriction endonuclease makes it possible to create artificial nucleases inducing specific double-stranded breaks in the genomic DNA [28].

TALENs are another type of engineered nucleases that exhibit better specificity and efficiency than ZFNs [7, 29]. Similar to ZFNs, TALENs consist of a nonspecific DNA cleavage domain fused to a customizable sequence-specific DNA-binding domain to generate double-stranded breaks in the DNA sequence [4, 7]. The DNA-binding domain consists of monomers where each of the monomers binds one nucleotide in the target nucleotide sequence. The first studies constructing a chimeric TALE nuclease was designed by inserting the DNA-binding domain of TALE into a plasmid vector previously used for creating ZFNs [8]. Hence, the modification pattern is the same for TALENs as with ZFNs where the dimerized *FokI* introduces a double-stranded break into the targeted site. However, compared to triplet-confined zinc finger proteins, there is no need to redesign the linkage between repeats constituting arrays of TALENs. In other words, TALENs consist of long arrays of repeats assembled in various ways to specifically target any nucleotide in the genome, while ZFNs are codon specific [30].

One drawback in terms of cloning repeated TALE arrays, is the large scale of identical repeat sequences that must be designed [30]. Other disadvantages with endonuclease based ZFNs and TALENs are the need of re-engineering the enzyme to fit each target sequence, and the demand of being synthesized separately for each case. A more efficient and less expensive gene editing tool, also known as the clustered regularly interspaced short palindromic repeats (CRISPR)-associated (Cas) system, is therefore favorable.

1.2.1 The CRISPR-Cas System

CRISPRs were originally discovered in *E.coli* in 1987 [31], but the function of the short repeated sequences remained unclear for several years. It was not until in 2005 that subsequent experiments demonstrated that these sequences took part in bacterial and archaea adaptive immune defense by inducing RNA-guided DNA cleavage against invading DNA (Figure 1.3) [32–34]. The CRISPR-Cas9 system compromises two components, a single-stranded guide RNA (sgRNA) and a Cas9 endonuclease derived from *Streptococcus pyogenes* (SpCas9) [5]. When used as an adaptive immunity pathway in bacteria, small fragments from the phage genome, called spacers, are inserted into the CRISPR-array. This array consists of fragments from various phage genomes that the bacterium has encountered previously [5]. The CRISPR array is transcribed as a long precursor-CRISPR RNA (pre-crRNA) repeat transcript as shown in Figure 1.3. Each of the repeats

binds to the transactivating crRNA (tracrRNA) to form double-stranded RNA (dsRNA) sequences. RNase III binds to the RNA duplex and cleaves it such as the spacer and repeat regions are separated from the pre-crRNA transcripts [35]. The CRISPR RNA (crRNA) is responsible for DNA targeting, while the tracrRNA is responsible of forming a complex with Cas9. The formation of this crRNA:tracrRNA complex constitutes the sgRNA which directs Cas9 to the target site. Cas9 is then activated and will search for the protospacer adjacent motif (PAM) sequences in the viral genome. The PAM sequence is essential for the compatibility with the Cas proteins, and allows the system to differentiate between non-self and self [36]. Once Cas9 detects a PAM sequence, it sits on the DNA strand and begin unwinding the PAM strands. If the crRNA loaded onto Cas9 matches the protospacer, the unwinding continues and terminates in the formation of an R-loop. Finally, this activates the cleavage domains of Cas9 and a double-stranded cut is initiated within the protospacer, three nucleotides upstream of the PAM sequence [9]. Hence, DNA targeting by the hallmark protein Cas9, relies on a 20-nucleotide long spacer and the PAM site.

The advantages of CRISPR-Cas9 compared to other technologies are the simplicity, efficiency, and the potential of editing multiple loci simultaneously [37].

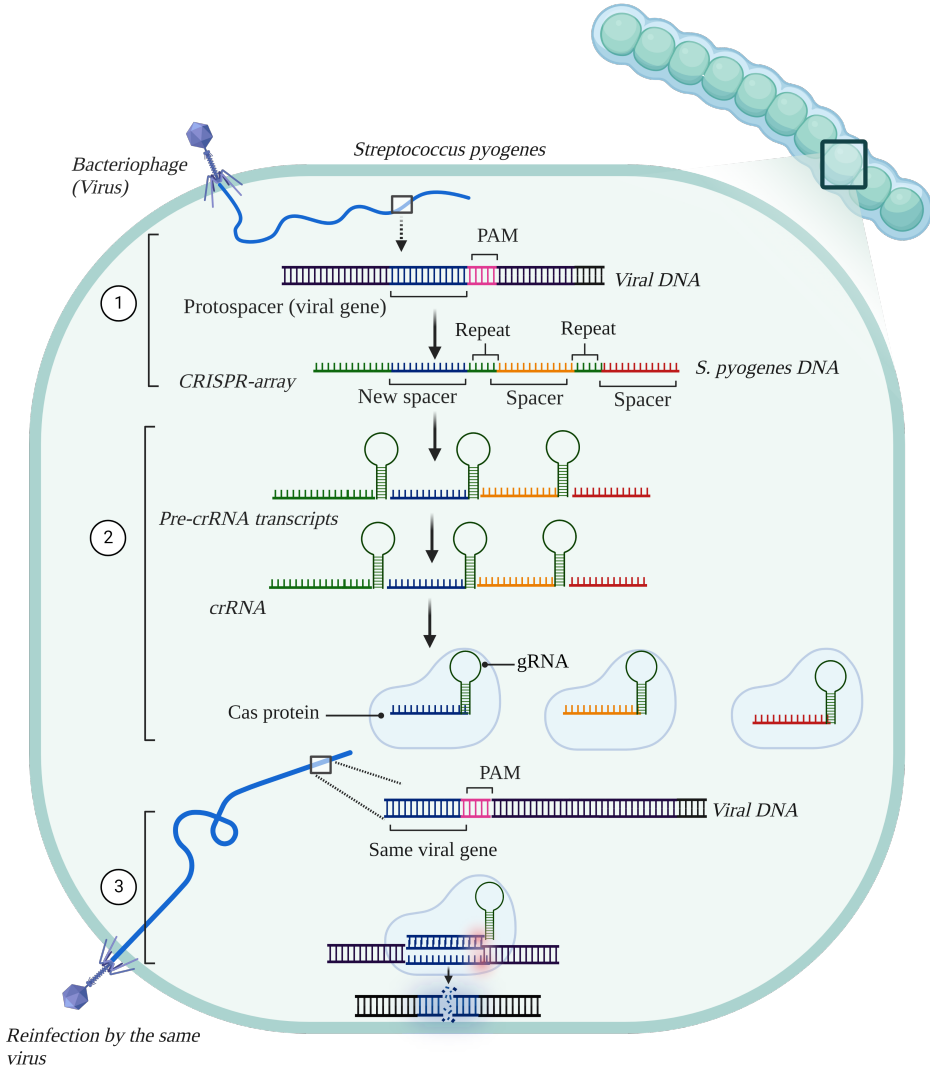

Figure 1.3: **The CRISPR-based adaptive immunity in bacteria.**
CRISPR immune system targets DNA or RNA, this illustration depicts DNA targeting. The three steps to immunity are: 1) acquisition of CRISPR spacer sequence matching an infectious agent, 2) transcription and formation of Cas-RNA complexes, where the maturation of the active crRNAs from the CRISPR precursor transcript (pre-crRNA) is one of the key events for CRISPR activation, and 3) the activation of DNA cutting mechanism. If the bacterium is infected by the same virus, the Cas9:gRNA generated during the first infection recognizes the PAM-motif in the viral genome. Thus, Cas9-mediated cleavage occurs to prevent re-infection. Created with BioRender (`https://www.biorender.com/`) with inspiration from Wang and Doudna [38].

1.2.2 Other CRISPR-Based Techniques

With continuous research in the CRISPR gene-editing systems, new CRISPR tools are being discovered. Type II Cas9 orthologs are currently being studied to expand the CRISPR toolbox capable of recognizing multiple PAMs [39]. Similarly, Cas12 orthologs and Cas13 have shown promise in creating novel platforms for nucleic acid detection [40].

In many circumstances we are interested in using CRISPR to generate specific

point mutations at desired sites. However, standard Cas nucleases introduce double-stranded breaks in the DNA sequence, often resulting in the formation of undesired indels and translocations. To circumvent this, base editors have been developed which utilize fusions between a catalytically impaired Cas nuclease and a base-modification enzyme that operates on single-stranded DNA [41, 42]. The catalytically disabled nuclease nicks the non-edited DNA strand, forcing the cells to repair the nicked strand by using the edited strand as a template. The two classes of DNA base editors described thus far in literature are cytosine base editors and adenine base editors. These base editors are capable of converting a CG pair to a TA base pair, and AT base pair into a GC base pair, respectively [41, 42]. Newby et al. generated an adenine base editor which converts the mutant allele causing sickle-cell disease (SCD) into a benign variant, by editing $CD34^+$ hematopoietic stem and progenitor cells (HSPCs) [43]. Moreover, the first clinical trials using base editing therapy began in late August 2022, where the goal is to develop a medicine that potentially could alleviate the effects of mutations causing SCD by editing $CD34^+$ HSPCs *ex vivo* (`https://clinicaltrials.gov/`, identifier number NCT05456880). Targeted adenosine conversion to inosine has also been developed using both antisense [44, 45] and Cas13-guided [46] RNA-targeting methods.

Another newly developed technology that avoids the creation of double-stranded breaks is prime editing. Prime editing uses Cas9 nickase (nCas9) fused with a reverse transcriptase, while the traditional gRNA is replaced with a prime editing guide RNA (pegRNA) [47]. The pegRNA is linked to a gene specific RNA sequence containing a primer binding site (PBS), which contains a complementary sequence to the target region of the edited DNA sequence. nCas9 nicks the non-edited strand to produce a single-stranded DNA break which then serves as a primer and binds the PBS site in the pegRNA. A new DNA fragment is produced utilizing reverse transcriptase and the newly synthesized DNA replaces the target DNA. Thus, prime editing is replacing targeted DNA sequences without the need of a DNA template. A recent study by Everette et al. demonstrates the development of a prime editing strategy in HSPCs that rescues sickle-cell disease phenotypes after engraftment in mice [48].

1.3 Therapeutic Use of mRNA

In light of the global severe acute respiratory syndrome coronavirus 2 (SARS-CoV-2) pandemic, mRNA proved to be the ideal basis for the development of new vaccines against infectious pathogens [49–51]. Thus, making novel vaccines within very short time span at limited financial investments is of great importance for future pandemic scenarios. With an mRNA based approach it is theoretically possible to produce any protein or peptide via the protein synthesis machinery processed in the transfected cells *in vitro* or *in vivo* [52]. Compared to DNA-based drugs, mRNA transcripts have a relatively high transfection efficiency and low toxicity as they do not need to enter the nucleus to be functional [53]. Besides, mRNA carries no risk of genomic integration which gives mRNA a safety advantage over DNA-based therapeutics. Nevertheless, challenges still remain, such as insufficient knowledge of mRNA structure instability and immunogenicity, in addition to the potential induction of an immune response with associated toxicity.

A mature mRNA harbors a 5'cap, the coding region including exons, untranslated regions (UTRs), and the poly(A) tail (Figure 1.4). mRNA, transcribed in the nucleus, undergoes modifications such as splicing before it is translated into proteins in the cytoplasm. In addition to splicing, precursors mRNA (pre-mRNA) undergoes 5' and 3' end modifications. The 5'end cap protects the mature mRNA from degradation, while the addition of poly(A) tail confers stability to the mRNA and assists in the export of the mRNA to the cytosol. Based on the vital importance of these functional elements, numerous studies have focused on the optimization of mRNA structure. This include, but are not limited to, developing series of 5' cap analogs [54, 55], changing the poly(A) tail length [56], and encoding various functional peptides or viral replication machinery of open reading frames (ORFs) [57].

Figure 1.4: **Illustration of mature mRNA**
including the 5' cap, the coding region with exons, the 5' and 3' UTRs, and the poly(A) tail. Created with BioRender (`https://www.biorender.com/`).

Even though mRNA-based therapeutics are promising when it comes to developing human medicine, there are still several hurdles remaining. First, preventing the degradation of mRNA caused by ribonucleases (RNases) [58] by for instance co-delivering recombinant RNase inhibitors [59, 60]. Secondly, research revolves heavily around engineering T7 RNA polymerase to produce mRNA lacking immunostimulatory byproducts such as double-stranded RNA [61]. And finally, circumventing the formation of double-stranded RNA, which might lead to immunostimulatory responses, could be solved by including selected chaotropic agents during the *in vitro* transcription protocol [62]. Since the immune response to viral infection is normally initiated when viral double-stranded RNA is detected by double-stranded RNA-binding proteins in the host [63], examples of such proteins are Toll-like receptors (TLRs) [64], and retinoic-acid inducible gene I (RIG-I) or melanoma differentiation associated factor gene 5 (MDA5) (RIG-I-like receptors) [65].

Furthermore, mRNA delivery remains a great challenge for current mRNA-based therapeutics. To enhance mRNA delivery, various modalities of delivery have been designed and synthesized, including lipid nanoparticles (LNPs) [66], polymeric nanoparticles [67], in addition to other delivery systems [68]. The advantages associated with LNP-based mRNA delivery systems are their high stability, the transfection efficiency, the safety, and the low cost of manufacturing processes.

mRNA-based therapeutics are expected to become a powerful therapy for a variety of refractory diseases, such as infectious diseases, metabolic genetic diseases, cancer, cardiovascular and cerebrovascular disease, and other diseases. mRNA is easily synthesized through an *in vitro* transcription process, is relatively easy to manufacture, and can be quickly applied to various therapies.

1.4 Synthesis of mRNA by *in vitro* Transcription

There are different strategies for *in vitro* synthesis of mRNA, however, RNA can be efficiently synthesized by *in vitro* transcription.

As mentioned previously, a functional mRNA requires a 7-methylgunaylate cap at the 5'end and a poly(A) tail at the 3'end, in addition to a coding region flanked by UTRs. Post-transcriptional capping is important to evade cellular innate immune response against foreign RNA by obtaining a Cap-1 structure [54].

Incorporating a cap analog during transcription is known as co-transcriptional capping. The most common cap analog used are the standard 7-methyl guanosine (m7G) cap analog or anti-reverse cap analog (ARCA) (Figure 1.5) [54]. Methylated 3'position of m7G prevents RNA elongation by phosphodiester bond formation at this position. The 7-methylated G functions as a terminal residue allowing the correct orientation of 5'm7G cap structures to the synthesized transcripts. A cap analog and modified nucleotides are introduced into the transcription reaction. The incorporation of naturally modified nucleotides enhance stability and translational capacity of mRNA, in addition to diminishing its immunogenecity *in vivo* [69]. Studies have shown that using CleanCap Reagent AG results in a more stable, progressive, and less immunologically triggering mRNA [54] compared with traditional dinucleotide co-transcriptional capping. One criteria using CleanCap Reagent AG is that the DNA template must contain an "AG" instead of a "GG" following the T7 promoter in the initial sequence.

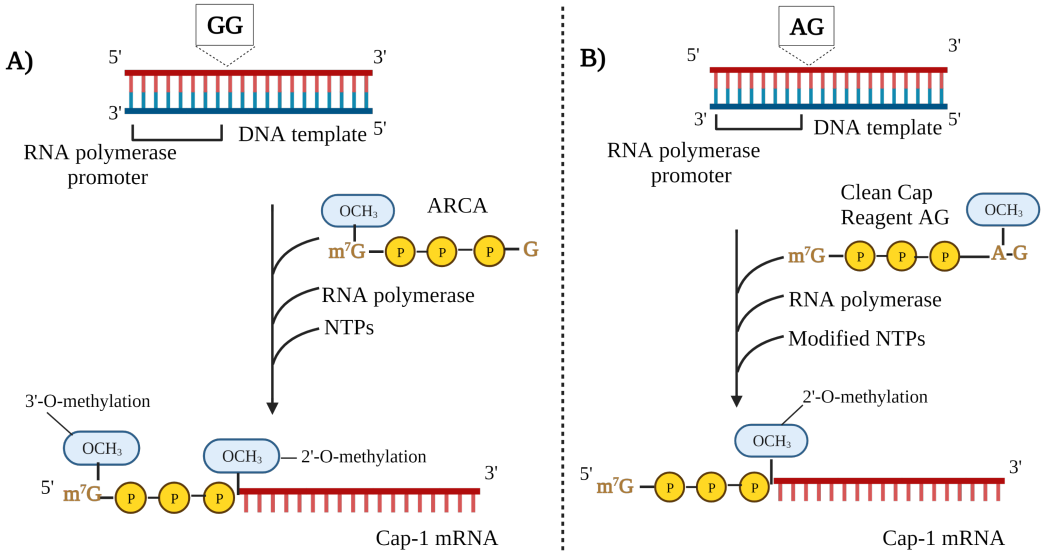

Figure 1.5: **Illustration of co-transcriptional capping** with an mRNA cap analog (shown in yellow) in transcription reaction. **A)** The anti-reverse cap analog (ARCA) contains an additional 3'-O-methyl group on the 7-methylguanosine to facilitate incorporation in the correct orientation. The inclusion of the mRNA cap 2'-O-Methyltransferase results in the formation of the Cap-1 structure. **B)** Co-transcriptional capping with CleanCap reagent AG requires a modified template initiation sequence. The incorporation of this trinucleotide in the beginning of a transcript results in a Cap-1 structure [54]. Created with BioRender (`https://www.biorender.com/`) and adapted from NEB Expressions Spring 2022 (`https://bionordika.no/`).

1.5 Detection Methods for Precise Editing

It is crucial to be able to detect and distinguish between the two repair pathway outcomes. Droplet digital polymerase chain reaction (ddPCR) is an easy and rapid method to quantify genome editing outcomes with high sensitivity and specificity [70–72].

ddPCR divides the target and background DNA randomly into 20,000 nanoliter-sized droplets. The spherical droplets are composed of an oil surface and an aqueous core containing the PCR reaction mix. A reference probe, labelled with for instance HEX fluorochrome, is included and binds to the sequence of interest. In addition, specific NHEJ and HDR fluorochrome probes are added to the ddPCR Supermix. Hence, in ddPCR there are 20,000 individually reactions taking place compared to a single reaction in normal PCR. Each reaction contains the standard materials such as enzyme, primers, and probes, while the distribution of droplets containing the region of interest is random [73]. The droplets are subjected to thermal cycling in a standard PCR machine, then read one by one by the Droplet Reader (Bio-Rad). The data is displayed in a two-dimensional

plot of positive, double-positive, and double-negative droplets in the QuantaSoft software.

A disadvantage with ddPCR is that it cannot distinguish between different types of indel formation. As the NHEJ probe drop-off when indels are introduced to the sequence, ddPCR cannot tell if the indels are insertions or deletions. DNA sequencing is a method that can accurately detect NHEJ. This can be done using Next-generation sequencing (NGS) or Sanger sequencing combined with specific data analyses tools, such as Inference of CRISPR Edits (ICE) software [74]. In contrast to Sanger sequencing where one single DNA fragment is sequenced, NGS platforms sequence millions of DNA fragments simultaneously per run of DNA [75]. Even though NGS provides accurate estimates of indel size, frequency, and sequence identity, this method requires time and effort for library preparation and bioinformatics capability to analyze the data [70].

1.6 Aim of Thesis

In present thesis, the three main research questions are (i) will a time-controlled two-step transfection protocol of Cas9wt and Cas9 coupled to HMGB1-fusion improve HDR editing in human PBMCs, (ii) is it possible to optimize the mRNA production to create a more stable Cas9wt mRNA, and (iii) will addition of RNase inhibitors prior to electroporation enhance the editing outcomes.

An overall overview of the experimental setup is presented in Figure 1.6. Based on a paper by Yang et al. [76], we preform a time-controlled Two-step Electroporation of Cas9wt mRNA and Cas9-HMGB1 mRNA to enhance the efficiency of installing silent mutations by nonviral ssODN in human PBMCs. Chromatin modulator HMGB1 is fused to Cas9 to improve Cas9 activity [22]. Furthermore, as demonstrated by Piao et al. [62], we hypothesize that adding a chaotropic agent such as urea to the *in vitro* transcription protocol will disrupt the pairing of newly formed single-stranded RNAs into double-stranded RNA. In addition, extendend purification of RNA is going to be performed as well. We also test the inclusion of RNase inhibitors to the sgRNA-Cas9wt mRNA mix prior to electroporation of human PBMCs, with inspiration from Laoharawee and co-workers [60].

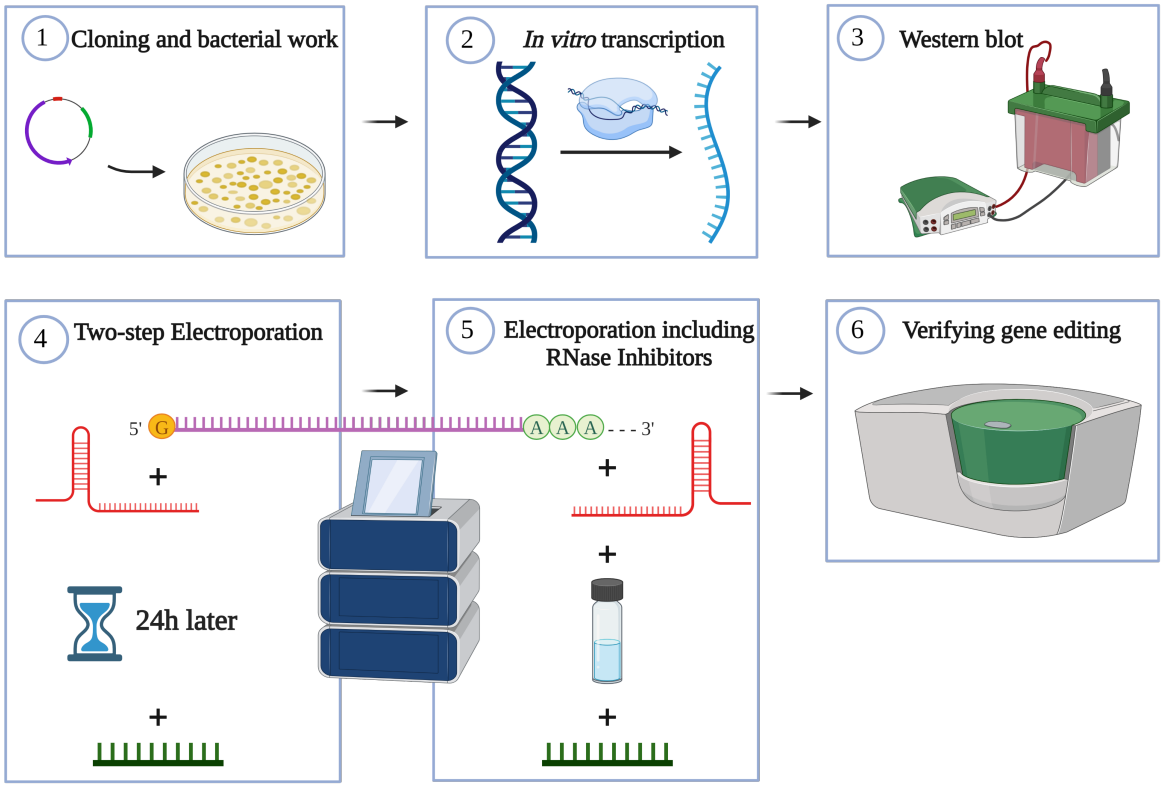

Figure 1.6: **The workflow of experimental design.**
1. Cloning and bacterial work of pDEST40, pDEST40 Cas9wt, and pDEST40 Cas9-HMGB1 plasmid utilizing CcdB and *DH5α* competent cells. Moreover, generating a nucleotide change in the T7 promoter by T7 mutagenesis to be able to use a CleanCap for the *in vitro* transcription protocol. 2. *In vitro* transcription of Cas9wt and Cas9-HMGB1, in addition, optimizing the protocol by adding urea to the mRNA synthesis and extendend purification of RNA. 3. Validating the expression of Cas9wt and Cas9-HMGB1 constructs in HEK293T cells. Furthermore, verifying time-point protein expression of optimized Cas9wt mRNA in PBMCs by western blot. 4. Time-controlled Two-step Electroporation of Cas9wt and Cas9-HMGB1 mRNA in PBMCs. Thus, single-stranded repair template is included 24 hours post-first-electroporation. 5. Adding RNase inhibitors to Cas9wt mRNA in PBMCs prior to electroporation. 6. Verifying gene editing by ddPCR. Created with BioRender (`https://www.biorender.com/`).

2 Methods

All materials are given in Appendix A Materials, including lab equipment, kits, buffers and chemicals, and cell culture media (Table A.1-4).

2.1 Statistical Methods

All statistical analyses were performed using GraphPad Prism 9.3.1 software utilizing one-way or two-way ANOVA followed by Tukey's multiple comparison tests ($^{****}P < 0.0001$,$^{***}P < 0.001$, $^{**}P < 0.01$, $^{*}P < 0.05$ as shown in figures).

2.2 Amplification of Plasmids by Bacterial Transformation

To amplify DNA fragments and to produce large amounts of identical plasmids from the initial stock sample of pDEST40, pDEST40 Cas9wt, and pDEST40 Cas9-HMGB1, we used bacterial transformation.

Firstly, 50 μL of $DH5\alpha$ competent bacteria cells (Thermo Fisher) were aliquoted into Eppendorf tubes, and 1 μL of DNA (10 pg- 100 ng) was added to the competent cells. The DNA mixture was incubated for 30 minutes on ice, then heat-shocked at 42°C for 45 seconds in a water bath before incubating for another 2 minutes on ice. At the end, 500 μL of SOC media without antibiotic was added to the bacteria prior to plating 100 μL on agar plates containing ampicillin. The next day, one colony from each plate was picked and single colonies were expanded overnight at 37°C. The following day, plasmid DNA from the successfully transfected *E. colis* were isolated using Miniprep Kit or Maxiprep Kit, following the QIAprep Spin Miniprep Kit protocol (QIAGEN) or the PureLink® HiPure Plasmid Filter Purification Kits (Invitrogen). The Miniprep Kit follows a bind-wash-elute procedure, while the Maxiprep Kit uses columns combining filtration for lysate clarification.

2.3 Introduction of a Single Nucleotide Change in the T7 Promoter Sequence by T7 Promoter Mutagenesis

To change a Guanine to Adenine in the T7 promoter sequence we used site mutagenesis. The common pDEST40 backbone plasmid was used, in addition to pDEST40 Cas9wt

and pDEST40 Cas9-HMGB1. The plasmid maps and corresponding plasmid sequences are listed in Appendix F Plasmid Maps and Plasmid Sequences.

To generate one nucleotide change in the T7 promoter sequence, the Q5® Site-Directed Mutagenesis Kit was used according to the manufacturer's protocol. In brief this protocol encompass 5 steps. First, the region of mutagenesis is amplified by PCR using a pair of primers resulting in two PCR products. Second, a kinase, ligase and Dpnl (KLD) treatment step ligates the two PCR products forming double-stranded DNA plasmids bearing the mutation. Third, competent cells are utilized for bacterial transformation. Fourth, surviving colonies are picked and plated onto agar plates containing ampicillin. Lastly, plasmid DNA is isolated and purified by Miniprep Kit.

For PCR primer design, the pair of primers with the best annealing temperature had been ordered previously by another researcher, following the instructions on NEBaseChanger's© website (`https://nebasechanger.neb.com/`) (Appendix B Primer and Probe Sequences). The region of mutagenesis was amplified by PCR and both primers were used as the 5'ends of the primers are located head-to-head and the amplification starts from the same spot but into different directions. The KLD treatment step ensured ligation of the two PCR products and creation of double-stranded DNA plasmid bearing the desired mutation. The thermocycling condition was set at 61°C for elongation for all plasmids containing the pDEST40 backbone, while the elongation temperature for the positive control in the Q5 Site-Directed Mutagenesis Kit followed the manufacturer's protocol.

After exponential amplification of plasmids, the plasmids were cloned into bacteria according to the One Shot® ccdB Survival™ 2 T1R Chemically Competent Cells protocol (NEB) or according to the $DH5\alpha$ Competent Bacteria Cells protocol (Thermo Fisher). For plasmid pDEST40, the One Shot ccdB Survival Competent Cells were used as the plasmid backbone contains the *ccdB* gene coding for the toxic protein CcdB, which causes cell death [77]. By using a special strain of *E.coli* that tolerates the expression of the toxic gene, it is possible to identify desired clones due to the selection against vectors that do not take up the insert [78]. By using the CcdB-resistant strain ccdB Survival (Invitrogen) a successful insertion will completely replace the ccdB gene with the insert of interest. For the pDEST40 Cas9-HMGB1 plasmid, the $DH5\alpha$ Competent Bacteria Cells were used as these bacteria cells are sensitive to CcdB. The surviving colonies should then

contain the desired, recombined construct since the CcdB protein inhibits the growth of CcdB sensitive *E.coli* strains [79].

Colonies were picked the next day and plasmid DNA from the successfully transfected *E. colis* were isolated using Miniprep Kit. The cultures were collected according to the QIAprep Spin Miniprep Kit protocol (QIAGEN). The samples were then sent for Sanger sequencing to Eurofins (`https://eurofinsgenomics.eu/`) for confirmation of desired mutation.

After T7 mutagenesis, the desired sequence should be the following: taatacgactcactataag, where the underlined nucleotide in bold, red font is the nucleotide changed from a Guanine to Adenine. The sequence analysis was performed in SnapGene® (version 6.0.6).

2.4 Synthesizing mRNA by *in vitro* Transcription

To produce a poly(A) tailed mRNA including CleanCap, the mRNA was transcribed *in vitro* following the HiScribe T7 mRNA Kit with CleanCap Reagent AG protocol (NEB) with small modifications. In brief, the *in vitro* transcription protocol encompass 5 steps. First, circular plasmid DNA is linearized by *MssI* restriction enzyme. Second, gel electrophoresis is run to verify the linearization and product size of the cut plasmid. Third, mRNA is synthesized by mixing the linearized plasmid DNA with modified nucleotides, the m7G CleanCap, T7 RNA Polymerase Mix, and buffer, followed by DNase treatment and adding the poly(A) tail. Lastly, the mRNA is purified and run on gel electrophoresis to observe the quality of obtained mRNA. For all steps in the *in vitro* protocol, the surfaces and equipment were disinfected with RNase away before and during the production steps to prevent degradation of mRNA.

First, the DNA template was linearized by using 2 μL of *MssI* digestion enzyme and 2 μL of restriction digestion buffer FastAP or FastDigestion. For the linearization reaction, 8000 ng of plasmid template was used. Subsequently, nuclease-free water was added to get a total reaction volume of 20 μL. The mixture was incubated at 37°C overnight.

The next day, agarose gel electrophoresis was performed to verify linearization and product size. 500 ng of each linearized plasmid was loaded per well in addition to 20 μL of water into the remaining empty wells of the E-Gel slide (2% SYBR Safe). The gel was

run for 26 minutes choosing the program "E-gel $0.8-2\%$" prior to visualizing the gel on the UV transilluminator (Bio-Rad). mRNA synthesis was prepared as described in Table 2.1 and incubated at 37°C for 2 hours. For each linearized plasmid the amount was 1000 ng per *in vitro* transcription reaction.

Table 2.1: **Reagents and volume required for mRNA synthesis.**
The volume of 'x' depends on the concentration of template DNA added to the mix. The mixture was topped up with nuclease-free water to get a final volume of 20 μL.

Reagents	**Volume [μL]**
ATP [60 mM]	2
CTP [50 mM]	2
GTP [50 mM]	2
N1-Methylpseudouridine-5'-Triphosphate [50 mM]	2
Cap Analog [40 mM]	2
10X T7 CleanCap Reagent AG Reaction Buffer	2
RNase out [40 U/μL]	0.5
Template DNA [1 μg]	x
T7 RNA Polymerase Mix	2
Nuclease-free H_2O	x
TOTAL	**20**

In order to remove the DNA template, 2 μL of DNase enzyme was added to each tube of the mRNA synthesis mix. The mixture was incubated at 37°C for 15 minutes. Then, the poly(A) tail was added to the mRNA by mixing 5 μL of 10x PolyA polymerase Reaction buffer and 5 μL of PolyA polymerase. To get a total volume of 50 μL, 20 μL of nuclease-free water was added. At the end, the mixture was incubated for another 30 minutes at 37°C. Finally, 75 μL of LiCl solution was added to the transcription reaction to purify the mRNA. The mRNA was stored at -20°C overnight.

The next day, the RNA was centrifuged at 21,000 g at 4°C for 17 minutes to pellet the RNA. The pellet was rinsed by slowly adding 500 μL of cold 70% EtOH and centrifuged at 21,000 g at 4°C for 12 minutes. After carefully removing the ethanol, residual liquid was removed and the pellet was air dried until it turned transparent ($\sim$ 4-5 minutes). Subsequently, to completely dissolve the mRNA, the mRNA was resuspended

in 30 μL of nuclease-free water and heated at 65°C for 5 minutes. After measuring the concentration by NanoDrop, an aliquot was taken for preparing the mRNA sample while the remaining mRNA was stored at −80°C. The mRNA sample was made by mixing 20 μL of Formaldehyde Loading Dye and 0.5 μL of Ethidium Bromide together with 1 μL of the aliquoted mRNA.

The concentration of the Millennium RNA Marker (Thermo Fisher) ladder was 4000 ng while the total amount of loaded mRNA varied between 1000-3000 ng. At the end, the mRNA samples were heat-denatured at 70°C for 15 minutes before loading 24 μL of mRNA ladder and 22 μL of mRNA samples onto the pre-made agarose denaturating formaldehyde gel (Appendix A Materials, Table A.3 Buffers and Chemicals). The gel was run for approximately 1.5 hours at 95 V. At the end, the gel was visualized under the UV transilluminator (Bio-Rad).

2.4.1 Synthesizing mRNA by Optimizing the *in vitro* Transcription Protocol

It has been demonstrated that including selected chaotropic agents at optimized concentrations during *in vitro* transcription prevents undesired double-stranded RNA formation [62]. Thus, 8M of urea was added accordingly to previous protocol (Table 2.1) by dissolving 0.48 g urea in 0.5 mL Milli-Q water. Further, the MEGAclear™ Transcription Clean-Up Kit was used to remove additional nonreacted nucleotides, proteins, and salts from the RNA.

2.5 Transfection of HEK293T Cells by Lipofectamine and FuGENE

Transfection is a nonviral method of introducing foreign DNA into eukaryotic cells. Different transfection methods are either chemical, biological or physical, resulting in a change in the properties of cells, allowing the study of gene function and protein expression [80]. Lipofectamine and FuGENE are cationic lipid formulations designed for delivering DNA into various cell lines. As plasmids are not easily transfected to primary cells, we used HEK293T cells instead to transfect Cas9wt and Cas9-HMGB1 plasmid.

2.5.1 Cell Preparation and Transfection Procedure

The cells were thawed and maintained as described in Subsection 2.7.1 Thawing Cells and Subsection 2.7.2 Splitting Fibroblasts and HEK293T Cells, respectively. The cells were plated on a 24-well plate the day before transfection to obtain an optimal confluency of 80-90% (see Appendix H Cell Pictures). The required number of cells was 1.25 x 10^5 cells/well in 500 μL of Recovery medium supplemented with 1X Penicillin-Streptomycin (P/S) (Appendix A Materials, Table A.4 Cell Culture Media).

On the day of transfection, media was changed to fresh Expansion medium without P/S. The Transfection Master Mixes for Lipofectamine and FuGENE were made as shown in Table 2.2.

For Lipofectamine transfection, Mixture 1 was incubated for 5 minutes at room temperature before adding Mixture 1 to Mixture 2. The transfection mixture was then incubated for another 20 minutes at room temperature.

For FuGENE transfection, the transfection mixture was incubated for 15 minutes at room temperature. The transfection mixes were then distributed drop-wise to each well prior to incubating the plate at 37°C, 5% CO_2 level for 24 hours.

Table 2.2: **Reagents and volume required for one sample of transfection** in a 24-well plate according to manufacturer.

(a) Lipofectamine transfection

Reagents	**24 well/1 sample [μL]**
Mixture 1	
Opti-MEM	50
Lipofectamine 2000	2
Mixture 2	
Opti-MEM	50
Plasmid DNA [μg]	0.8
Total volume	**100**

(b) FuGENE transfection

Reagents	**24 well/1 sample [μL]**
Opti-MEM	50
FuGENE	2.4
Plasmid DNA [μg]	0.8
Total volume	**50**

2.5.2 Cell Collection for Protein Lysates

Cells were pelleted by centrifugation at 500 g for 5 minutes at 4°C. Then, the cells were washed twice in cold 1X PBS and centrifuged at 500 g for 5 minutes. 50 μL of RIPA lysis buffer and HALT protease inhibitor was added before incubating the tubes for 30 minutes on ice, flicking the tubes before, during, and after incubation. At the end, the samples were centrifuged at 14,000 g for 15 minutes at 4°C. Finally, 40 μL of supernatant was transferred to a new Eppendorf tube and stored at -20°C. The protein lysates were later subjected for western blotting.

2.6 Protein Expression by Western Blotting

A western blot allows detection of a single protein within a mixture of proteins by first separating the proteins based on molecular weight, then by its charge. The separated proteins are then transferred to a membrane in order to immobilize the proteins and to

make them accessible for detection by antibodies.

To validate the Cas9wt and Cas9-HMGB1 plasmid constructs, HEK293T cells were transfected and collected 24 hours later as described in Subsection 2.5.2 Collection for Protein Lysates. Initially, cells were lysed in order to collect the protein lysate. The protein concentration was measured with the Bicinchoninic acid (BCA) Kit. Electroporated PBMC and fibroblast samples were also included, where PBMC samples were collected at different time-points (2-24 hours) post-electroporation described in Subsection 2.8.4 Media Change and Cell Collection.

2.6.1 BCA Assay- Protein Quantification, Sample Normalization and Sample Preparation

The standard curve dilutions were prepared according to the BCA assay protocol (Appendix C BCA Standard Curve Dilutions). The working solution was prepared using the following formula to determine the total volume of reagents required:

(9 standards + number of unknowns) x (2 replicas) x (200 μL of working reagent per sample)= total volume working reagent required.

The amount of working reagent was prepared by mixing 50 parts of BCA Reagent A with 1 part of BCA Reagent B. Then, 2 μL of the protein samples and 2 μL of the standard curve diluted samples were pipetted in duplicates into a 96-well plate. Each sample was topped with 198 μL of working solution and incubated at 37°C for 30 minutes. The readout was performed at 560 nm on the Infinite® microplate reader (Tecan). The protein amount in the samples were standardized to even concentrations between the samples. Then, samples were prepared for boiling by adding 7.5 μL of 4xLaemmli in combination with the reducing agent 2-mercaptoethanol to 10 μg protein. At the end, the samples were topped up with RIPA lysis buffer and HALT protease inhibitor to obtain a final volume of 30 μL. The samples were boiled at 95°C for 5 minutes and kept at -20°C.

2.6.2 Protein Electrophoresis and Transblotting Proteins from Gel to Membrane

The pre-casted TGX gel (4-20%) was applied to the electrophoresis cassette, and 8 μL of protein ladder and 25 μL of boiled samples were loaded onto the gel. The electrophoresis ran for 5 minutes at 50 V before adjusting the voltage up to 90 V for 90 minutes or until the blue line on the gel reached the green chamber line.

To transblot the proteins from gel to polyvinylidene difluoride (PVDF) membrane, the instructions for Trans-Blot Turbo Mini transfer for sandwich assembly were followed. First, the running buffer was discarded from the cassette and the transblotting cassette was cracked open using specialized tools. The gel was placed gently on top of the membrane and the plastic slide was removed. Second, the bottom part of the sandwich was placed on the bottom part of the transblotting cassette. It is important that the membrane is placed in such manner that the negatively charged proteins migrate from the gel to the membrane. Finally, the upper part of the sandwich was placed on top prior to pressing firmly the parts together as sufficient contact between the gel and the membrane is crucial to obtain clear bands. Air bubbles were also removed with a rolling tool to prevent blurry bands on the blot. At the end, the sandwich was applied to the Trans-Blot Turbo Cassette (Bio-Rad), and the Trans-Blot Turbo Transfer System (Bio-Rad) was set at High Molecular Weight program for 10 minutes.

2.6.3 Blocking the Membrane and Incubating with Primary and Secondary Antibodies

After transblotting, the membrane was put into blocking solution TBST (5% skimmed powder milk or 5% BSA) and blocked for 1 hour on a rocking machine. The composition of buffers and antibodies used is listed in Appendix A Materials, Table A.3 Buffers and Chemicals.

Cas9 and α-tubulin antibody were diluted in 5% skimmed powder milk and 5% BSA, respectively, and the membrane was incubated in primary antibodies at 4°C overnight on a rocking machine.

The next day, the membrane was washed three times in TBS at 20 minutes intervals on a rocking machine. The secondary antibody mixture diluted in 5% skimmed powder milk was added and incubated for 1 hour at room temperature. The membrane was again washed three times in TBS at 20 minutes intervals.

2.6.4 Enhanced Chemiluminescence Incubation and Developing the Membrane

Enhanced chemiluminescence (ECL) is a method used to visualize the protein. The development mixture was prepared by mixing 1:1 Enzyme Mix and Enhancer Master Mix. The membrane was kept on a rocking machine for 5 minutes in a box with lid to keep the membrane away from light. Once completed, the membrane was placed in a foil to protect against light and pictures of the membrane were taken. The ChemiDoc Imaging System (Bio-Rad) was set to colorimetric for protein ladder detection and chemiluminiscent for protein-antibody conjugate detection.

2.7 Handling Cell Line and Primary Cells

All work handling cell lines and primary cells was done in a sterile BL-2 laminar hood. Aseptic techniques were strictly followed. The different types of media used are listed in Appendix A Materials, Table A.4 Cell Culture Media. In addition, images of cells at various states and conditions are shown in Appendix H Cell Pictures.

Countess® (Thermo Fisher) was utilized for cell counting. A mixture of 10 μL of Trypan Blue cell counting dye and 10 μL of cells were loaded onto the counting slide.

2.7.1 Thawing Cells

Cells were transferred from -150°C into dry ice and thawed in a 37°C water bath for approximately 2 minutes. The thawed cells were poured into 10 mL of Thawing medium without P/S and centrifuged at 0.3 g for 5 minutes at room temperature. The pellet was resuspended in 1 mL pre-warmed Expansion medium without P/S and topped up to 10 mL. Everything was seeded into an appropriate cell culture flask prior to adjusting the volume of Expansion medium to obtain between 0.5-2.0 x 10^6 cells/mL. Finally, the cell culture flask was left in the incubator at 37°C, 5% CO_2 for three days.

2.7.2 Splitting Fibroblasts and HEK293T Cells

First, old cell culture medium was discarded before the cells were washed in 10 mL of pre-warmed phosphate buffered saline (PBS). PBS was discarded and cells were detached from the surface by adding 5 mL of pre-warmed trypsin. The flask was incubated at 37°C, 5% CO_2 for 5 minutes or until all cells were detached. The cells were resuspended in 25 mL of pre-warmed fibroblast/HEK293T Recovery medium supplemented with 1X P/S prior to transferring the suspension into a 50 mL Falcon tube for centrifugation at 0.3 g for 5 minutes at room temperature. The supernatant was discarded, and cells were resuspended in 1 mL Recovery medium supplemented with 1X P/S and topped up to 10 mL. At the end, the cell suspension was seeded onto T175 cell culture flasks containing 5 mL of cell suspension and 30 mL of pre-warmed Recovery medium supplemented with 1X P/S.

2.8 Electroporation of Primary Cells

2.8.1 Cell Preparation for Electroporation

For fibroblasts, cells were harvested following the same procedure as described in Subsection 2.7.2 Splitting Fibroblasts and HEK293T Cells. The concentration of an aliquot was measured to calculate the volume of cells needed to obtain 0.5-1.0 x 10^6 cells per sample. For human PBMCs, cells were harvested and the concentration of an aliquot was measured to calculate the volume of cells needed to obtain 1.0-2.0 x 10^6 cells per sample.

The appropriate volume was centrifuged at 0.3 g for 5 minutes and the pellet was resuspended in 1 mL pre-warmed PBS. The cell suspension was topped up to 10 mL of PBS and centrifuged at 0.3 g for 5 minutes. The prepared cells were resuspended in 20 μL Electroporation buffer (20 μL per well).

2.8.2 Preparation of Electroporation Mix

For standard RNP transfection, 100 pmol of sgRNA (100 μM stock, IDT) and 61 pmol of Cas9wt as protein (500 μM stock, IDT) was added to a 96-well plate using an electronic pipette. The plate was sealed, spun down and mixed by tapping the wells. The plate was then incubated for 15 minutes at 37°C, 5% CO_2 and placed on ice. 100 pmol of *ADA2* forward repair template (100 μM stock, IDT) was added onto the RNP complexes before

the plate was spun down and kept on ice until cells were ready for electroporation.

Working with Cas9wt and Cas9-HMGB1 mRNA, including optimized Cas9wt mRNA (PBMCs), 100 pmol sgRNA (100 μM stock, IDT) and 100 pmol of *ADA2* forward ssODN repair template (100 μM stock, IDT) were pipetted into a 96-well plate placed on an ice holder to prevent degradation of mRNA. The plate was sealed and spun down before pipetting 1000 ng of Cas9wt or Cas9-HMGB1 mRNA directly into the mix to the corresponding wells with an electronic pipette. Then, 20 μL of cells resuspended in Electroporation buffer was added to the wells with a multichannel pipette. Finally, 21-22 μL of cell-reagent mix was transferred to the 16-well electroporation strip.

For conditions without *ADA2* forward ssODN repair template, 100 pmol sgRNA (100 μM stock, IDT) and 1000 ng of Cas9wt mRNA were added to the 96-well plate.

For the Two-step Electroporation conditions, 100 pmol of *ADA2* forward ssODN repair template (100 μM stock, IDT) was added 24 hours after the first electroporation of the sgRNA:mRNA mix.

For samples containing RNase Out or RNase Inhibitor (PBMCs), 40 units was added to the respective wells.

All conditions were pipetted in triplicates except mock samples.

2.8.3 Electroporation

The pellet from Subsection 2.8.1 Cell Preparation for Electroporation was resuspended in 20 μL Electroporation buffer (20 μL per well). The cell suspension was pipetted into the wells of the 96-well plate containing the previously prepared Electroporation mix. The mix was then transferred to a 16-well strip before loading the strip to the Lorenza electroporation machine (Lorenza). The electroporation solution program used for fibroblasts was "Primary Cell P3" with pulse code "CA-137". For PBMCs, the electroporation solution program used was "Primary Cell P3" with pulse code "EO-115".

After the program was finished, 80-85 μL of pre-warmed Cell Recovery medium without P/S was added and the strip was incubated at 37°C, 5% CO_2 for 15 minutes. For fibroblasts, a 6-well plate containing 2 mL of pre-warmed Recovery medium without P/S and 2 mL of PBS in the remaining empty wells was prepared. For PBMCs, a 12-well plate containing 1 mL of pre-warmed Recovery medium without P/S and 1 mL of PBS in the remaining empty wells was prepared.

Finally, 100 μL of electroporated cells were transferred to the designated wells. The electroporation strip was cleaned with 100 μL of cell culture media to wash out excess cells. The cell culture plate was placed in the incubator at 37°C, 5% CO_2 to rest over night.

2.8.4 Media Change and Cell Collection

The next day, for fibroblasts, old media was discarded and replaced with 2 mL fresh pre-warmed Recovery medium supplemented with 1X P/S. For PBMCs, half of the initial media was removed and supplemented with the same volume of fresh Recovery medium supplemented with 1X P/S. The medium change was repeated again two days later.

Cells were harvested 4 days post-electroporation. To verify Cas9 protein expression in fibroblasts and PBMCs, cells were collected 24 hours post-electroporation following Subsection 2.5.2 Cell Collection for Protein Lysates. Comparing protein expression between Cas9wt mRNA and optimized Cas9wt mRNA with urea and purified with MegaClear Kit (PBMCs), cell were collected 2, 4, 6, 8, and 24 hours post-electroporation for protein lysates.

2.9 Detection of Editing with ddPCR

To be able to detect editing with ddPCR, the samples must first be prepared for droplet generation prior to exponential amplification by standard PCR. Finally, the detection of NHEJ and HDR is analyzed in the two-dimensional droplet cluster plot in the software.

The samples were diluted according to calculations using the Qubit concentration results to get a total amount of 64 ng for each DNA sample. The Master Mix and Primer-Probe Mix for NHEJ and HDR were prepared as shown in Table 2.3. Initially, the Primer-Probe Mixes were prepared in two separate Eppendorf tubes before adding the Master Mixes to the respectively Primer-Probe Mixes. The designed primers and probes are listed in Appendix B Primer and Probe Sequences.

Table 2.3: **Master Mix and Primer-Probe Mix made for 1 sample of NHEJ and HDR.** Primers and probes were resuspended in buffer provided by IDT according to manufacturer's protocol to get a final concentration of 100 μM.

(a) NHEJ

Master Mix NHEJ	**Volume for 1 sample [μL]**
ddPCR Supermix (no dUTP)	10
Primer-Probe Mix (NHEJ)	1
Milli-Q H_2O	1
Primer-Probe Mix NHEJ	**For 100 μL**
Milli-Q H_2O	54
Forward primer	18
Reverse primer	18
NHEJ probe (FAM)	5
Reference probe (HEX)	5

(b) HDR

Master Mix HDR	**Volume for 1 sample [μL]**
ddPCR Supermix (no dUTP)	10
Primer-Probe Mix (HDR)	1
Milli-Q H_2O	1
Primer-Probe Mix HDR	**For 100 μL**
Milli-Q H_2O	54
Forward primer	18
Reverse primer	18
HDR probe (FAM)	5
Reference probe (HEX)	5

An electronic pipette was used to distribute 12 μL of the Master Mix NHEJ and 12 μL of the Master Mix HDR to the semi-skirted 96-well plate assigned to the NHEJ and the HDR reactions. Then, 64 ng of each DNA sample normalized to 8 ng/μL were added to the corresponding wells. The remaining empty wells were filled up with 20 μL of water prior to loading the plate onto the Automated Droplet Generator (Bio-Rad).

Immediately after the program was done, the plate containing the generated droplets was heat-sealed at 170°C. The sealed plate was then placed in the PCR machine with the following program shown in Table 2.4.

Table 2.4: **PCR thermocycler program for amplification of generated droplets.**
* Step 2 and 3 are repeated 42 times.

	Temperature [°C]	**Time**
1	95	10:00 min
2*	94	0:30 sec
3*	56	3:00 min
4	98	10:00 min
5	4	Hold

After the thermocycler was completed, the QuantaSoft™ software (version 1.7.4) was launched and the Droplet Reader (Bio-Rad) was initiated. The plate reading parameters were set as shown below:

Experiment: RED (Rare target sequence detection- rare event detection)
SuperMix: ddPCR Supermix for Probes (no dUTP)
Target 1, type: Ch1 Unknown
Target 2, type: Ch2 Unknown

The data obtained from the droplet reader was then gated in a two-dimensional amplitude plot in the QuantaSoft software (version 1.7.4).

2.9.1 gDNA Extraction and Measuring DNA Concentration with Qubit and Nanodrop

DNA was extracted following the DNeasy Blood & Tissue Kit protocol (QIAGEN).

The DNA concentration was measured with Qubit® according to the Qubit® dsDNA High Sensitive Assay Kits Molecular Probes (Thermo Fisher) and NanoDrop™ 2000/2000c Spectrophotometers (Thermo Fisher). Qubit measures the absolute amount of DNA in the sample, while NanoDrop gives an overview of the samples' purity.

The Qubit dsDNA High Sensitive Assay Kit reads the concentration using a fluorometer [81]. Two different standards of 10 μL are required, diluted in 190 μL of working

solution. Each sample tube was prepared with 1 μL of DNA diluted in 199 μL of working solution. The working solution was prepared by diluting the Qubit dsDNA High Sensitive Reagent in a 1:200 ratio of Qubit dsDNA High Sensitive Buffer. At the end, the tubes were incubated at room temperature for 2-5 minutes before measuring the standards and samples on the Qubit 2.0 Fluorometer.

For NanoDrop™, 1 μL of DNA sample was pipetted directly onto the measurement pedestal. A ratio absorbance at 260 nm and 280 nm assesses the purity of DNA or RNA. Measuring DNA, a 260/280 ratio of $\sim$1.8 is accepted as pure, while for RNA this value is $\sim$2.0. Obtaining a lower ratio might indicate the presence of protein, phenol or other contaminants that absorbs near or strongly at 280 nm. The 260/230 ratio is a secondary measurement on nucleic acid purity. A pure value is commonly in the range of 1.8-2.2. If the ratio is appreciable lower, this might indicate the presence of co-purified contaminants [82].

2.9.2 Detection of NHEJ and HDR Edits

As ddPCR measures NHEJ and HDR simultaneously, specific probes are designed to distinguish the two major repair pathways. A reference probe that is nonoverlapping with the cut site and that always binds to the genomic DNA is required. Then, the NHEJ probe is a wild type probe that binds to the wild type sequence, while the HDR probe binds to the specific sequence from the repair template. Thus, the NHEJ probe and HDR probe will only bind if the reference probe has bound to the DNA fragment of interest.

The QuantaSoft software measures the number of positive and negative droplets for each fluorophore in each sample. Hence the positive droplets for HDR and NHEJ (FAM) is plotted against the positive droplets for the reference probe (HEX) shown in Figure 2.1.

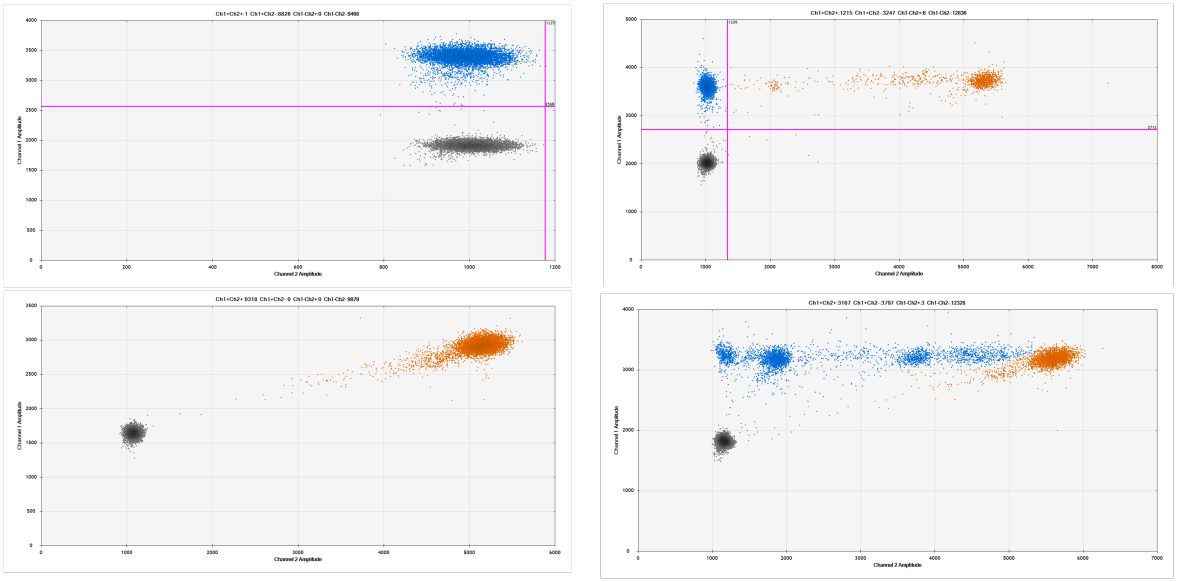

(a) Gating strategy of negative control

(b) Gating strategy of RNPs

Figure 2.1: **Gating strategy of Mock and RNPs**
in a two-dimensional cluster for quantifying gene editing with ddPCR. The upper panel represents HDR, while lower panel represents NHEJ. Channel 1 Amplitude fluorescence (FAM probe) is plotted against Channel 2 Amplitude fluorescence (HEX probe). Black dots represent droplets of DNA fragments without DNA of interest (no reference probe has bound). For HDR, the blue dots represent population that is HEX positive. The DNA marker probe has bound, but not the specific sequence from repair template. The repair template has thus not been incorporated into the genome and no HDR has occurred. For NHEJ, the orange dots represent population that is HEX positive. The DNA marker probe has bound, in addition to the NHEJ probe indicating that no indels was introduced into the sequence and no DNA sequence change has occurred.

In summary, to detect HDR editing, the HEX reference probe binds to the sequence of interest and the FAM HDR probe binds to the sequence on the introduced repair template. To detect NHEJ editing, the HEX reference probe binds to the sequence of interest, and the FAM NHEJ probe does not bind as there are indels introduced to the sequence. The NHEJ probe binds to the wild type sequence, and is often referred to as the drop-off probe.

3 Results

In current thesis, the experimental workflow was as follow: generating plasmids by cloning in bacteria and introducing a nucleotide change in the T7 promoter, synthesising mRNA *in vitro* and optimizing the mRNA protocol, verification of Cas9 protein expression by western blot, electroporating various conditions of Cas9wt mRNA and Cas9-HMGB1 mRNA in human PBMC, and verifying editing with ddPCR.

3.1 Introducing a Single Nucleotide Change in the T7 promoter

The aim was to make one nucleotide change in the T7 promoter sequence to be able to employ a CleanCap structure in the *in vitro* protocol. After changing a Guanine to Adenine in the T7 promoter, *in vitro* transcription was performed to produce mRNA from linearized DNA template. At the end, the obtained mRNA was delivered by electroporation to human PBMCs for CRISPR gene editing.

The different conditions of the experimental setup of T7 mutagenesis are shown in Table 3.1. A reaction without the polymerase mix was included as a control to verify that no amplification took place when the Master Mix was excluded. In addition, only heat shocked bacteria were plated onto the ampicillin plate to verify the properties of the competent cells. The PCR reagents were adjusted to a final volume of 25 μL for all conditions.

Table 3.1: **Experimental setup for the T7 mutagenesis experiment**
including positive and negative controls. 1. pDEST40, and 2. pDEST40 Cas9-HMGB1.

Condition	**Plasmid**	**Bacteria**
Original T7 mutagenesis	pDEST40, pDEST40 Cas9-HMGB1	ccdB[1], $DH5\alpha$[2]
Reaction excluding the polymerase mix	pDEST40, pDEST40 Cas9-HMGB1	ccdB[1], $DH5\alpha$[2]
Heat shocked bacteria	pDEST40 Cas9-HMGB1	$DH5\alpha$
Positive control from the Q5 Site-Directed Mutagenesis Kit	CLuc AG Control Template	$DH5\alpha$

As expected, after transformation there were no colonies on the plates of the reaction without polymerase mix and only heat shocked bacteria. No colonies were picked from the pDEST40 plate as this plasmid was included as a positive control.

To verify the ligation of the two PCR products and creation of plasmid double-stranded DNA, 20 μL of the plasmids with and without KLD treatment was loaded onto a pre-made 1% agarose gel (Appendix A Materials, Table A.3 Buffers and Chemicals) (Figure 3.1). The gel was run at 90 V for approximately 45 minutes and visualized under

the UV transilluminator (Bio-Rad) with SYBR Safe. We observed circularization of the KLD treated PCR product (Figure 3.1, red boxes).

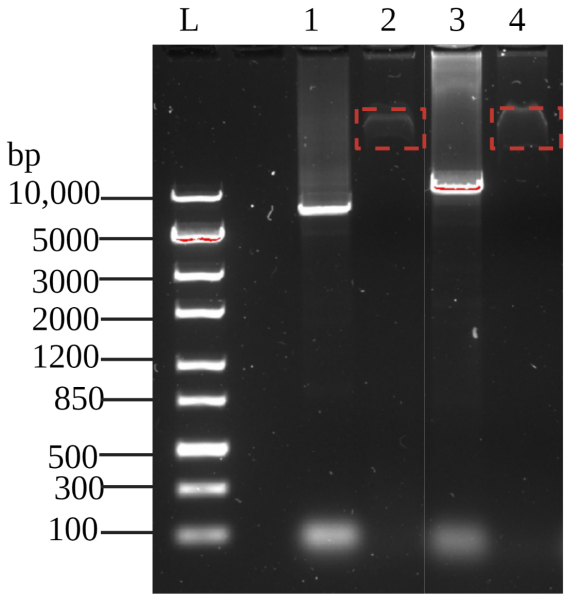

Figure 3.1: **Verification of ligation of the two PCR products.**
L. DNA ladder ZipRuler Express 1, 1. pDEST40 Cas9wt without KLD treatment, 2. pDEST40 Cas9wt with KLD treatment, 3. pDEST40 Cas9-HMGB1 wihtout KLD treatment, and 4.pDEST40 Cas9-HMGB1 with KLD treatment.

At the end, four samples of pDEST40 Cas9-HMGB1 from the Original T7 mutagenesis condition were sent for Sanger sequencing. Receiving the sequencing results from Eurofins (`https://www.eurofins.no/`), 8 out of 10 sequences had the desired mutation: taatacgactcactataag, where the underlined nucleotide in bold, red font is the one being changed. Out of these 8 passed sequences, one sample of pDEST40 Cas9-HMGB1 was chosen for *in vitro* transcription.

3.2 Producing a More Stable and Less Immunologically Triggering mRNA

We obtained mRNA by synthesizing mRNA *in vitro* (Figure 3.2b). It is crucial to cut the circular plasmid before proceeding with *in vitro* transcription as T7 polymerase utilizes the linearized DNA as template. If the plasmid is not completely linearized, no transcription will occur. We verified linearization and product size by gel electrophoresis followed by confirmation of mRNA product by formaldehyde gel (Figure 3.2). One sharp band indicates a completely linearized plasmid, whereas two or more bands indicate that some

of the plasmid is still in a circular form (Figure 3.2a). The cut plasmid is moving faster in the gel due to its open double-stranded DNA conformation. For all lanes, we loaded 500 ng of circular and linearized plasmid, except Cas9wt linearized in FastAP buffer (Figure 3.2a, lane 5). The gel was visualized under the UV transilluminator (Bio-Rad) with SYBR Safe.

The mRNA bands appeared clear without significant degradation for all lanes, except Cas9wt mRNA purified with MegaClear Kit (lane 6), which did not show any band on the gel (Figure 3.2b). The amount of mRNA loaded onto the gel varied between 1000-3000 ng. The measured concentrations along with the purity are show in Appendix D mRNA Concentration and Purity.

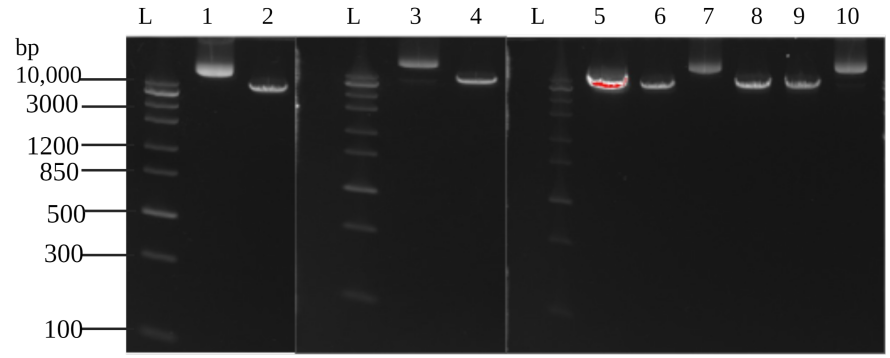

(a) Linearization quality and product size verification

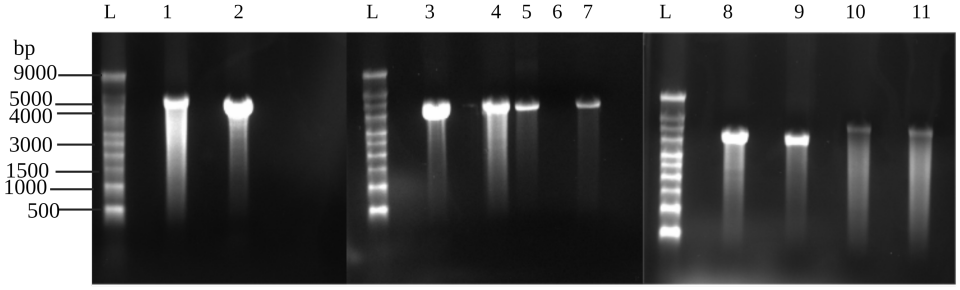

(b) mRNA gel

Figure 3.2: **The linearization quality and product size verification and mRNA gel of Cas9wt and Cas9-HMGB1 plasmids.**
The amount of mRNA gel loaded onto the gel is written in brackets. **A)** Linearization quality and product size verification of Cas9wt and Cas9-HMGB1 plasmids. L. DNA ladder ZipRule Express 1, 1. Cas9wt circular plasmid, 2. Cas9wt linearized plasmid, 3. Cas9-HMGB1 circular plasmid, 4.Cas9-HMGB1 linearized plasmid, 5. Cas9wt linearized plasmid in FastAP buffer, 6. Cas9wt linearized plasmid in FastDigestion buffer, 7. Cas9wt circular plasmid, 8. Cas9-HMGB1 linearized plasmid in FastAP buffer, 9. Cas9-HMGB1 linearized plasmid in FastDigestion buffer, 10. Cas9-HMGB1 circular plasmid. **B)** mRNA gel of Cas9wt and Cas9-HMGB1. L. DNA ladder ZipRule Express 1 (4000 ng), 1. Cas9wt mRNA (3000 ng), 2.Cas9-HMGB1 mRNA (3000 ng), 3. Cas9wt mRNA with urea (3000 ng), 4. Cas9wt mRNA before purified with MegaClear Kit (3000 ng), 5. Cas9wt mRNA with urea before purified with MegaClear Kit (1000 ng), 6. Cas9wt mRNA purified with MegaClear Kit (2000 ng), 7. Cas9wt mRNA with urea and purified with MegaClear Kit (700 ng), 8. Cas9wt mRNA before purified with MegaClear Kit (3000 ng), 9. Cas9wt mRNA purified with MegaClear Kit (2000 ng), 10. Cas9-HMGB1 mRNA with urea (3000 ng), 11. Cas9-HMGB1 mRNA with urea and purified with MegaClear Kit (3000 ng).

3.3 Detection of Protein Expression in HEK293T Cells, Fibroblasts and PBMCs

Transfection of HEK293T cells with Lipofectamine and FuGENE was initiated to verify which method was best suited for HEK293T cell line. Comparing these methods, transfection with Lipofectamine obtained higher transfection efficiency, while transfection with FuGENE obtained better quality in terms of band size (Figure 3.3a, upper

panel). We chose to proceed with Lipofectamine because of the optimization possibilities when it comes to the amount of proteins loaded onto the gel and extending the time for boiling samples and blocking/washing the membrane. In addition, the Lipofectamine reagent is less expensive than the FuGENE reagent. The overall aim was to detect if the Cas9-HMGB1 fusion affected protein expression and in which direction. Figure 3.3b gives a clear picture of the Cas9 expression in Cas9wt and Cas9-HMGB1 plasmid. As demonstrated in Figure 3.3b, the fusion migrated shorter in the gel compared to Cas9wt due to its bigger size (approximately 800 base pairs longer than Cas9wt). The ladder is shown in Appendix I Western Blot Ladder.

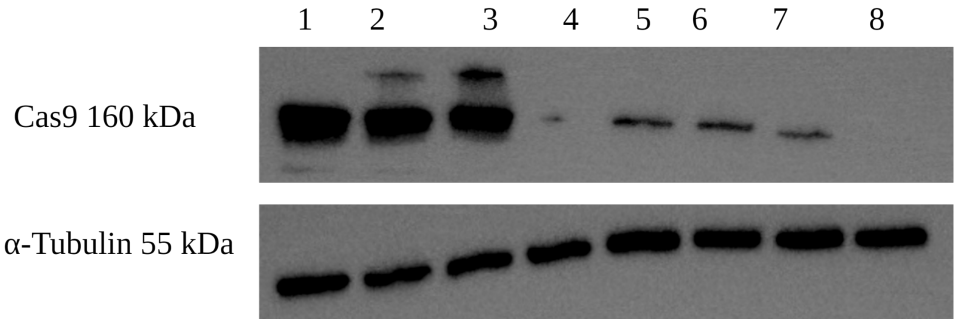

(a) Lipofectamine and FuGENE

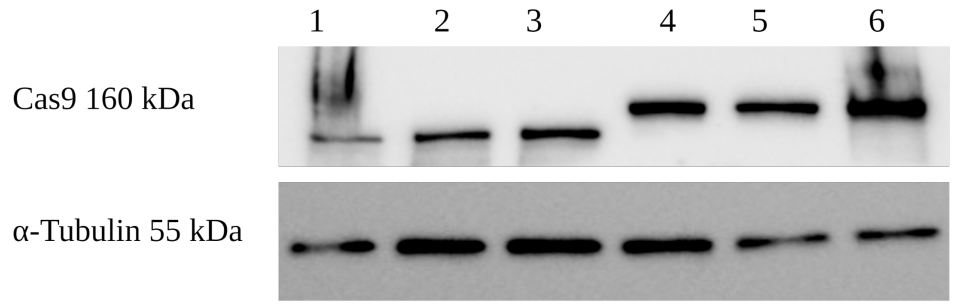

(b) Lipofectamine

Figure 3.3: **Protein expression of Cas9 and α-tubulin in HEK293T cells.**
The Bio-Rad machine was set at chemilimuniscence for pictures of protein expression and colorimetric for pictures of the Protein Dual color Standard ladder. **A)** Testing out Lipofectamine and FuGENE transfection to verify which method was best suited to detect protein expression of Cas9wt plasmid. Upper panel represents Cas9 (160 kDa). 1., 2., 3. Lipofectamine transfection, 4. Lipofectamine transfection Mock, 5., 6., 7. FuGENE transfection, and 8. FuGENE Mock. The faint band in lane 4 may be spillover in the Lipofectamine mock sample. Second panel represents the expression of α-tubulin (55 kDa) in the same order as for Cas9 expression. **B)** Lipofectamine transfection of Cas9 (160 kDa). 1., 2., 3. Cas9wt plasmid, 4., 5., 6. Cas9-HMGB1 plasmid. Second panel represents the expression of α-tubulin (55 kDa) with the same numbering as for Cas9.

Western blot was initially performed in fibroblasts and PBMCs (Figure 3.4a). A western blot was also performed in PBMCs to verify and compare Cas9 protein expression at different time-point (2, 4, 6, 8, and 24 hours post-electroporation) for Cas9wt mRNA and optimized Cas9wt mRNA. The first western blot experiment conducted with PBMCs and fibroblasts employing Cas9wt mRNA, did not show any Cas9 protein expression for either cell type (Figure 3.4a, upper panel). Surprisingly, the expression of the housekeeping gene α-tubulin was not detectable in PBMCs, but in fibroblasts (Figure 3.4a, lower panel).

To detect and compare Cas9 protein expression between Cas9wt mRNA and optimized Cas9wt mRNA, and to establish at what time point the Cas9 protein expression peaked, we ran a time-point experiment. Unfortunately, Cas9 protein expression was poor and not possible to distinguish (Figure 3.4b, upper panel), however, bands representing α-tubulin were robust (Figure 3.4b, lower panel).

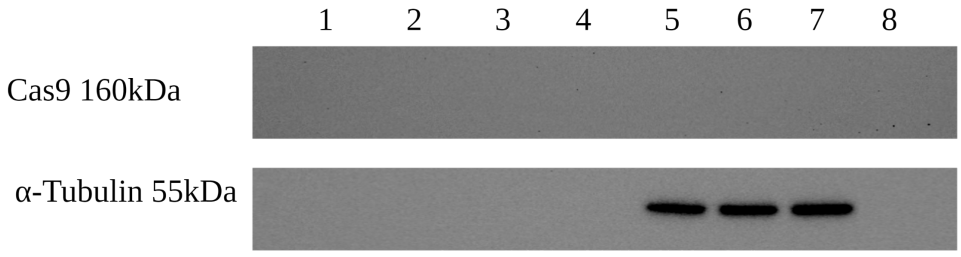

(a) PBMCs and fibroblasts

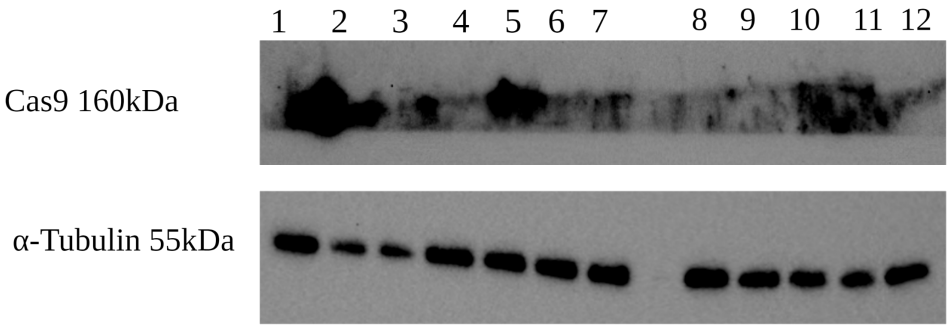

(b) PBMCs

Figure 3.4: **Protein expression of Cas9 and α-tubulin in PBMC and fibroblasts.** The Bio-Rad machine was set at chemilimuniscence for pictures of protein expression and colorimetric for pictures of the Protein Dual color Standard ladder. **A)** Western blot experiment with PBMCs and fibroblasts. Upper panel represents the expression of Cas9 (160 kDa) of PBMCs (band 1.4) and fibroblasts (band 5-8). The loading order was as follow: 1.,2.,3. PBMC replicates, 4. PBMC Mock, 5., 6., 7. fibroblasts replicates, and 8. fibroblasts Mock. Second panel represents α-tubulin (55 kDa) in the same order as for Cas9 expression of PBMCs and fibroblasts. Bands are observed for fibroblasts replicates, but not for PBMCs. **B)** Time-point collection of PBMCs. Upper panel represents the protein expression of Cas9 (160 kDa). Second panel represents the protein expression of α-tubulin (55 kDa). 1. Spike in Cas9 x100 diluted, 2. PBMC Mock, 3., 4., 5., 6., 7. Cas9wt mRNA collected 2, 4, 6, 8, and 24 hours post-electroporation, respectively, 8., 9., 10., 11., 12. optimized Cas9wt mRNA collected 2, 4, 6, 8, and 24 hours post-electroporation, respectively.

3.4 Electroporating RNPs and mRNA

Electroporation allows for controlled dosage and high-efficiency delivery of the Cas9wt mRNA. Extended training of electroporation with RNPs in PBMCs was necessary before moving on to electroporating mRNA (Figure 3.5a). To verify synthesized mRNA, we delivered Cas9 as mRNA to PBMCs by electroporation, and measured the viability and cell count throughout the whole experiment. RNPs of Cas9wt as protein were included as control, while the ssODN was excluded in one condition to verify whenever the single-stranded repair template had an effect on the editing outcome. In addition, Cas9wt mRNA and Cas9-HMGB1 mRNA were first delivered to fibroblasts, mainly because it is

easier to work with fibroblasts compared to PBMCs, but also to observe how the mRNA affected the editing in these primary cells (Figure 3.5b and Figure 3.5c).

The editing outcomes of RNPs were relatively low in the first training experiment in PBMCs (Figure 3.5a, dots). The events of NHEJ were slighter higher than for HDR. In the second electroporation experiment, the number of biological replicates were reduced to n=3 mainly to decrease the number of samples electroporated at the same time and thus increasing the chances to obtain higher editing (Figure 3.5a, triangles). Albeit the editing results increased for the second experiment, there were more spread between replicates (Figure 3.5c). The gating strategy for Mock and RNPs in fibroblasts are shown in Figure 3.6, while the remaining gating strategies are in Appendix G Gating Strategy for HDR and NHEJ.

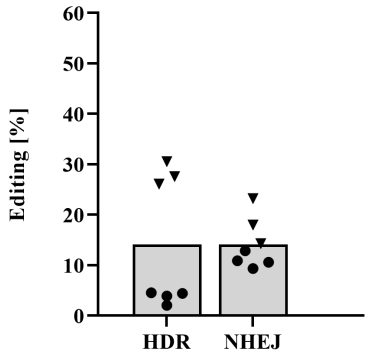

(a) RNPs (PBMCs)

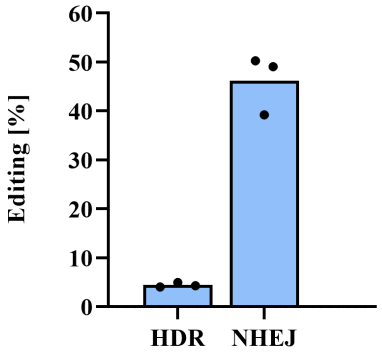

(b) Cas9wt mRNA (fibroblasts)

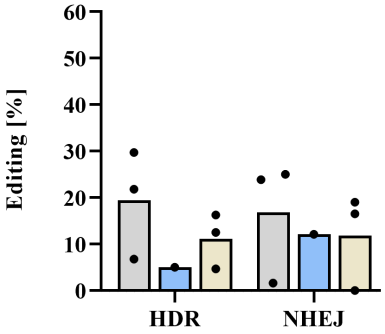

(c) Cas9wt and Cas9-HMGB1 mRNA (fibroblasts)

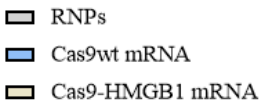

Figure 3.5: **Editing results of RNPs in PBMCs and of Cas9wt mRNA and Cas9-HMGB1 mRNA in fibroblasts.**
A) Editing results of RNPs in PBMCs when delivering Cas9 as protein. Dots represent biological replicates of donor M30 (n=4) and triangles represent biological replicates donor F26 (n=3). **B)** Editing results from first experiment working with mRNA in fibroblasts. Only one condition was included to limit the amount of replicates and to get hands-on experience working with mRNA. Dots represent biological replicates for one experiment (n=3). **C)** Editing results in fibroblasts when delivering Cas9wt as mRNA or fused to HMGB1. Dots represent biological replicates for one experiment (n=3).

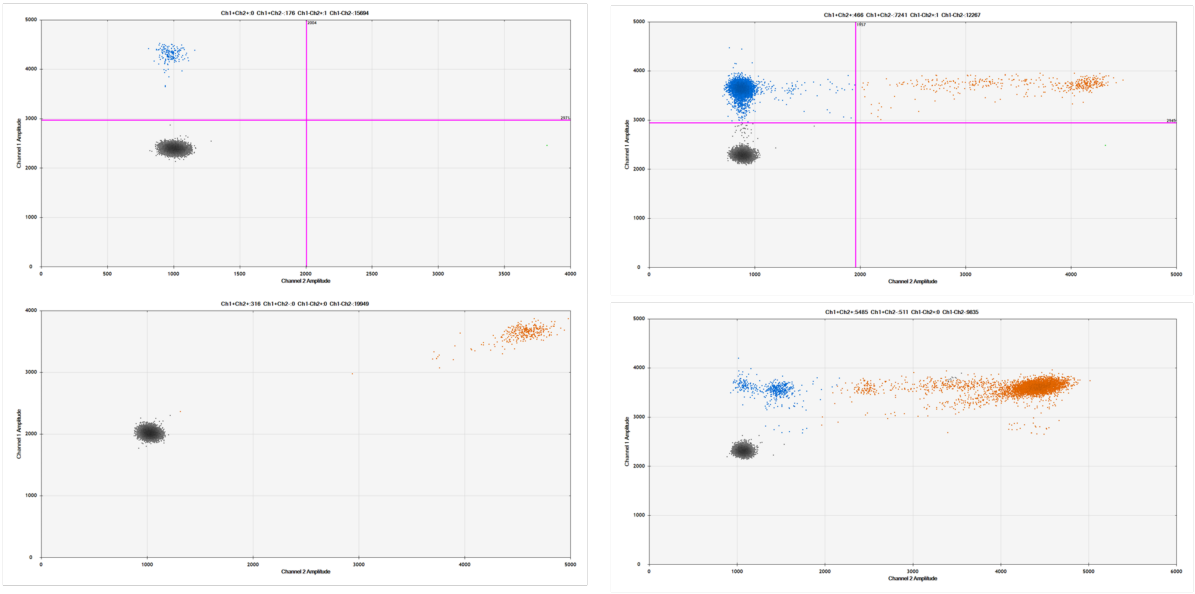

(a) Gating strategy of negative control

(b) Gating strategy of RNPs

Figure 3.6: **Gating strategy of Mock and RNPs of fibroblasts**
in a two-dimensional cluster for quantifying gene editing with ddPCR. The upper panel represents HDR, while lower panel represents NHEJ. Channel 1 Amplitude fluorescence (FAM probe) is plotted against Channel 2 Amplitude (HEX probe). Black dots represent droplets of DNA fragments without DNA of interest (no reference probe has bound). For HDR, the blue dots represent population that is HEX positive. The DNA marker probe has bound, but not the specific sequence from repair template. Hence, the repair template has not been incorporated into the genome and no HDR has occurred. For NHEJ, the orange dots represent population that is HEX positive. The DNA marker probe has bound, in addition to the NHEJ probe indicating that no indels was introduced into the sequence and no DNA sequence change has occurred.

The first electroporation experiment with Cas9wt mRNA in fibroblasts gave sufficient editing (Figure 3.5b) to proceed with electroporation of several conditions simultaneously. As a consequence, the spread in replicates increased and two replicates of Cas9wt mRNA were lost due to a systemic error (Figure 3.5c). Furthermore, as expected, lower editing is observed when using mRNA compared to RNPs.

Two independent experiments with various conditions of Cas9wt mRNA were performed. Time-controlled two-step transfection protocol might substantially improve the efficiency of installing silent mutations in primary T cells [76]. Thus, nonviral ssODN repair template was delivered 24 hours post-electroporation to enhance HDR gene editing.

The initial number of cells in each well were 2 millions. The viability and cell count of each conditions were measured 24 hours post-electroporation and on the day of collection (96 hours post-electroporation) (Figure 3.7, a-d). Two independent experiments were initiated using cells from the same donor (M41), where the dots represent the biological

mean of replicates (n=3) for each experiment. Comparing the replicates, the spread in viability and cell count between first and second experiment are most likely due to the improvement of the electroporation technique.

To easier observe the differences in number of cells before and after electroporation, a recovery ratio was calculated for each condition. A recovery rate < 1 demonstrates a decrease of number of cells compared to the initial number of cells. Contrarily, a recovery rate > 1 demonstrates an increase of number of cells compared to the initial number of cells. The variation in recovery ratio differed among conditions (Figure 3.7, e-f).

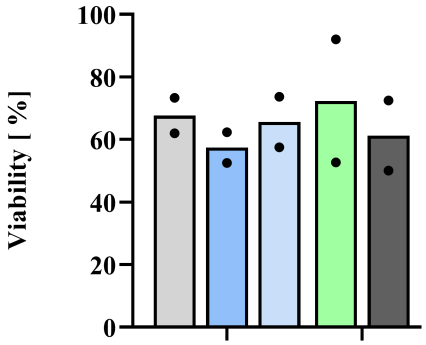

(a) Viability 24 hours post-electroporation

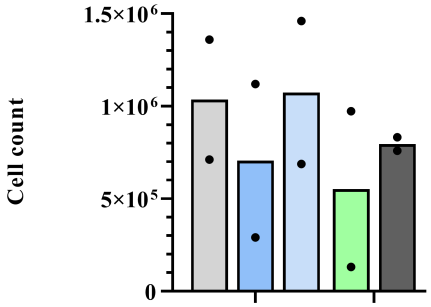

(b) Cell count 24 hours post-electroporation

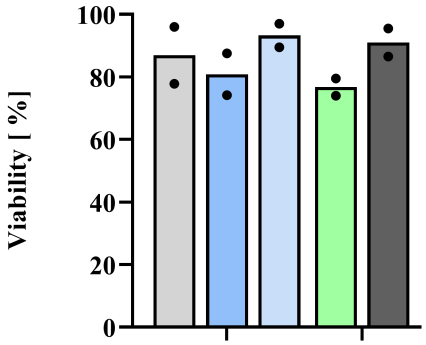

(c) Viability 96 hours post-electroporation

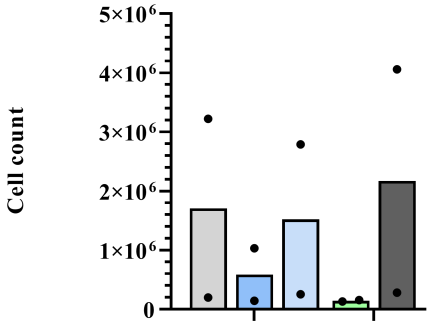

(d) Cell count 96 hours post-electroporation

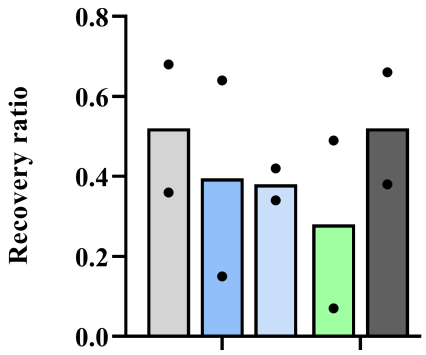

(e) Recovery rate 24 hours post-electroporation

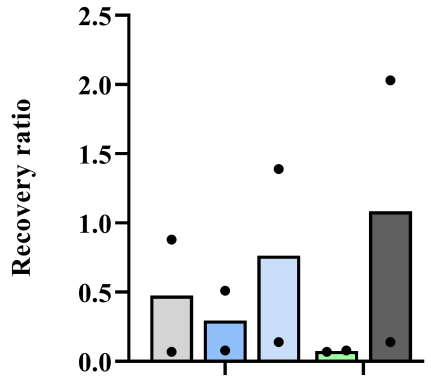

(f) Recovery rate 96 hours post-electroporation

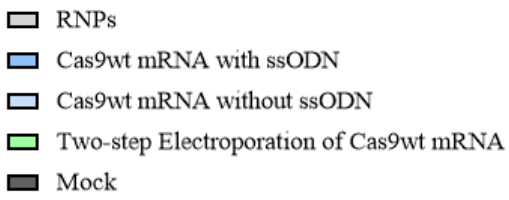

Figure 3.7: **Viability and cell count of Cas9wt mRNA with and without ssODN repair templates and Two-step Electroporation.**
The initial number of cells in each conditions were 2 millions. Dots represent the mean of biological replicates of donor M41 (n=3, two independent experiments).

Viability and cell count dropped right after electroporation mostly due to high level of cellular stress. Furthermore, measuring the viability and cell count the day of collection (96 hours post-electroporation), we observed that the condition without repair template and Mock had proliferated (Figure 3.7f), while the remaining conditions did not recover. Statistics were not performed on cell count values due to the significant variation between number of cells probably caused by systemic errors.

3.5 Time-controlled Electroporation with Cas9wt mRNA and Cas9-HMGB1 mRNA

The Two-step Electroporation experiment with Cas9wt mRNA and Cas9-HMGB1 mRNA was conducted twice in two different donors, F54 (squares) and D12 (triangles). The same measurements for viability and cell count were perform as previously shown, in addition to measuring the viability and cell count 24 hours post Two-step Electroporation (Figure 3.8, c-d). The viability and cell count decreased drastically after the second electroporation, however, the cells recovered to post-electroporated states at the day of collection (96 hours post first electroporation).

The recovery rate 24 hours post Two-step Electroporation was < 0.2 which indicated a significant loss of cells (Figure 3.9b), suggesting that electroporation might trigger numerous pathways of cell signalling, including stress or cell death pathways. For Mock and RNPs, the cells had proliferated significantly 96 hours post-electroporation (Figure 3.9c).

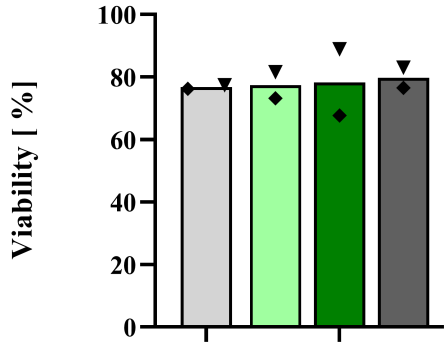

(a) Viability 24 hours post-electroporation

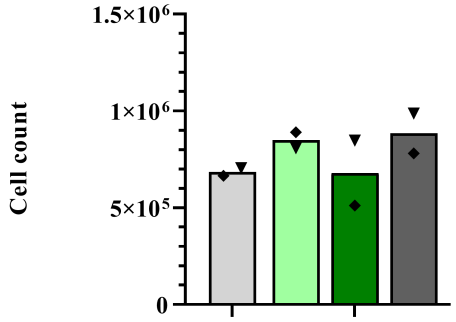

(b) Cell count 24 hours post-electroporation

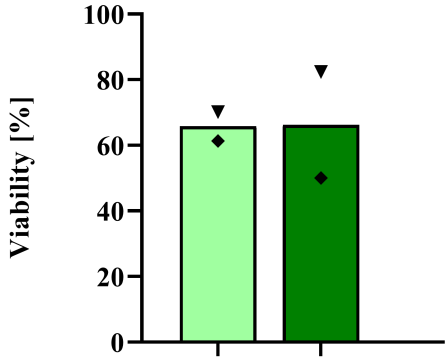

(c) Viability 24 hours post Two-step Electroporation

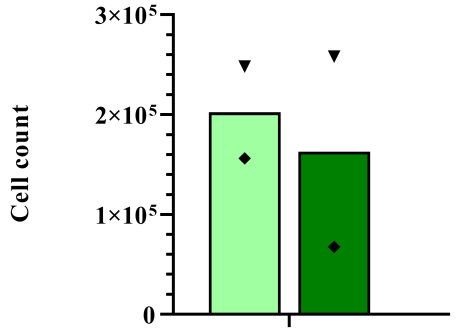

(d) Cell count 24 hours post Two-step Electroporation

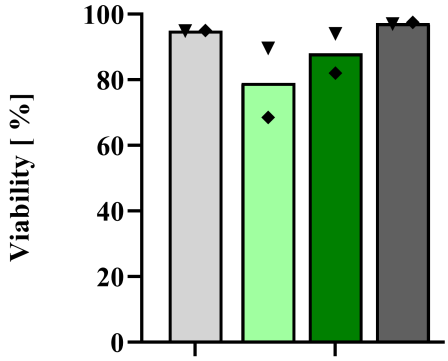

(e) Viability 96 hours post-electroporation

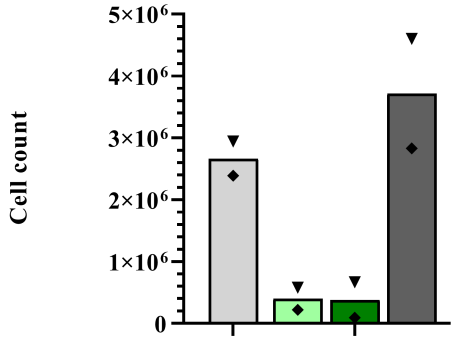

(f) Cell count 96 hours post-electroporation

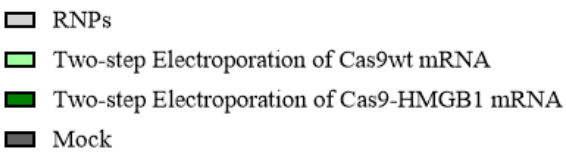

Figure 3.8: **Viability and cell count of Two-step Electroporation of Cas9wt and Cas9-HMGB1 mRNA.**
The initial number of cells in each conditions were 2 millions. Triangles represent the mean of biological replicates of donor D12 (n=3) and squares represent the mean of biological replicates of donor F54 (n=3).

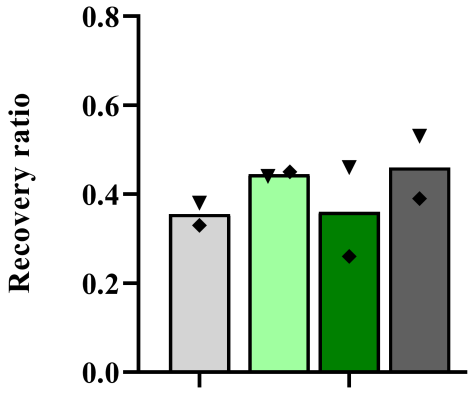

(a) 24 hours post-electroporation

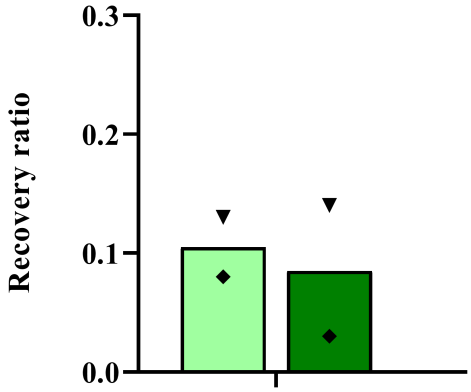

(b) 24 hours post Two-step Electroporation

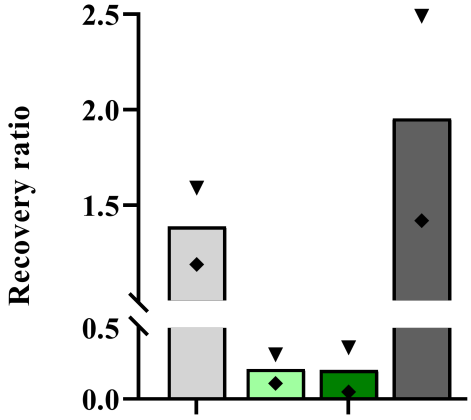

(c) 96 hours post-electroporation

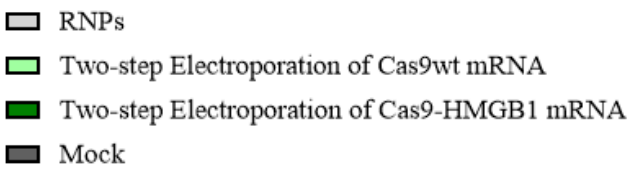

Figure 3.9: **The recovery ratio of Two-step Electroporation.**
The initial number of cells in each conditions were 2 millions. Triangles represent the mean of biological replicates of donor D12 (n=3) and squares represent the mean of biological replicates of donor F54 (n=3).

3.6 Adding Urea to the mRNA Synthesis Procedure and Electroporation of Optimized Cas9wt mRNA

Immunostimulatory double-stranded RNA is created during *in vitro* transcription affecting the protein expression and the potency and safety particularly in therapeutic applications. Due to its similar sizes and intrinsic characteristics it is challenging to reduce the undesired byproducts from the desired mRNA. Common methods for double-stranded RNA removal rely heavily on complex purification processes such as reverse-phase high-pressure liquid chromatography (RP-HPLC) [83]. Nevertheless, this method is time-consuming often resulting in increased RNA degradation, decreased quality and/or decreased yield. Thus, it would be ideal to eliminate the double-stranded RNA removal purification steps. By including selected chaotropic agents during *in vitro* transcription, a mild denaturing environment is created. This prevents the undesired intermolecular or intramolecular base-pairing that is thought to promote RNA-templated double-stranded RNA formation by RNA polymerase [62]. We added 8M urea to the *in vitro* protocol and purified the obtained RNA further following the MEGAclear™ Transcription Clean-Up Kit. To verify the affect of urea and the purification kit, three conditions were tested out: one condition with urea, one condition with extended purification with the MegaClear Kit, and the final condition including both urea and the purification kit. There was a significant difference in viability 24 hours post-electroporation between RNPs and Cas9wt with urea, and Cas9wt with urea and the remaining conditions (Figure 3.10a). In terms of viability, conditions with extendend purification and conditions with urea and extendend purification performed better than the condition with urea. Analyzing the recovery rate, the cells never recovered back to post-electroporated shape, which might indicate that the cells were not able to repair the membrane damage caused by electroporation.

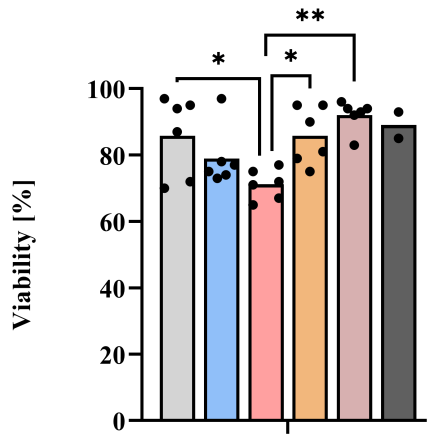

(a) Viability 24 hours post-electroporation

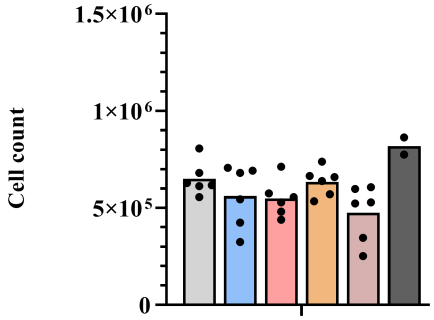

(b) Cell count 24 hours post-electroporation

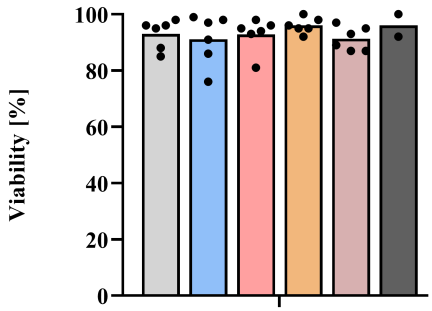

(c) Viability 96 hours post-electroporation

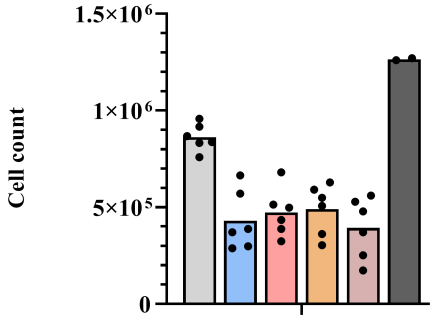

(d) Cell count 96 hours post-electroporation

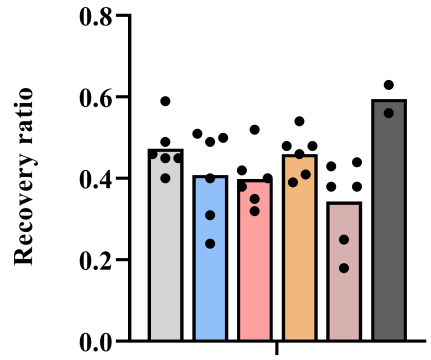

(e) Recovery rate 24 hours post-electroporation

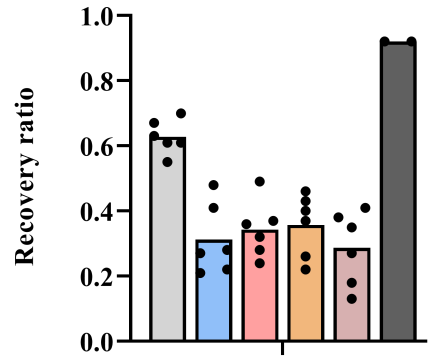

(f) Recovery rate 96 hours post-electroporation

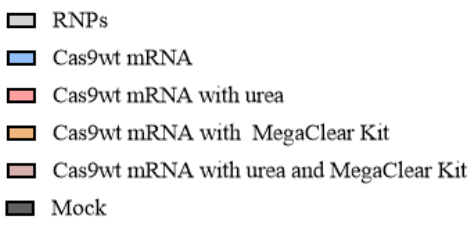

Figure 3.10: **Viability, cell count, and recovery rate of Cas9wt mRNA with urea and MegaClear Kit.**
The initial number of cells in each conditions were 1 millions. Dots represent biological replicates of donor F40 (n=3). $^{**}P < 0.01$, $^{*}P < 0.05$, one-way ANOVA.

3.7 Adding RNase Inhibitors to Cas9wt mRNA Prior to Electroporation

RNases have the ability to enter cells by endocytosis subsequently causing complete degradation of intracellular RNA [84]. Several studies have been conducted to identify the intracellular activity of RNases and how these enzymes act as a barrier to efficient expression of exogenous mRNA in for instance nonhuman primate models of HSPCs [59] and in mRNA encoded genome editing tools in primary human monocytes [60]. Hence, we hypothesized that employing RNase Out or RNase Inhibitor in the electroporation reaction allowed for a higher mRNA expression and enhanced mRNA-based genome engineering in PBMCs. The viability and cell count was measured as described in previous sections (Figure 3.11, a-d), in addition to the recovery ratio (Figure 3.11, e-f).

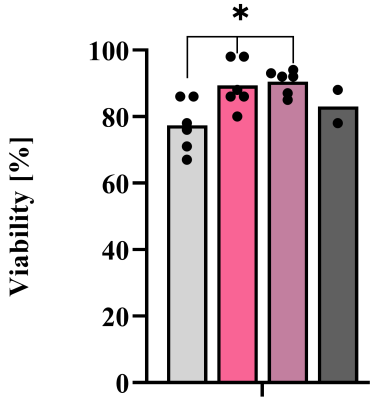

(a) Viability 24 hours post-electroporation

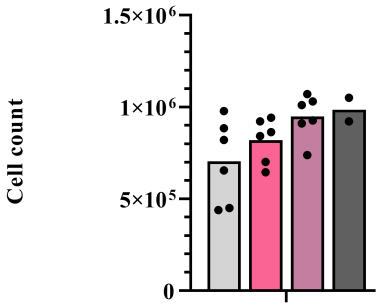

(b) Cell count 24 hours post-electroporation

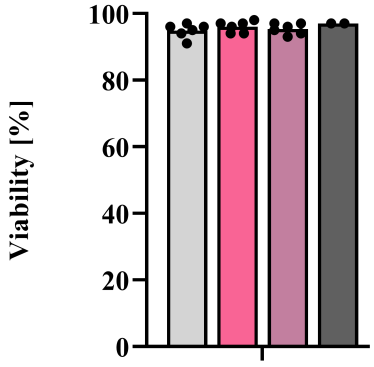

(c) Viability 96 hours post-electroporation

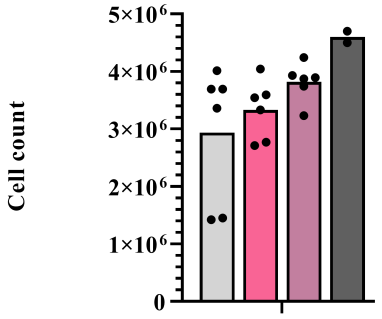

(d) Cell count 96 hours post-electroporation

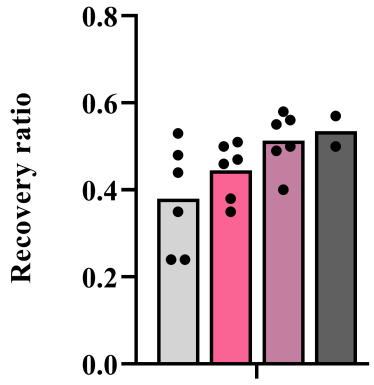

(e) Recovery rate 24 hours post-electroporation

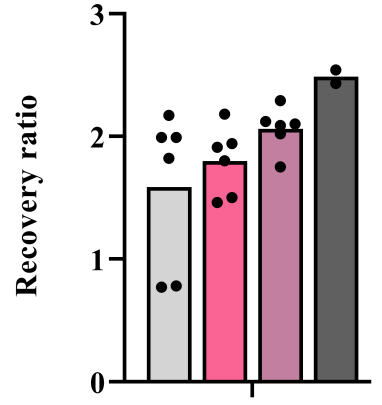

(f) Recovery rate 96 hours post-electroporation

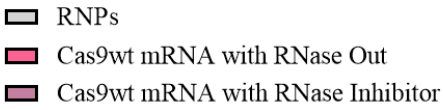

Figure 3.11: **Viability, cell count, and recovery rate of Cas9wt mRNA with RNAse Out and RNAse Inhibitor.**
The initial number of cells in each conditions were 1 millions. Dots represent biological replicates for donor D12 (n=3). $^*P < 0.05$, one-way ANOVA.

The recovery ratio clearly demonstrated that viability and cell count dropped right after electroporation (24 hours post-electroporation) (Figure 3.12d. Furthermore, measuring viability and cell count the day of collection (96 hours post-electroporation), we observed that the majority of replicates had proliferated significantly (Figure 3.11f). The conditions with RNase Inhibitor seemed to preform slightly better than RNase Out in terms of cell count and recovery rate.

3.8 Gene Editing of Human PBMCs

Presenting the editing results of PBMCs in one graph clearly points out the editing outcomes in RNPs varies between donors (Figure 3.12). There were significant differences between RNPs and remaining conditions for all editing results, except for NHEJ in Cas9wt mRNA with and without repair template (Figure 3.12a). Analyzing and comparing gene editing outcomes across conditions, the conditions with RNase Inhibitor performed the highest in terms of editing efficiency. The editing outcomes of RNPs for this condition were $\sim 55\%$, moreover, the recovery rate was close to 2.0 at the day of collection (Figure 3.11f). This might indicate that donor D12 contained higher levels of available T cells compared to remaining donors. The NHEJ of Cas9wt conditions (Figure 3.12a) was relatively high, and to some extent close to or higher than the control RNPs, while HDR was $< 3\%$ for conditions except control RNPs. The Two-step Electroporation conditions of Cas9wt mRNA and Cas9-HMGB1 mRNA were $< 3\%$ for NHEJ and $< 1\%$ for HDR (Figure 3.12b). Comparing the editing outcomes between Figure 3.12a and Figure 3.12b, the latter experiment was conducted in two different donors (D12 and F54), while the first experiment was conducted with the same donor (M41) in two independent experiment. For the optimized mRNA with inclusion of urea and extended purification, NHEJ and HDR were $< 3\%$ as well. The gating strategy for Mock and RNPs are shown in Figure 3.13, while the remaining gating strategies are in Appendix G Gating Strategy for HDR and NHEJ. Nevertheless, our results demonstrated no significant improvement in HDR for none of the conditions tested.

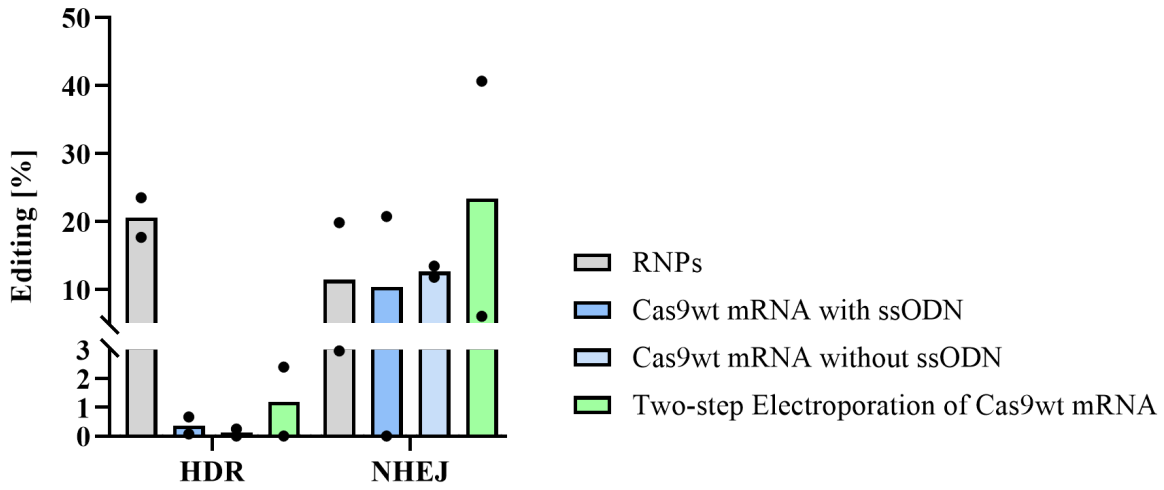

(a) Various conditions of Cas9wt mRNA

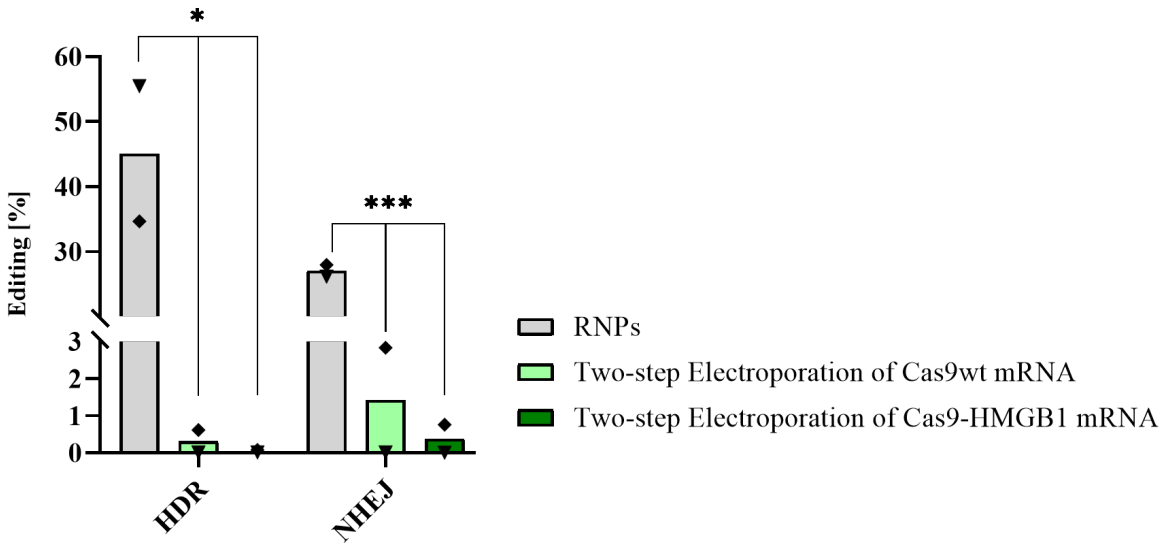

(b) Two-step Electroporation of Cas9wt mRNA and Cas9-HMGB1 mRNA)

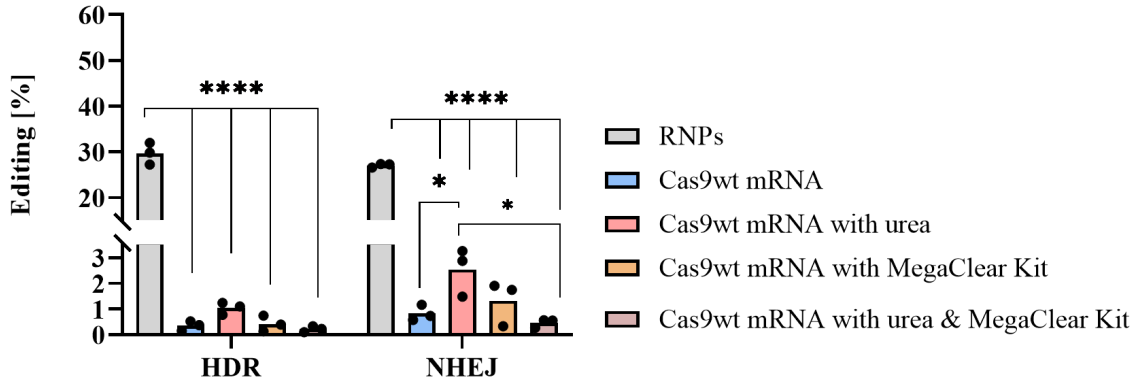

(c) Optimized Cas9wt mRNA

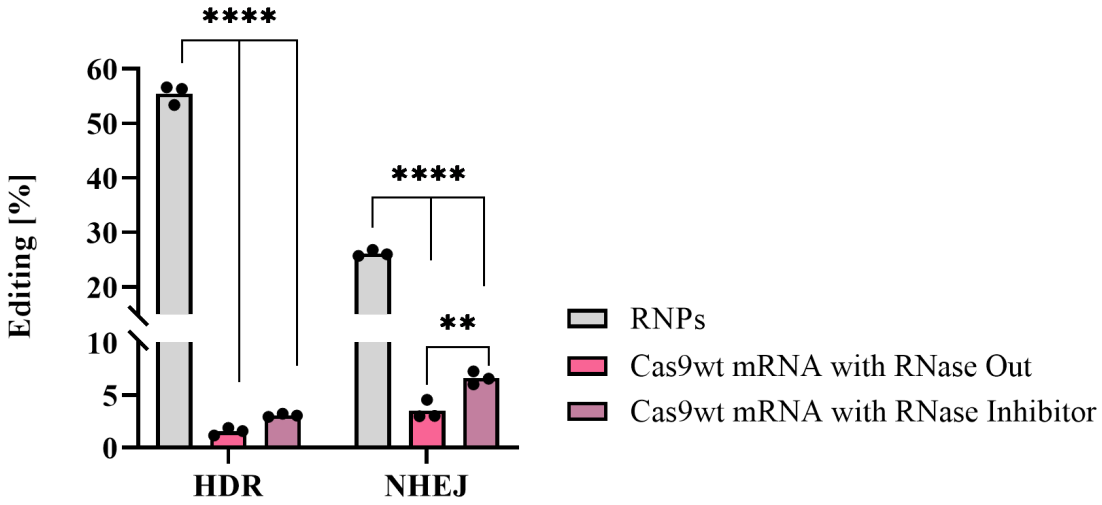

(d) RNase inhibitors in Cas9wt mRNA

Figure 3.12: **Gene editing in human PBMCs.**
A) Gene editing in conditions with and without repair template and time-point delivery of repair template. Dots represent the mean of biological replicates of donor M41 (n=3) in two independent experiments. $^{*}P < 0.05$, two-way ANOVA, calculated on triplicates. **B)** Gene editing of Two-step Electroporation in Cas9wt and Cas9-HMGB1 mRNA. Triangles represent the mean of biological replicates of donor D12 (n=3), and squares represent the mean of biological replicates of donor F54 (n=3).$^{****}P < 0.0001$, two-way ANOVA, calculated on triplicates. **C)** Optimizing Cas9wt mRNA by adding urea to the mRNA synthesis procedure and additional cleaning of RNA. Dots represent biological replicates of donor F40 (n=3).$^{****}P < 0.0001$, $^{*}P < 0.05$, one-way ANOVA. **D)** Gene editing adding RNase inhibitors prior to electroporation of Cas9wt mRNA. Dots represent biological replicates of donor D12 (n=3).$^{****}P < 0.0001$, $^{**}P < 0.01$, one-way ANOVA.

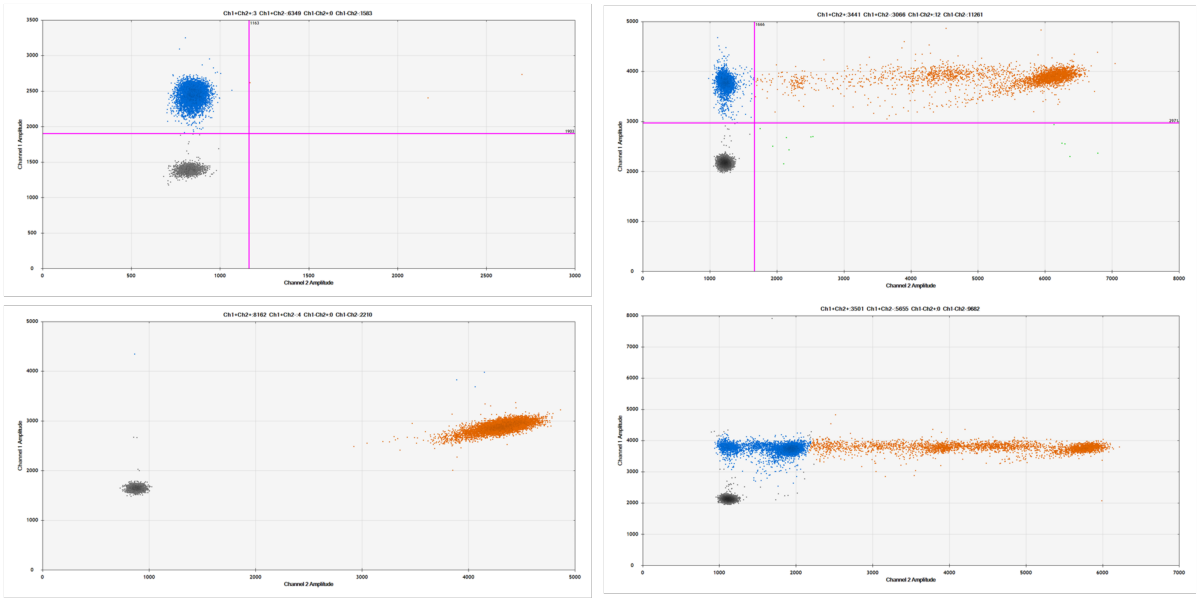

(a) Gating strategy of negative control

(b) Gating strategy of RNPs

Figure 3.13: **Gating strategy of Mock and RNPs in PBMCs**
in a two-dimensional cluster for quantifying gene editing with ddPCR. The upper panel represents HDR, while lower panel represents NHEJ. Channel 1 Amplitude fluorescence (FAM probe) is plotted against Channel 2 Amplitude (HEX probe). Black dots represent droplets of DNA fragments without DNA of interest (no reference probe has bound). For HDR, the blue dots represent population that is HEX positive. The DNA marker probe has bound, but not the specific sequence from repair template. Hence, the repair template has not been incorporated into the genome and no HDR has occurred. For NHEJ, the orange dots represent population that is HEX positive. The DNA marker probe has bound, in addition to the NHEJ probe indicating that no indels was introduced into the sequence and no DNA sequence change has occurred.

4 Discussion

The three main research questions in present thesis were: (i) is it possible to enhance HDR gene editing in human PBMCs by delivering the single-stranded repair template at a later time-point to the sgRNA:Cas9 mRNA mix, where Cas9 is also coupled to a chromatin modulating fusion, (ii) can the production of mRNA be optimized by including a chaotropic agent to the mRNA synthesis and by extended purification of the RNA, and (iii) would implementation of RNase inhibitors to the sgRNA:mRNA mix prior to electroporation result in higher HDR editing. In the following discussion the focus will be mainly on the electroporation results, however, as the detection of Cas9 protein expression in PBMCs was poor, potential causes leading to this will be presented as well.

4.1 Detection of Cas9 Expression by Western Blot

As the primary antibody binds to the protein band immobilized on the membrane, it is important to block the nonspecific sites present on the membrane that do not have any protein attached but can still bind the primary antibody. An inefficient blocking may therefore give rise to the detection of several bands as observed in Figure 3.3a, upper panel. Another factor leading to multiple bands could be overloading of the gel, promoting a non-specific binding to proteins of excessive abundance resulting in "ghost bands". The protein expression of Cas9wt in PBMCs shows poor/smeared bands (Figure 3.4b, upper panel). A smeared band might be caused by non-specific binding of the antibody or a low signal-to-noise caused by weak detection. Other factors could be insufficient contact between the membrane and the gel, the presence of air bubbles, or excess buffer remained between the blot and gel.

For the first western blot experiment with PBMCs and fibroblasts there were no bands present on the membrane for protein expression of Cas9 and α-tubulin for PBMCs (Figure 3.4a). One reason might be that during the electroporation process, Cas9wt mRNA was not pipetted directly into the mix, but on the side of the wells. We assumed that this lead to loss or degradation of mRNA even before electroporation. For the second western blot experiment with time-point collection of PBMCs, poor bands were observed for Cas9 (Figure 3.4b, upper panel). Potential causes for this could have been insufficient contact between the membrane and the gel, the presence of air bubbles, or excess buffer

remained between the blot and the gel might have influenced the result. The gel had to be re-adjusted which might have had a negative outcome on the blot transfer. Another reason for the uneven signal across the blot might be that the membrane allowed to dry during handling.

In conclusion, the results demonstrated that several steps during the western blot procedure impact the blot signal detection, and working with PBMCs is in overall challenging to obtain protein expression. Other methods that could have been performed to detect mRNA expression are enzyme-linked immunosorbent assay (ELISA) or flow cytometry as both methods hold the potential to detect specific protein in a complex mixture.

4.2 Precise Gene Editing with Cas9wt and Cas9-HMGB1 mRNA in Human PBMCs is Challenging

mRNA-based therapeutics are expected to become a powerful therapy for a variety of diseases. Even though the benefits of gene editing utilizing programmable nucleases are promising, several technical challenges remain to be solved prior to translating theory into practice. The ease of producing a less immunologically triggering mRNA is one approach to improve the accuracy and efficacy in gene editing.

4.2.1 Tackling Electroporation of Human PBMCs

Our results revealed that precise gene editing did not improve significantly across the different conditions tested in human PBMCs. Delivering Cas9 as protein or mRNA resulted in various editing in terms of HDR and NHEJ outcomes. First of all, analyzing the first editing results in PBMCs (Figure 3.5) with the latest PBMC experiment initiated (Figure 3.12), the editing of RNPs increased from less than 10% to up to 55% HDR. Even though there was no significant difference between donors, the increase in editing outcome of RNP controls gives an estimate of how important it is to master the electroporation technique to obtain high levels of precise gene editing. On the other hand, comparing fibroblasts and PBMCs, our results demonstrated a higher NHEJ in Cas9wt mRNA (Figure 3.5b), indicating that cell lines are more susceptible to electroporation compared to primary cells. One possibility might be the fact that PBMCs are immune cells and

are able to sense more foreign nucleic acids than fibroblasts. In other words, working with PBMCs requires more competence and laboratory skills to obtain the same editing results as for fibroblasts.

As we proceeded with the electroporation experiments, it became clear that including fewer conditions led to higher editing and less spread between replicates. At least in the beginning of the thesis work when the confidence and required laboratory skills were lacking. Thus, electroporating mRNA for the first time, one fibroblast condition was electroporated (Figure 3.5b). For the second electroporation experiment working with mRNA, RNPs were included as control, in addition to Cas9-HMGB1 mRNA (Figure 3.5c). The spread between replicates was much higher compared to electroporating one condition. Nevertheless, we concluded that the editing was sufficient to proceed with electroporating PBMCs. On the contrary, due to an error when transferring the cells to the electroporation strip, all of the Cas9wt replicates were lost. The remaining cells ($<$ 0.95 x 10^6) were prepared and electroporated immediately after the first electroporation. Therefore, only one replicate was collected for gDNA extraction (Figure 3.5c.)

4.2.2 Time-controlled Electroporation and Optimization of the *in vitro* Transcription Protocol Require Further Testing

Our Two-step Electroporation conditions did not perform as expected. Based on published literature, we hypothesized that adding the repair template 24 hours post-electroporation would substantially improve the efficiency of installing silent mutations in human PBMCs [76]. In our case, we electroporated 2 million cells instead of 1 million cells recommended by Yang et al. [76], as this has been tested out previously in Haapaniemi lab. Yang et al. performed nonviral transgene integration in primary T cells by TALEN-mediated gene editing. They showed that the maximum knock-in frequency occurred 16 hours post-TALEN electroporation with a mean of 40%, as for our case, HDR editing was close to 0% for the majority of conditions.

However, NHEJ of Two-step Electroporation of Cas9wt mRNA obtained the highest editing with $< 2\%$[1] (Figure 3.12b). In addition, we delivered the single-stranded repair template 24 hours post first electroporation due to the ease of experimental setup. Optimization of the second transfection timing is therefore required. Considerations regarding the kinetics of the nuclease expression and double-stranded break creation, in addition to the format of the delivered nucleases, must be taken into account. For instance, delivering Cas9 as protein, which do not require the nuclease expression step, the creation of double-stranded breaks would most likely occur faster, thus, a shorter delay of the second transfection is probably needed.

We also hypothesized that optimizing the *in vitro* protocol by adding a chaotropic agent during mRNA synthesis would decrease the formation of double-stranded RNA [62], thus preventing possible interactions with immune sensors. Even though Piao et al.[62] provided a straight-forward and cost-effective approach for producing mRNA with reduced formation of double-stranded RNA, they did not test their mRNA in primary cells. Here, we demonstrate that *in vitro* transcribed mRNA containing urea does not improve editing in primary cells. Another consideration to take into account is the stability of the obtained mRNA. The bands on the mRNA gel were clear, but to some extent degraded (Figure 3.2b). Improvements when it comes to proper RNase free technique is necessary, and in our case, challenges still remain to obtain an mRNA that does not show any signs of degradation. In conclusion, adding urea to Cas9wt mRNA increased NHEJ to $\sim 3\%$ compared to 1% in normal Cas9wt mRNA, but HDR remained $< 1\%$. Nevertheless, the experiment was conducted once in one donor, and further testing should be conducted to support these results. As we did not obtain any Cas9 protein expression in PBMCs by western blot, the affect of urea in primary cells should be investigated with for instance ELISA or flow cytometry.

For the extended purification step, stock samples of Cas9wt mRNA with and without urea were aliquoted before proceeding with the purification kit. Since one band was observed for the Cas9wt sample, but not for the purified Cas9wt sample (Figure 3.2b,

[1]Comparing NHEJ outcomes in donor M41 (Figure 3.12a) with donor D12 and F54 (Figure 3.12b) of Two-step Electroporation of Cas9wt mRNA, the high editing in donor M41 ($\sim 40\%$) might indicate that this donor could be one of the better. Nevertheless, as the data presented in Figure 3.12a was conducted as one of the first electroporation experiment working with mRNA, several technical problems arose. We therefore conclude that the editing outcomes for this experiment should be questioned.

lane 6), we assumed that the mRNA had been lost or degraded during the purification procedure. Therefore, extended purified Cas9wt was also included in the second *in vitro* transcription experiment together with the Cas9-HMGB1. Furthermore, we observed low concentration of cut plasmid when using the FastAP buffer, thus, another restriction-digestion buffer was tested (Figure 3.2a, lane 5-10). Comparing the concentration of mRNA before and after extended purification of Cas9-HMGB1 with the same condition of Cas9wt, there is almost no decrease in concentration in Cas9-HMGB1 mRNA (3362 ng/μL to 3328 ng/μL) compared to Cas9wt mRNA (3301 ng/μL to 779 ng/μL). This supports the importance of hands-on experience and repeating the technique to improve the outcomes.

Extended purification of RNA with MegaClear Kit did not affect the 260/280 and the 260/230 ratio significantly. The RNA concentration decreased instead as more steps were added to the *in vitro* transcription protocol (Appendix D mRNA Concentration and Purity). As the 260/280 ratio was lower than 2.0 for all samples, there might still be proteins and leftovers from the kit present in the samples. Based on these numbers, consideration whether it is necessary to perform extended purification must be taken into account since the kit adds another 1-1.5 hours to the *in vitro* transcription protocol. Moreover, the editing outcomes were almost the same as in the Cas9wt mRNA sample ($< 2\%$ versus $\sim 1\%$, respectively)(Figure 3.12c).

4.2.3 Including RNase Inhibitors Performed Best Among Conditions Tested

As the time-controlled electroporation experiment did not increase HDR editing, nor the inclusion of urea to the *in vitro* transcription protocol, we implemented RNase inhibitors post-electroporation [60] to minimize the degradation of RNA. Our results revealed that adding RNase inhibitors might have a positive impact when it comes to precise gene editing compared to the other conditions tested in current thesis. Laoharawee et al. [60] electroporated primary human monocytes using mRNA-based engineering reagents. They demonstrated that the optimal dilutions of RNase inhibitor was 1:50, therefore we utilized 40 units in our samples. The RNase Inhibitor conditions resulted in a slightly higher editing than RNase Out (5% NHEJ versus 4% NHEJ)(Figure 3.12d). Nevertheless, this experiment was conducted once in one donor and should therefore be tested in several donors, in addition to verify the optimal mRNA:RNase inhibitor ratio in PBMCs.

5 Conclusion

The purpose of current thesis was to enhance HDR editing by time-point delivery of single-stranded repair template to the previously electroporated sgRNA-mRNA PBMCs. Moreover, the *in vitro* transcription protocol was optimized to produce a more stable mRNA, and the implementation of RNase inhibitors prior to electroporation of mRNA was tested.

We demonstrated the challenges of precise gene editing of human PBMCs as our proposed strategies did not improve HDR editing significantly. First and foremost, the produced mRNA was to a certain degree degraded, hence, obtaining an mRNA with no signs of degradation should be pursued. Second, the concentration of RNase inhibitors included should be further optimized. And third, a better understanding of how PBMCs respond to mRNA transfection and how to stimulate primary cells in terms of precise gene editing is needed for further advances using Cas9 mRNA delivery methods. PBMCs are difficult to work with and to manipulate, and the methodology used in the thesis was challenging to master in a short time-frame of thesis work.

In general, even though CRISPR-Cas is a promising gene editing tool, the bottlenecks supported by our data include, but are not limited to, the use of the cellular DNA repair machinery to create a precise double-strand break in the genome, proper expression of the nuclease within the target cell, and enhancing editing efficiency. Lastly, the challenge in regulating the activation of the immune system *in vivo* upon mRNA delivery requires clarification. Nevertheless, the development of mRNA as a delivery method has accelerated greatly and has the potential to provide solutions for prevention and treatment of currently incurable diseases in the next decades.

References

[1] H. Li, Y. Yang, W. Hong, M. Huang, M. Wu, and X. Zhao, "Applications of genome editing technology in the targeted therapy of human diseases: mechanisms, advances and prospects," *Signal transduction and targeted therapy*, vol. 5, no. 1, p. 1, 2020.

[2] H. A. Rees and D. R. Liu, "Base editing: precision chemistry on the genome and transcriptome of living cells," *Nature reviews genetics*, vol. 19, no. 12, pp. 770–788, 2018.

[3] Y.-G. Kim, J. Cha, and S. Chandrasegaran, "Hybrid restriction enzymes: zinc finger fusions to fok i cleavage domain.," *Proceedings of the National Academy of Sciences*, vol. 93, no. 3, pp. 1156–1160, 1996.

[4] M. J. Moscou and A. J. Bogdanove, "A simple cipher governs dna recognition by tal effectors," *Science*, vol. 326, no. 5959, pp. 1501–1501, 2009.

[5] M. Jinek, K. Chylinski, I. Fonfara, M. Hauer, J. A. Doudna, and E. Charpentier, "A programmable dual-rna–guided dna endonuclease in adaptive bacterial immunity," *science*, vol. 337, no. 6096, pp. 816–821, 2012.

[6] M. Bibikova, D. Carroll, D. J. Segal, J. K. Trautman, J. Smith, Y.-G. Kim, and S. Chandrasegaran, "Stimulation of homologous recombination through targeted cleavage by chimeric nucleases," *Molecular and cellular biology*, vol. 21, no. 1, pp. 289–297, 2001.

[7] J. Boch, H. Scholze, S. Schornack, A. Landgraf, S. Hahn, S. Kay, T. Lahaye, A. Nickstadt, and U. Bonas, "Breaking the code of dna binding specificity of tal-type iii effectors," *Science*, vol. 326, no. 5959, pp. 1509–1512, 2009.

[8] M. Christian, T. Cermak, E. L. Doyle, C. Schmidt, F. Zhang, A. Hummel, A. J. Bogdanove, and D. F. Voytas, "Targeting dna double-strand breaks with tal effector nucleases," *Genetics*, vol. 186, no. 2, pp. 757–761, 2010.

[9] G. Gasiunas, R. Barrangou, P. Horvath, and V. Siksnys, "Cas9–crrna ribonucleoprotein complex mediates specific dna cleavage for adaptive immunity in bacteria," *Proceedings of the National Academy of Sciences*, vol. 109, no. 39, pp. E2579–E2586, 2012.

[10] D. B. Roth and J. H. Wilson, "Relative rates of homologous and nonhomologous

recombination in transfected dna.," *Proceedings of the National Academy of Sciences*, vol. 82, no. 10, pp. 3355–3359, 1985.

[11] D. B. Roth, T. Porter, and J. Wilson, "Mechanisms of nonhomologous recombination in mammalian cells," *Molecular and cellular biology*, vol. 5, no. 10, pp. 2599–2607, 1985.

[12] F. Liang, M. Han, P. J. Romanienko, and M. Jasin, "Homology-directed repair is a major double-strand break repair pathway in mammalian cells," *Proceedings of the National Academy of Sciences*, vol. 95, no. 9, pp. 5172–5177, 1998.

[13] M. Sachdeva, B. W. Busser, S. Temburni, B. Jahangiri, A.-S. Gautron, A. Maréchal, A. Juillerat, A. Williams, S. Depil, P. Duchateau, *et al.*, "Repurposing endogenous immune pathways to tailor and control chimeric antigen receptor t cell functionality," *Nature communications*, vol. 10, no. 1, p. 5100, 2019.

[14] E. Senís, C. Fatouros, S. Große, E. Wiedtke, D. Niopek, A.-K. Mueller, K. Börner, and D. Grimm, "Crispr/cas9-mediated genome engineering: an adeno-associated viral (aav) vector toolbox," *Biotechnology journal*, vol. 9, no. 11, pp. 1402–1412, 2014.

[15] H. Yin, R. L. Kanasty, A. A. Eltoukhy, A. J. Vegas, J. R. Dorkin, and D. G. Anderson, "Non-viral vectors for gene-based therapy," *Nature Reviews Genetics*, vol. 15, no. 8, pp. 541–555, 2014.

[16] T. L. Roth, C. Puig-Saus, R. Yu, E. Shifrut, J. Carnevale, P. J. Li, J. Hiatt, J. Saco, P. Krystofinski, H. Li, *et al.*, "Reprogramming human t cell function and specificity with non-viral genome targeting," *Nature*, vol. 559, no. 7714, pp. 405–409, 2018.

[17] V. Hornung and E. Latz, "Intracellular dna recognition," *Nature Reviews Immunology*, vol. 10, no. 2, pp. 123–130, 2010.

[18] J.-B. Renaud, C. Boix, M. Charpentier, A. De Cian, J. Cochennec, E. Duvernois-Berthet, L. Perrouault, L. Tesson, J. Edouard, R. Thinard, *et al.*, "Improved genome editing efficiency and flexibility using modified oligonucleotides with talen and crispr-cas9 nucleases," *Cell reports*, vol. 14, no. 9, pp. 2263–2272, 2016.

[19] S. Iyer, A. Mir, J. Vega-Badillo, B. P. Roscoe, R. Ibraheim, L. J. Zhu, J. Lee, P. Liu, K. Luk, E. Mintzer, *et al.*, "Efficient homology-directed repair with circular single-stranded dna donors," *The CRISPR Journal*, vol. 5, no. 5, pp. 685–701, 2022.

[20] B. R. Shy, M. S. MacDougall, R. Clarke, and B. J. Merrill, "Co-incident insertion

enables high efficiency genome engineering in mouse embryonic stem cells," *Nucleic acids research*, vol. 44, no. 16, pp. 7997–8010, 2016.

[21] S. Lin, B. T. Staahl, R. K. Alla, and J. A. Doudna, "Enhanced homology-directed human genome engineering by controlled timing of crispr/cas9 delivery," *elife*, vol. 3, p. e04766, 2014.

[22] X. Ding, T. Seebeck, Y. Feng, Y. Jiang, G. D. Davis, and F. Chen, "Improving crispr-cas9 genome editing efficiency by fusion with chromatin-modulating peptides," *The CRISPR journal*, vol. 2, no. 1, pp. 51–63, 2019.

[23] G. Reint, Z. Li, K. Labun, S. Keskitalo, I. Soppa, K. Mamia, E. Tolo, M. Szymanska, L. A. Meza-Zepeda, S. Lorenz, *et al.*, "Rapid genome editing by crispr-cas9-pold3 fusion," *Elife*, vol. 10, p. e75415, 2021.

[24] A. Ghosh, K. Myacheva, M. Riester, C. Schmidt, and S. Diederichs, "Chimeric oligonucleotides combining guide rna and single-stranded dna repair template effectively induce precision gene editing," *RNA biology*, vol. 19, no. 1, pp. 588–593, 2022.

[25] B. Zorin, P. Hegemann, and I. Sizova, "Nuclear-gene targeting by using single-stranded dna avoids illegitimate dna integration in chlamydomonas reinhardtii," *Eukaryotic cell*, vol. 4, no. 7, pp. 1264–1272, 2005.

[26] G. Silva, L. Poirot, R. Galetto, J. Smith, G. Montoya, P. Duchateau, and F. Pâques, "Meganucleases and other tools for targeted genome engineering: perspectives and challenges for gene therapy," *Current gene therapy*, vol. 11, no. 1, pp. 11–27, 2011.

[27] J. Smith, M. Bibikova, F. G. Whitby, A. Reddy, S. Chandrasegaran, and D. Carroll, "Requirements for double-strand cleavage by chimeric restriction enzymes with zinc finger dna-recognition domains," *Nucleic acids research*, vol. 28, no. 17, pp. 3361–3369, 2000.

[28] J. Guo, T. Gaj, and C. F. Barbas III, "Directed evolution of an enhanced and highly efficient foki cleavage domain for zinc finger nucleases," *Journal of molecular biology*, vol. 400, no. 1, pp. 96–107, 2010.

[29] A. J. Bogdanove and D. F. Voytas, "Tal effectors: customizable proteins for dna targeting," *Science*, vol. 333, no. 6051, pp. 1843–1846, 2011.

[30] T. Gaj, C. A. Gersbach, and C. F. Barbas, "Zfn, talen, and crispr/cas-based methods

for genome engineering," *Trends in biotechnology*, vol. 31, no. 7, pp. 397–405, 2013.

[31] Y. Ishino, H. Shinagawa, K. Makino, M. Amemura, and A. Nakata, "Nucleotide sequence of the iap gene, responsible for alkaline phosphatase isozyme conversion in escherichia coli, and identification of the gene product," *Journal of bacteriology*, vol. 169, no. 12, pp. 5429–5433, 1987.

[32] R. Barrangou, C. Fremaux, H. Deveau, M. Richards, P. Boyaval, S. Moineau, D. A. Romero, and P. Horvath, "Crispr provides acquired resistance against viruses in prokaryotes," *Science*, vol. 315, no. 5819, pp. 1709–1712, 2007.

[33] C. Pourcel, G. Salvignol, and G. Vergnaud, "Crispr elements in yersinia pestis acquire new repeats by preferential uptake of bacteriophage dna, and provide additional tools for evolutionary studies," *Microbiology*, vol. 151, no. 3, pp. 653–663, 2005.

[34] A. Bolotin, B. Quinquis, A. Sorokin, and S. D. Ehrlich, "Clustered regularly interspaced short palindrome repeats (crisprs) have spacers of extrachromosomal origin," *Microbiology*, vol. 151, no. 8, pp. 2551–2561, 2005.

[35] E. Deltcheva, K. Chylinski, C. M. Sharma, K. Gonzales, Y. Chao, Z. A. Pirzada, M. R. Eckert, J. Vogel, and E. Charpentier, "Crispr rna maturation by trans-encoded small rna and host factor rnase iii," *Nature*, vol. 471, no. 7340, pp. 602–607, 2011.

[36] F. J. Mojica, C. Díez-Villaseñor, J. García-Martínez, and C. Almendros, "Short motif sequences determine the targets of the prokaryotic crispr defence system," *Microbiology*, vol. 155, no. 3, pp. 733–740, 2009.

[37] L. Cong, F. A. Ran, D. Cox, S. Lin, R. Barretto, N. Habib, P. D. Hsu, X. Wu, W. Jiang, L. A. Marraffini, *et al.*, "Multiplex genome engineering using crispr/cas systems," *Science*, vol. 339, no. 6121, pp. 819–823, 2013.

[38] J. Y. Wang and J. A. Doudna, "Crispr technology: A decade of genome editing is only the beginning," *Science*, vol. 379, no. 6629, p. eadd8643, 2023.

[39] J. Wei, L. Hou, J. Liu, Z. Wang, S. Gao, T. Qi, S. Gao, S. Sun, and Y. Wang, "Closely related type ii-c cas9 orthologs recognize diverse pams," *Elife*, vol. 11, p. e77825, 2022.

[40] J. S. Gootenberg, O. O. Abudayyeh, M. J. Kellner, J. Joung, J. J. Collins, and F. Zhang, "Multiplexed and portable nucleic acid detection platform with cas13, cas12a, and csm6," *Science*, vol. 360, no. 6387, pp. 439–444, 2018.

[41] A. C. Komor, Y. B. Kim, M. S. Packer, J. A. Zuris, and D. R. Liu, "Programmable editing of a target base in genomic dna without double-stranded dna cleavage," *Nature*, vol. 533, no. 7603, pp. 420–424, 2016.

[42] N. M. Gaudelli, A. C. Komor, H. A. Rees, M. S. Packer, A. H. Badran, D. I. Bryson, and D. R. Liu, "Programmable base editing of a• t to g• c in genomic dna without dna cleavage," *Nature*, vol. 551, no. 7681, pp. 464–471, 2017.

[43] G. A. Newby, J. S. Yen, K. J. Woodard, T. Mayuranathan, C. R. Lazzarotto, Y. Li, H. Sheppard-Tillman, S. N. Porter, Y. Yao, K. Mayberry, *et al.*, "Base editing of haematopoietic stem cells rescues sickle cell disease in mice," *Nature*, vol. 595, no. 7866, pp. 295–302, 2021.

[44] M. F. Montiel-Gonzalez, I. Vallecillo-Viejo, G. A. Yudowski, and J. J. Rosenthal, "Correction of mutations within the cystic fibrosis transmembrane conductance regulator by site-directed rna editing," *Proceedings of the National Academy of Sciences*, vol. 110, no. 45, pp. 18285–18290, 2013.

[45] M. Fukuda, H. Umeno, K. Nose, A. Nishitarumizu, R. Noguchi, and H. Nakagawa, "Construction of a guide-rna for site-directed rna mutagenesis utilising intracellular a-to-i rna editing," *Scientific reports*, vol. 7, no. 1, pp. 1–13, 2017.

[46] D. B. Cox, J. S. Gootenberg, O. O. Abudayyeh, B. Franklin, M. J. Kellner, J. Joung, and F. Zhang, "Rna editing with crispr-cas13," *Science*, vol. 358, no. 6366, pp. 1019–1027, 2017.

[47] A. V. Anzalone, P. B. Randolph, J. R. Davis, A. A. Sousa, L. W. Koblan, J. M. Levy, P. J. Chen, C. Wilson, G. A. Newby, A. Raguram, *et al.*, "Search-and-replace genome editing without double-strand breaks or donor dna," *Nature*, vol. 576, no. 7785, pp. 149–157, 2019.

[48] K. A. Everette, G. A. Newby, R. M. Levine, K. Mayberry, Y. Jang, T. Mayuranathan, N. Nimmagadda, E. Dempsey, Y. Li, S. V. Bhoopalan, *et al.*, "Ex vivo prime editing of patient haematopoietic stem cells rescues sickle-cell disease phenotypes after engraftment in mice," *Nature biomedical engineering*, pp. 1–13, 2023.

[49] E. Fang, X. Liu, M. Li, Z. Zhang, L. Song, B. Zhu, X. Wu, J. Liu, D. Zhao, and Y. Li, "Advances in covid-19 mrna vaccine development," *Signal Transduction and Targeted Therapy*, vol. 7, no. 1, p. 94, 2022.

[50] L. R. Baden, H. M. El Sahly, B. Essink, K. Kotloff, S. Frey, R. Novak, D. Diemert,

S. A. Spector, N. Rouphael, C. B. Creech, *et al.*, "Efficacy and safety of the mrna-1273 sars-cov-2 vaccine," *New England journal of medicine*, vol. 384, no. 5, pp. 403–416, 2021.

[51] A. B. Vogel, I. Kanevsky, Y. Che, K. A. Swanson, A. Muik, M. Vormehr, L. M. Kranz, K. C. Walzer, S. Hein, A. Güler, *et al.*, "Bnt162b vaccines protect rhesus macaques from sars-cov-2," *Nature*, vol. 592, no. 7853, pp. 283–289, 2021.

[52] K.-J. Kallen and A. Theß, "A development that may evolve into a revolution in medicine: mrna as the basis for novel, nucleotide-based vaccines and drugs," *Therapeutic advances in vaccines*, vol. 2, no. 1, pp. 10–31, 2014.

[53] R. M. Conry, A. F. LoBuglio, M. Wright, L. Sumerel, M. J. Pike, F. Johanning, R. Benjamin, D. Lu, and D. T. Curiel, "Characterization of a messenger rna polynucleotide vaccine vector," *Cancer research*, vol. 55, no. 7, pp. 1397–1400, 1995.

[54] S. Vaidyanathan, K. T. Azizian, A. A. Haque, J. M. Henderson, A. Hendel, S. Shore, J. S. Antony, R. I. Hogrefe, M. S. Kormann, M. H. Porteus, *et al.*, "Uridine depletion and chemical modification increase cas9 mrna activity and reduce immunogenicity without hplc purification," *Molecular Therapy-Nucleic Acids*, vol. 12, pp. 530–542, 2018.

[55] P. J. Sikorski, M. Warminski, D. Kubacka, T. Ratajczak, D. Nowis, J. Kowalska, and J. Jemielity, "The identity and methylation status of the first transcribed nucleotide in eukaryotic mrna 5 cap modulates protein expression in living cells," *Nucleic Acids Research*, vol. 48, no. 4, pp. 1607–1626, 2020.

[56] D. Strzelecka, M. Smietanski, P. J. Sikorski, M. Warminski, J. Kowalska, and J. Jemielity, "Phosphodiester modifications in mrna poly (a) tail prevent deadenylation without compromising protein expression," *RNA*, vol. 26, no. 12, pp. 1815–1837, 2020.

[57] K. Leppek, G. W. Byeon, W. Kladwang, H. K. Wayment-Steele, C. H. Kerr, A. F. Xu, D. S. Kim, V. V. Topkar, C. Choe, D. Rothschild, *et al.*, "Combinatorial optimization of mrna structure, stability, and translation for rna-based therapeutics," *Nature communications*, vol. 13, no. 1, p. 1536, 2022.

[58] P. Vrtačnik, Š. Kos, S. A. Bustin, J. Marc, and B. Ostanek, "Influence of trypsinization and alternative procedures for cell preparation before rna extraction on rna integrity," *Analytical biochemistry*, vol. 463, pp. 38–44, 2014.

[59] C. W. Peterson, R. Venkataraman, S. S. Reddy, D. Pande, M. R. Enstrom, S. Radtke, O. Humbert, and H.-P. Kiem, "Intracellular rnase activity dampens zinc finger nuclease-mediated gene editing in hematopoietic stem and progenitor cells," *Molecular Therapy-Methods & Clinical Development*, vol. 24, pp. 30–39, 2022.

[60] K. Laoharawee, M. J. Johnson, W. S. Lahr, C. J. Sipe, E. Kleinboehl, J. J. Peterson, C.-l. Lonetree, J. B. Bell, N. J. Slipek, A. T. Crane, *et al.*, "A pan-rnase inhibitor enabling crispr-mrna platforms for engineering of primary human monocytes," *International journal of molecular sciences*, vol. 23, no. 17, p. 9749, 2022.

[61] A. Dousis, K. Ravichandran, E. M. Hobert, M. J. Moore, and A. E. Rabideau, "An engineered t7 rna polymerase that produces mrna free of immunostimulatory byproducts," *Nature Biotechnology*, pp. 1–9, 2022.

[62] X. Piao, V. Yadav, E. Wang, W. Chang, L. Tau, B. E. Lindenmuth, and S. X. Wang, "Double-stranded rna reduction by chaotropic agents during in vitro transcription of messenger rna," *Molecular Therapy-Nucleic Acids*, vol. 29, pp. 618–624, 2022.

[63] Y. G. Chen and S. Hur, "Cellular origins of dsrna, their recognition and consequences," *Nature Reviews Molecular Cell Biology*, vol. 23, no. 4, pp. 286–301, 2022.

[64] L. Alexopoulou, A. C. Holt, R. Medzhitov, and R. A. Flavell, "Recognition of double-stranded rna and activation of nf-κb by toll-like receptor 3," *Nature*, vol. 413, no. 6857, pp. 732–738, 2001.

[65] Y.-M. Loo and M. Gale, "Immune signaling by rig-i-like receptors," *Immunity*, vol. 34, no. 5, pp. 680–692, 2011.

[66] M. A. Oberli, A. M. Reichmuth, J. R. Dorkin, M. J. Mitchell, O. S. Fenton, A. Jaklenec, D. G. Anderson, R. Langer, and D. Blankschtein, "Lipid nanoparticle assisted mrna delivery for potent cancer immunotherapy," *Nano letters*, vol. 17, no. 3, pp. 1326–1335, 2017.

[67] X. Jiang, K. Abedi, and J. Shi, "Polymeric nanoparticles for rna delivery," *Reference Module in Materials Science and Materials Engineering*, 2021.

[68] W. Ho, M. Gao, F. Li, Z. Li, X.-Q. Zhang, and X. Xu, "Next-generation vaccines: nanoparticle-mediated dna and mrna delivery," *Advanced Healthcare Materials*, vol. 10, no. 8, p. 2001812, 2021.

[69] K. Karikó, H. Muramatsu, F. A. Welsh, J. Ludwig, H. Kato, S. Akira, and D. Weiss-

man, "Incorporation of pseudouridine into mrna yields superior nonimmunogenic vector with increased translational capacity and biological stability," *Molecular therapy*, vol. 16, no. 11, pp. 1833–1840, 2008.

[70] Y. Miyaoka, J. R. Berman, S. B. Cooper, S. J. Mayerl, A. H. Chan, B. Zhang, G. A. Karlin-Neumann, and B. R. Conklin, "Systematic quantification of hdr and nhej reveals effects of locus, nuclease, and cell type on genome-editing," *Scientific reports*, vol. 6, no. 1, p. 23549, 2016.

[71] Y. Miyaoka, S. J. Mayerl, A. H. Chan, and B. R. Conklin, "Detection and quantification of hdr and nhej induced by genome editing at endogenous gene loci using droplet digital pcr," *Digital PCR: Methods and Protocols*, pp. 349–362, 2018.

[72] E. Mazaika and J. Homsy, "Digital droplet pcr: Cnv analysis and other applications," *Current protocols in human genetics*, vol. 82, no. 1, pp. 7–24, 2014.

[73] Bio-Rad, "Droplet digital™ pcr applications guide," 2014.

[74] D. Conant, T. Hsiau, N. Rossi, J. Oki, T. Maures, K. Waite, J. Yang, S. Joshi, R. Kelso, K. Holden, *et al.*, "Inference of crispr edits from sanger trace data," *The CRISPR Journal*, vol. 5, no. 1, pp. 123–130, 2022.

[75] M. F. Sentmanat, S. T. Peters, C. P. Florian, J. P. Connelly, and S. M. Pruett-Miller, "A survey of validation strategies for crispr-cas9 editing," *Scientific reports*, vol. 8, no. 1, p. 888, 2018.

[76] M. Yang, D. Tkach, A. Boyne, S. Kazancioglu, A. Duclert, L. Poirot, P. Duchateau, and A. Juillerat, "Optimized two-step electroporation process to achieve efficient nonviral-mediated gene insertion into primary t cells," *FEBS Open bio*, vol. 12, no. 1, pp. 38–50, 2022.

[77] P. Bernard, "Positive selection of recombinant dna by ccdb," 1996.

[78] M. G. Lemieux, "Plasmids 101: ccdb-the toxic key to efficient cloning," 2016.

[79] M. Soriano, "Plasmids 101: Gateway cloning," *Addgene's Blog, jan*, 2017.

[80] T. K. Kim and J. H. Eberwine, "Mammalian cell transfection: the present and the future," *Analytical and bioanalytical chemistry*, vol. 397, pp. 3173–3178, 2010.

[81] T. Scientific, "Qubit® dsdna hs assay kits manual," *Pub. No. MAN0002326. Rev. B. 0.*

[82] T. F. Scientific, "Nanodrop 2000/2000c spectrophotometer v1. 0 user manual," *Wilmington, DE*, vol. 19810, 2009.

[83] K. Karikó, H. Muramatsu, J. Ludwig, and D. Weissman, "Generating the optimal mrna for therapy: Hplc purification eliminates immune activation and improves translation of nucleoside-modified, protein-encoding mrna," *Nucleic acids research*, vol. 39, no. 21, pp. e142–e142, 2011.

[84] T.-Y. Chao and R. T. Raines, "Mechanism of ribonuclease a endocytosis: analogies to cell-penetrating peptides," *Biochemistry*, vol. 50, no. 39, pp. 8374–8382, 2011.

Appendices

A Materials

All laboratory equipment, chemicals, kits, media, buffers, and gels used in the experimental part are listed below (Table A1-4).

A.1 Lab Equipment

Table A.1: **Lab equipment, reagents, and chemicals**

Equipment/Reagent/Chemical	Catalog number	Manufacturer
Common materials		
1xPBS, pH 7.4	NA	Prepared in NCMM facilities
TE buffer, pH 8.0	AM9849	Invitrogen
Absolute Ethanol (96-100%)	600051/600068	Antibac
Biopak®Polisher, Milli-Q H_2O (RNAse/DNAse free)	CDUFBI001	Merck
Sub Aqua 5 Plus Unstirred Water Bath	NA	Grant Scientific
Thermo Scientific-MicroCL 21R centrifuge	75002470	Thermo Fisher
Zeiss Axiovert 40 C Inverted Phase Contrast Microscope	ZAXIO40C	Zeiss

Continued on next page

Table A.1 – *continued from previous page*

Equipment/Reagent/Chemical	Catalog number	Manufacturer
Thermoshaker	T1317	Eppendorf
ChemiDoc Imaging System	12003153	Bio-Rad
NanoDrop™2000 Spectrophotometer	ND2000	Thermo Fisher
Qubit™ 4 Fluorometer	Q33238	Invitrogen
Infinite®M Nano, single mode microplate reader	30190086	Tecan
Bacteria work		
CLuc AG Control Template (0.25 mg/mL)	N2078AVIAL	NEB-Bionordika
SOC media	15544034	Thermo Fisher
Ampicillin sodium salt (5 g)	A01665G	Sigma-Aldrich
LB media, pH 7.0	NA	Prepared in NCMM facilities
10 cm agar plates	NA	Prepared in NCMM facilities
Falcon™Round-Bottom Polypropylene Test Tube with Cap, miniprep culture tubes 14 mL	352059	Thermo Fisher

Continued on next page

Table A.1 – *continued from previous page*

Equipment/Reagent/Chemical	Catalog number	Manufacturer
Fisherbrand™Isotemp™ General Purpose Deluxe Water Bath	15355877	Fisher Scientific
Infors™Multitron Standard Incubation Shaker	11971582	Fisher Scientific
Eppendorf™centrifuge 5910R	5910R	Eppendorf
Floating tube holder	NA	NA
Subcloning Efficiency™ $DH5\alpha$™Competent Cells	18265017	Thermo Fisher
Mix & Go! Competent Cells $DH5\alpha$ 96 x 50 μL	T3009	Nordic Biosite
One Shot® ccdB Survival™ 2 T1R Chemically Competent Cells	A10460	Invitrogen
Gateway LR Clonase II Enzyme Mix	11791020/11791100	Thermo Fisher

Continued on next page

Table A.1 – *continued from previous page*

Equipment/Reagent/Chemical	Catalog number	Manufacturer
***In vitro* transcription**		
E-Gel™ Power Snap Electrophoresis Device	G8100	Invitrogen
E-Gel™ Agarose Gels with SYBR™ Safe DNA Gel Stain, 2%	G521802	Thermo Fisher
RNase away	7002	Thermo Fisher
RNaseOUT™ Recombinant Ribonuclease Inhibitor	10777019	Thermo Fisher
N1-Methylpseudouridine-5'-Triphosphate, 1 μmmol	N10811	Trilink Biotechnologies
E.coli Poly(A) polymerase	M0276L	NEB
Ultrapure™ Urea	15505035	Thermo Fisher
RNase A, (20mg/mL)	K182104A	Thermo Fisher
70 % EtOH	NA	Antibac
10X NorhternMax™ MOPS Gel Running Buffer	AM8671	Thermo Fisher
Formaldehyde, aqueous solution 36.5-38% in H_2O	F8775500ML	Sigma-Aldrich
Ethidium bromide solution	E151010ML	Sigma-Aldrich

Continued on next page

Table A.1 – *continued from previous page*

Equipment/Reagent/Chemical	Catalog number	Manufacturer
Millennium™ RNA Markers	AM7150	Thermo Fisher
ZipRuler Express DNA Ladder Set, ready-to-use, 2 x 50 μg	SM1373	Thermo Fisher
Filter cartrigdes	NA	NA
Transfection		
FuGENE® HD Transfection Reagent	E2312	Promega
Lipofectamine® 2000 Reagent	11668019	Invitrogen
Opti-MEM media	51985026	Life Technologies
Western Blot		
Pierce® BCA Protein Assay Kit	23227	Thermo Fisher
RIPA Lysis and Extraction Buffer 250 mL	89901	Thermo Fisher
Halt Protease Inhibitor Cocktail (100X) 1 mL	78430	Thermo Fisher
4x Laemmli Sample Buffer	1610747	Bio-Rad
2-Mercaptoethanol	1610710	Bio-Rad

Continued on next page

Table A.1 – *continued from previous page*

Equipment/Reagent/Chemical	Catalog number	Manufacturer
Tween®20, viscous liquid	SLCH6839	Sigma-Aldrich
TBS Tablets, pH 7.6	097500100	Medicago
Clarity®Western ECL Substrate	1705060	Bio-Rad
BSA (Bovine Serum Albumin)	SLCF3210	Sigma-Aldrich
Blocking-Grade Blocker	1706414	Bio-Rad
Recombinant Anti-CRISPR Cas9 primary antibody	ab191468	Abcam
Anti α-Tubulin primary antibody	ab7291	Abcam
Secondary anti-mouse antibody	ab6728	Abcam
No-Stain™ Protein Labeling Reagent	A44449	Thermo Fisher
Criterion™ TGX™ Precast Gels, 4-20%, 26 wells	5671095	Bio-rad
Trans-Blot Turbo Mini 0.2 μm PVDF Transfer Pack	1704156	Bio-Rad

Continued on next page

Table A.1 – *continued from previous page*

Equipment/Reagent/Chemical	Catalog number	Manufacturer
Trans-Blot Turbo Midi 0.2 μm PVDF Transfer Pack	1704157	Bio-Rad
Trans-Blot Turbo™ Transfer System	1704150	Bio-Rad
Trans-Blot Turbo™ Cassette	1704151	Bio-Rad
Cole-Parmer® Stuart® See-Saw Rocker	10637815	Fisher Scientific
PowerPac® Basic Power Supply	1645050	Bio-Rad
Scissors, tweezers, gel cracking tools, roller, and scapel	NA	NA
Electroporation		
RPMI 1640 Medium, GlutaMAX Supplement, HEPES	72400021	Gibco
DMEM, 1g/L D-Glucose, L-Glutamine, Pyruvate	31885023	Gibco
Fetal Bovine Serum (FBS), certified, heat inactivated	10082147	Gibco
Penicillin-Streptomycin (P/S), 10,000 U/mL	15140122	Thermo Fisher

Continued on next page

Table A.1 – *continued from previous page*

Equipment/Reagent/Chemical	Catalog number	Manufacturer
Alt-R® S.p. Cas9 Nuclease V3	1081059	IDT
Recombinant Human IL-2	20002	Peprotech
Recombinant Human IL-7	20007	Peprotech
Recombinant Human IL-15	20015	Peprotech
Dimethyl sulfoxide (DMSO)	276855	Sigma-Aldrich
Trypsin-EDTA (0.05%), Phenol red (500 mL)	25300062	Thermo Fisher
Lonza 4D Nucleofector System, Core Unit	AAF1002B	Lonza
Lonza 4D Nucleofector System, The X Unit up to 16 reactions	AAF1002X	Lonza
P3 Primary Cell 4D-Nucleofector™ X Kit S, up to 16 reactions	V4XP3032	Lonza
HyClone™ MaxCyte® Electroporation Buffer	EPB1	GE Healthcare Life Sciences
Precision™ General Purpose Bath	TSGP20	Thermo Fisher

Continued on next page

Table A.1 – *continued from previous page*

Equipment/Reagent/Chemical	Catalog number	Manufacturer
Eppendorf™ Centrifuge 5702R	5702R	Eppendorf
Armadillo PCR Plate, 96-well, orange, clear wells	AB2396O	Thermo Fisher
RNaseOUT™ Recombinant Ribonuclease Inhibitor	10777019	Thermo Fisher
Protector RNase Inhibitor 2000 Units	3335399001	Merck
In-Vitro Cell NuAire Direct Heat CO_2 Incubator	NU5810	NuAire
Countess™ Automated Cell Counter	C10227	Thermo Fisher
Countess™ Cell Counting Chamber Slides	C10228	Thermo Fisher
GeneAmp™ PCR System 9700	4339386	Thermo Fisher

Continued on next page

Table A.1 – *continued from previous page*

Equipment/Reagent/Chemical	Catalog number	Manufacturer
ddPCR		
ddPCR™ Supermix for Probes (No dUTP)	1863024	Bio-Rad
PCR primers, and FAM and HEX probes	see Table B	Designed individually for each target gene, purchased from IDT
Automated Droplet Generation Oil for Probes	1864110	Bio-Rad
ddPCR Droplet Reader Oil	1863004	Bio-Rad
Automated Droplet Generator	1864101	Bio-Rad
DG32™ Automated Droplet Generator Cartridges	1864108	Bio-Rad
ddPCR Plates, 96-wells, Semi-Skirted	12001925	Bio-Rad
Armadillo High Performance 96-Well PCR Plates	AB2396	Thermo Fisher
Pierceable Foil Heat Seal	1814040	Bio-Rad
Nunc™ Aluminum Sealing Tape for 96-well plates	232698	Thermo Fisher
QX200™ Droplet Reader	1864003	Bio-Rad

Continued on next page

Table A.1 – *continued from previous page*

Equipment/Reagent/Chemical	Catalog number	Manufacturer
PX1 PCR Plate Sealer	1814000	Bio-Rad
Biomek i-Series 90 μL Pipette Tips, sterile	B85884	Beckman Coulter

End of table

A.2 Kits

Table A.2: **Kits**
including catalog number and manufacturer.

Kits	Catalog number	Manufacturer
Q5® Site-Directed Mutagenesis Kit	E0554S	NEB
QIAprep® Spin Miniprep Kit	27104/27106	QIAGEN
PureLink® HiPure Plasmid Filter Purification Kits	K2100-17	Invitrogen
DNeasy Blood and Tissue Kit	69506	QIAGEN
Qubit® dsDNA HS Assay Kit	Q32851/Q32854	Life technologies
HiScribe™ T7 mRNA Kit with CleanCap® Reagent AG	E2080S	NEB-Bionordika
MEGAclear™ Transcription Clean-Up Kit	AM1908	Invitrogen
Pierce® BCA Protein Assay Kit	23227	Thermo Fisher

A.3 Buffers and Chemicals

Table A.3: **Buffers and chemicals** with its corresponding recipe.

Buffer/Chemical	Recipe
Agarose denaturating formaldehyde gel	
Running buffer	10X MOPS diluted to 1X in Milli-Q water
Denaturing gel	0.5 g agarose gel dissolved in 36 mL of Milli-Q water, 5 mL 10X MOPS running buffer, 9 mL 37 % formaldehyde
Agarose gel	
Running buffer	10X TAE buffer diluted to 1X in Milli-Q water
Agarose gel	2.0 g agarose gel dissolved in 200 mL of 1X TAE buffer
Western Blot	
Running buffer	10X stock, 1X working concentration; Tris/Glycine/SDS. 25 mM Tris, 190 mM Glycine, 0.1% SDS
TBS	2 TBS tablets and Tween: 20 mM Tris, pH 7.5, 150 mM NaCl, 0.1% Tween
TBST	Combined Milli-Q water, TBS tablet (2 tablets) and Tween: 20 mM Tris, pH 7.5, 150 mM NaCl, 0.1% Tween
Blocking solution	5 % BSA (Bovine Serum Albumin, Sigma-Aldrich, # SLCF3210) and 5% nonfat dry milk (Blocking-Grade Blocker, Bio-Rad, # 170-6414)

Continued on next page

Table A.3 – *continued from previous page*

Buffer/Chemical	Recipe
Primary antibodies	Recombinant Anti-CRISPR Cas9 primary antibody (Abcam, %ab191468) diluted 1:1000 in 10 mL of 5% nonfat dry milk (Blocking-Grade Blocker, Bio-Rad, # 170-6414), Anti α-Tubulin primary antibody (Abcam, %ab7291) diluted 1: 10,000 in 10 mL of 5 % BSA (Bovine Serum Albumin, Sigma, # SLCF3210)
Secondary antibody	Secondary anti-mouse antibody diluted 1:10,000 in 10 mL of 5 % nonfat dry milk (Blocking-Grade Blocker, Bio-Rad, # 170-6414)

End of table

A.4 Cell Culture Media

The different cell culture media used is listed in Table A.4. The major difference working with PBMCs and fibroblasts/HEK293T cells is the stimulation of T cells by including cytokines to the PBMCs. All work prior to electroporation does not include P/S, while media post-electroporation contains 1X P/S.

Table A.4: **Media used for cell culturing.**

Type of media	**Components**
PBMCs	
Thawing medium	RPMI 1640 Medium, GlutaMAX Supplement, HEPES (Gibco, # 72400-021) supplemented with 10 % FBS (Fetal Bovine Serum, certified, heat inactivated, Gibco, # 10082147)
Expansion medium	RPMI 1640 Medium, GlutaMAX Supplement, HEPES (Gibco, # 72400-021) supplemented with 10 % FBS (Fetal Bovine Serum, certified, heat inactivated, Gibco, # 10082147), 1X P/S (Penicillin-Streptomycin, Thermo Fisher, # 15140122), 15 μL/mL anti-human CD3/CD28 (StemCell Technologies, # 10970), 120U/mL IL-2 (Recombinant Human IL-2, Peprotech, # 200-02), 3ng/mL IL-7 (Recombinant Human IL-7, Peprotech, # 200-07), 3ng/mL IL-15 (Recombinant Human IL-15, Peprotech, # 200-15)
Recovery medium after electroporation	RPMI 1640 Medium, GlutaMAX Supplement, HEPES (Gibco, # 72400-021) supplemented with 10 % FBS, and IL-2 (Recombinant Human IL-2, Peprotech, # 200-02) at 250 U/mL

Continued on next page

Table A.4 – *continued from previous page*

Type of media	Components
Recovery medium for change/splitting	RPMI 1640 Medium, GlutaMAX Supplement, HEPES (Gibco, # 72400-021) supplemented with 10 % FBS (Fetal Bovine Serum, certified, heat inactivated, Gibco, # 10082147), 1X P/S (Penicillin-Streptomycin, Thermo Fisher, # 15140122), 120U/mL IL-2 (Recombinant Human IL-2, Peprotech, # 200-02)
Fibroblasts and HEK293T cells	
Thawing medium	DMEM, 1g/L D-Glucose, L-Glutamine, Pyruvate (Gibco, # 31885-023) supplemented with 10 % FBS (Fetal Bovine Serum, certified, heat inactivated, Gibco, # 10082147)
Expansion medium	DMEM, 1g/L D-Glucose, L-Glutamine, Pyruvate (Gibco, # 31885-023) supplemented with 10 % FBS (Fetal Bovine Serum, certified, heat inactivated, Gibco, # 10082147) supplemented with 1X P/S (Penicillin-Streptomycin, Thermo Fisher, # 15140122)
Recovery medium after electroporation	DMEM, 1g/L D-Glucose, L-Glutamine, Pyruvate (Gibco, # 31885-023) supplemented with 10 % FBS (Fetal Bovine Serum, certified, heat inactivated, Gibco, # 10082147)

Continued on next page

Table A.4 – *continued from previous page*

Type of media	Components
Recovery medium for change/splitting	DMEM, 1g/L D-Glucose, L-Glutamine, Pyruvate (Gibco, # 31885-023) supplemented with 10 % FBS (Fetal Bovine Serum, certified, heat inactivated, Gibco, # 10082147) supplemented with 1X P/S (Penicillin-Streptomycin, Thermo Fisher, # 15140122)

End of table

B Primer and Probe Sequences

For each primer or probe listed in Table B.1; name, sequence and source are noted. In the case of *ADA2* repair template, the nucleotides in red, bold font are the ones that are changed, thus introduced in the repair template. The nucleotides in red, bold font marked with an asterisk indicate the chemical modifications (2PT) on the repair template.

Table B.1: **List of primer and probe sequences**

Primer/Probe name	Sequence 5' to 3'	Source
T7 mutagenesis		
T7 mutagenesis forward primer	ACTCACTATAAGGAGACCCAAG	NEB
T7 mutagenesis reverse primer	CGTATTAATTTCGATAAGCCAG	NEB
Electroporation		

Continued on next page

Table B.1 – *continued from previous page*

Primer/Probe name	Sequence 5'to 3'	Source
ADA2 sgRNA #3, 20 bp (WT to SNP)	tgctggaggattatcggaag	IDT
ADA2 repair template, 3'2PT, forward, 100 bp (WT to SNP)	ccccgtccatcagaaaaatgttccaagtggatt ctgctggaggactacagagcagaacgtcac tgagtttgatgacaggtgagtagtagt*t*c	IDT
ddPCR		
ADA2 primer forward	GGTGAGGAATGTCACCTACA	IDT
ADA2 primer reverse	GTACCAAGGGAGACACCTAC	IDT
ADA2 reference probe	/56-FAM/GCCACATCTG TTTCACCCCA/3BHQ_1/	IDT
ADA2 HDR probe	/5HEX/CTGGAGGACTA CAGAAAGCGG/3BHQ_1/	IDT
ADA2 NHEJ probe	/5HEX/attatcggaa gcgggtgcaga/3BHQ_1/	IDT

End of table

C BCA Assay Standard Curve Dilutions

Table C.1: **Dilution scheme for standard test tube protocol of diluted albumin (BSA) standards.**
The working range is between 20-2,000 μg/mL. Use the same lysis buffer for dilutions as for lysis of the samples.

Vial	Volume of dilutent [μL]	Volume of BSA [μL]	Final concentration [μg/mL]
A	0	300 of stock	2000
B	125	375 of stock	1500
C	325	325 of stock	1000
D	175	175 of vial B dilution	750
E	325	325 of vial C dilution	500
F	325	325 of vial E dilution	250
G	325	325 of vial F dilution	125
H	400	100 of vial G dilution	25
I	400	0	0=blank

D mRNA Concentration and Purity

Table D.1: **mRNA concentration and purity of the optimized *in vitro* transcription**. Measurements were done with NanoDrop before and after extended purification utilizing the MegaClear Kit.

Sample ID	Concentration [ng/μL]	260/280	260/230
Cas9wt mRNA	3372	1.94	2.12
Cas9wt mRNA with urea	3301	1.95	2.16
Cas9wt mRNA purified with MegaClear Kit	2295	1.87	2.08
Cas9wt mRNA with urea and purified with MegaClear Kit	779	1.86	2.10
Cas9-HMGB1 mRNA with urea	3362	1.94	2.26
Cas9-HMGB1 with urea and purified with MegaClear Kit	3328	1.95	2.19

E Softwares and Online Resources

Table E.1: **List of softwares and online resources**

Software/Online resource	Application	Supplier
BioRender	Creating illustrations, figures and flow charts	https://www.biorender.com/
Eurofins Genomics	Sending plasmids and DNA for Sanger sequencing	https://eurofinsgenomics.eu/
GraphPad Prism (version 9.4.0)	Making graphs and calculating staticstics	GraphPad Prism
GXCapture (version 7.1.1.2)	Taking pictures of cells compatible with GXCAM-5	https://gtvision.co.uk/
Inkscape (version 1.0.2.2)	Vector graphics software to merge several graphs into one figure	https://inkscape.org/
QuantaSoft (version 1.7.4.0917)	Analyzing gene editing outcomes, compatible with Droplet Reader	Bio-Rad Laboratories
SnapGene (version 6.0.6)	Molecular biology software to make plasmid maps and interpreting DNA sequences	https://www.snapgene.com/
Tecan Magellan Pro (version 7.5)	Plate reading software for Tecan Plate readers	Tecan

End of table

F Plasmid Maps and Plasmid Sequences

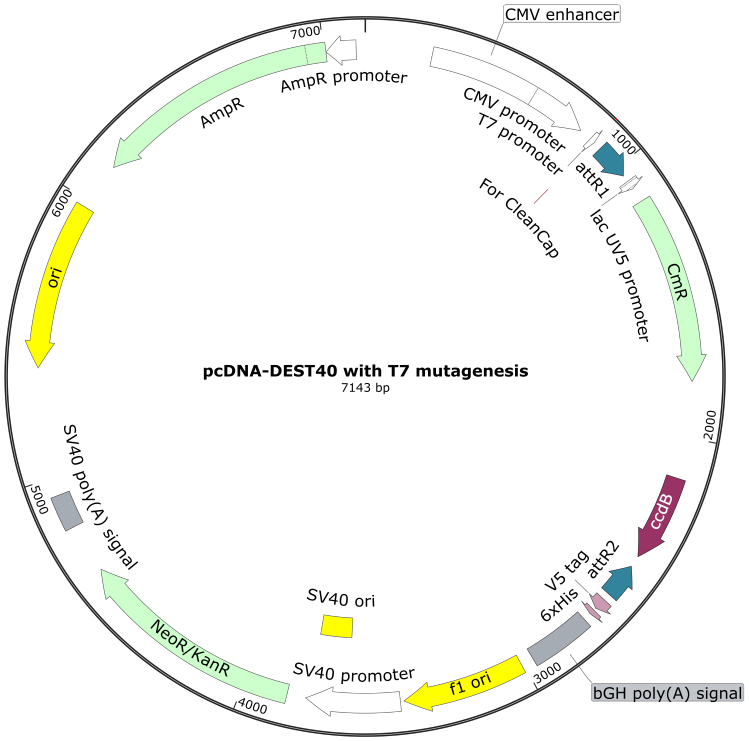

(a) pDEST40 with T7 mutagenesis

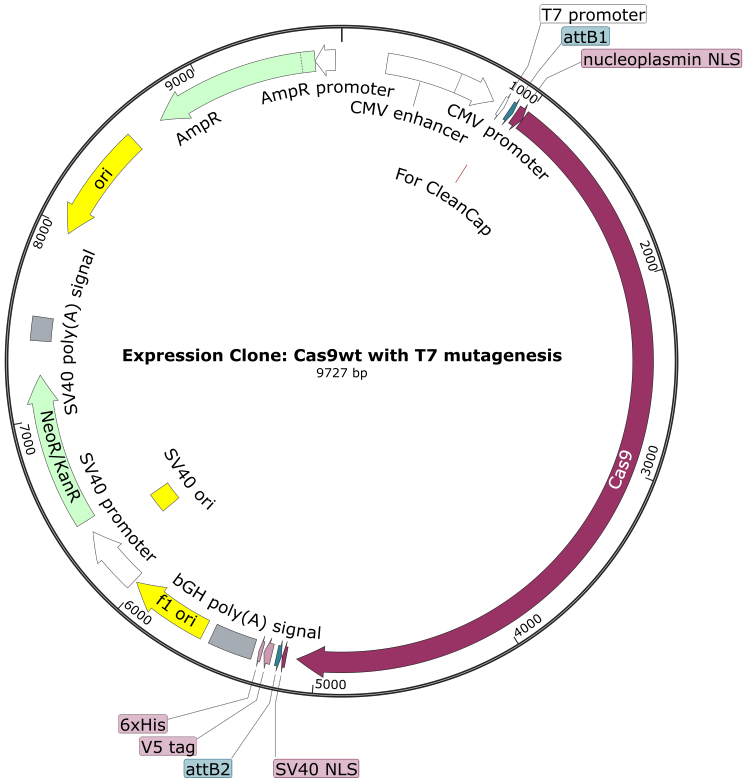

(b) pDEST40 Cas9wt with T7 mutagenesis

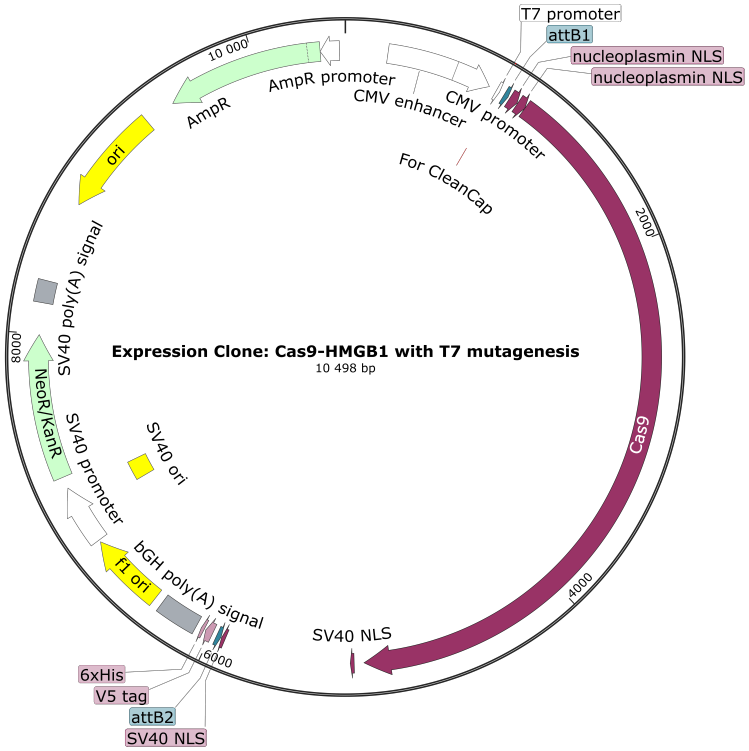

(c) pDEST40 Cas9-HMGB1 with T7 mutagenesis

Figure F.1: **Plasmid maps**
made in SnapGene (version 6.0.6), `https://www.snapgene.com/`.

pDEST40 with T7 mutagenesis

GACGGATCGGGAGATCTCCCGATCCCCTATGGTGCACTCTCAGTACAATCTGCTCTGATGCCGCATAGTTAAGCCAGTATCTGCTCCCTGCTTGTG
TGTTGGAGGTCGCTGAGTAGTGCGCGAGCAAAATTTAAGCTACAACAAGGCAAGGCTTGACCGACAATTGCATGAAGAATCTGCTTAGGGTTAGG
CGTTTTGCGCTGCTTCGCGATGTACGGGCCAGATATACGCGTTGACATTGATTATTGACTAGTTATTAATAGTAATCAATTACGGGGTCATTAGTTC
ATAGCCCATATATGGAGTTCCGCGTTACATAACTTACGGTAAATGGCCCGCCTGGCTGACCGCCCAACGACCCCCGCCCATTGACGTCAATAATGA
CGTATGTTCCCATAGTAACGCCAATAGGGACTTTCCATTGACGTCAATGGGTGGAGTATTTACGGTAAACTGCCCACTTGGCAGTACATCAAGTGT
ATCATATGCCAAGTACGCCCCCTATTGACGTCAATGACGGTAAATGGCCCGCCTGGCATTATGCCCAGTACATGACCTTATGGGACTTTCCTACTT
GGCAGTACATCTACGTATTAGTCATCGCTATTACCATGGTGATGCGGTTTTGGCAGTACATCAATGGGCGTGGATAGCGGTTTGACTCACGGGGAT
TTCCAAGTCTCCACCCCATTGACGTCAATGGGAGTTTGTTTTGGCACCAAAATCAACGGGACTTTCCAAAATGTCGTAACAACTCCGCCCCATTGA
CGCAAATGGGCGGTAGGCGTGTACGGTGGGAGGTCTATATAAGCAGAGCTCTCTGGCTAACTAGAGAACCCACTGCTTACTGGCTTATCGAAATT
AATACGACTCACTATAAGGAGACCCAAGCTGGCTAGTTAAGCTATCAACAAGTTTGTACAAAAAAGCTGAACGAGAAACGTAAAATGATATAAA
TATCAATATATTAAATTAGATTTTGCATAAAAAACAGACTACATAATACTGTAAAACACAACATATCCAGTCACTATGGCGGCCGCATTAGGCAC
CCCAGGCTTTACACTTTATGCTTCCGGCTCGTATAATGTGTGGATTTTGAGTTAGGATCCGGCGAGATTTTCAGGAGCTAAGGAAGCTAAAATGGA
GAAAAAAATCACTGGATATACCACCGTTGATATATCCCAATGGCATCGTAAAGAACATTTTGAGGCATTTCAGTCAGTTGCTCAATGTACCTATAA
CCAGACCGTTCAGCTGGATATTACGGCCTTTTTAAAGACCGTAAAGAAAAATAAGCACAAGTTTTATCCGGCCTTTATTCACATTCTTGCCCGCCT
GATGAATGCTCATCCGGAATTCCGTATGGCAATGAAAGACGGTGAGCTGGTGATATGGGATAGTGTTCACCCTTGTTACACCGTTTTCCATGAGCA
AACTGAAACGTTTTCATCGCTCTGGAGTGAATACCACGACGATTTCCGGCAGTTTCTACACATATATTCGCAAGATGTGGCGTGTTACGGTGAAAA
CCTGGCCTATTTCCCTAAAGGGTTTATTGAGAATATGTTTTTCGTCTCAGCCAATCCCTGGGTGAGTTTCACCAGTTTTGATTTAAACGTGGCCAAT
ATGGACAACTTCTTCGCCCCCGTTTTCACCATGGGCAAATATTATACGCAAGGCGACAAGGTGCTGATGCCGCTGGCGATTCAGGTTCATCATGCC
GTCTGTGATGGCTTCCATGTCGGCAGAATGCTTAATGAATTACAACAGTACTGCGATGAGTGGCAGGGCGGGGCGTAAAGATCTGGATCCGGCTT
ACTAAAAGCCAGATAACAGTATGCGTATTTGCGCGCTGATTTTTGCGGTATAAGAATATATACTGATATGTATACCCGAAGTATGTCAAAAAGAG
GTGTGCTATGAAGCAGCGTATTACAGTGACAGTTGACAGCGACAGCTATCAGTTGCTCAAGGCATATATGATGTCAATATCTCCGGTCTGGTAAGC
ACAACCATGCAGAATGAAGCCCGTCGTCTGCGTGCCGAACGCTGGAAAGCGGAAAATCAGGAAGGGATGGCTGAGGTCGCCCGGTTTATTGAAA
TGAACGGCTCTTTTGCTGACGAGAACAGGGACTGGTGAAATGCAGTTTAAGGTTTACACCTATAAAAGAGAGAGCCGTTATCGTCTGTTTGTGGAT
GTACAGAGTGATATTATTGACACGCCGGGCGACGGATGGTGATCCCCCTGGCCAGTGCACGTCTGCTGTCAGATAAAGTCTCCCGTGAACTTTAC
CCGGTGGTGCATATCGGGGATGAAAGCTGGCGCATGATGACCACCGATATGGCCAGTGTGCCGGTCTCCGTTATCGGGGAAGAAGTGGCTGATCT
CAGCCACCGCGAAAATGACATCAAAAACGCCATTAACCTGATGTTCTGGGGAATATAAATGTCAGGCTCCGTTATACACAGCCAGTCTGCAGGTC
GACCATAGTGACTGGATATGTTGTGTTTTACAGTATTATGTAGTCTGTTTTTTATGCAAAATCTAATTTAATATATTGATATTTATATCATTTTACGT
TTCTCGTTCAGCTTTCTTGTACAAAGTGGTTGATCTAGAGGGCCCGCGGTTCGAAGGTAAGCCTATCCCTAACCCTCTCCTCGGTCTCGATTCTACG
CGTACCGGTCATCATCACCATCACCATTGAGTTTAAACCCGCTGATCAGCCTCGACTGTGCCTTCTAGTTGCCAGCCATCTGTTGTTTGCCCCTCCC
CCGTGCCTTCCTTGACCCTGGAAGGTGCCACTCCCACTGTCCTTTCCTAATAAAATGAGGAAATTGCATCGCATTGTCTGAGTAGGTGTCATTCTAT
TCTGGGGGGTGGGGTGGGGCAGGACAGCAAGGGGGAGGATTGGGAAGACAATAGCAGGCATGCTGGGGATGCGGTGGGCTCTATGGCTTCTGAG
GCGGAAAGAACCAGCTGGGGCTCTAGGGGGTATCCCCACGCGCCCTGTAGCGGCGCATTAAGCGCGGCGGGTGTGGTGGTTACGCGCAGCGTGA
CCGCTACACTTGCCAGCGCCCTAGCGCCCGCTCCTTTCGCTTTCTTCCCTTCCTTTCTCGCCACGTTCGCCGGCTTTCCCCGTCAAGCTCTAAATCGG
GGGCTCCCTTTAGGGTTCCGATTTAGTGCTTTACGGCACCTCGACCCCAAAAAACTTGATTAGGGTGATGGTTCACGTAGTGGGCCATCGCCCTGA
TAGACGGTTTTTCGCCCTTTGACGTTGGAGTCCACGTTCTTTAATAGTGGACTCTTGTTCCAAACTGGAACAACACTCAACCCTATCTCGGTCTATT
CTTTTGATTTATAAGGGATTTTGCCGATTTCGGCCTATTGGTTAAAAAATGAGCTGATTTAACAAAAATTTAACGCGAATTAATTCTGTGGAATGT
GTGTCAGTTAGGGTGTGGAAAGTCCCCAGGCTCCCCAGCAGGCAGAAGTATGCAAAGCATGCATCTCAATTAGTCAGCAACCAGGTGTGGAAAGT
CCCCAGGCTCCCCAGCAGGCAGAAGTATGCAAAGCATGCATCTCAATTAGTCAGCAACCATAGTCCCGCCCCTAACTCCGCCCATCCCGCCCCTA
ACTCCGCCCAGTTCCGCCCATTCTCCGCCCCATGGCTGACTAATTTTTTTTATTTATGCAGAGGCCGAGGCCGCCTCTGCCTCTGAGCTATTCCAGA
AGTAGTGAGGAGGCTTTTTTGGAGGCCTAGGCTTTTGCAAAAAGCTCCCGGGAGCTTGTATATCCATTTTCGGATCTGATCAAGAGACAGGATGA
GGATCGTTTCGCATGATTGAACAAGATGGATTGCACGCAGGTTCTCCGGCCGCTTGGGTGGAGAGGCTATTCGGCTATGACTGGGCACAACAGAC
AATCGGCTGCTCTGATGCCGCCGTGTTCCGGCTGTCAGCGCAGGGGCGCCCGGTTCTTTTTGTCAAGACCGACCTGTCCGGTGCCCTGAATGAACT
GCAGGACGAGGCAGCGCGGCTATCGTGGCTGGCCACGACGGGCGTTCCTTGCGCAGCTGTGCTCGACGTTGTCACTGAAGCGGGAAGGGACTGGC
TGCTATTGGGCGAAGTGCCGGGGCAGGATCTCCTGTCATCTCACCTTGCTCCTGCCGAGAAAGTATCCATCATGGCTGATGCAATGCGGCGGCTGC
ATACGCTTGATCCGGCTACCTGCCCATTCGACCACCAAGCGAAACATCGCATCGAGCGAGCACGTACTCGGATGGAAGCCGGTCTTGTCGATCAG
GATGATCTGGACGAAGAGCATCAGGGGCTCGCGCCAGCCGAACTGTTCGCCAGGCTCAAGGCGCGCATGCCCGACGGCGAGGATCTCGTCGTGA
CCCATGGCGATGCCTGCTTGCCGAATATCATGGTGGAAAATGGCCGCTTTTCTGGATTCATCGACTGTGGCCGGCTGGGTGTGGCGGACCGCTATC
AGGACATAGCGTTGGCTACCCGTGATATTGCTGAAGAGCTTGGCGGCGAATGGGCTGACCGCTTCCTCGTGCTTTACGGTATCGCCGCTCCCGATT
CGCAGCGCATCGCCTTCTATCGCCTTCTTGACGAGTTCTTCTGAGCGGGACTCTGGGGTTCGCGAAATGACCGACCAAGCGACGCCCAACCTGCCA
TCACGAGATTTCGATTCCACCGCCGCCTTCTATGAAAGGTTGGGCTTCGGAATCGTTTTCCGGGACGCCGGCTGGATGATCCTCCAGCGCGGGGAT
CTCATGCTGGAGTTCTTCGCCCACCCCAACTTGTTTATTGCAGCTTATAATGGTTACAAATAAAGCAATAGCATCACAAATTTCACAAATAAAGCA
TTTTTTTCACTGCATTCTAGTTGTGGTTTGTCCAAACTCATCAATGTATCTTATCATGTCTGTATACCGTCGACCTCTAGCTAGAGCTTGGCGTAATC
ATGGTCATAGCTGTTTCCTGTGTGAAATTGTTATCCGCTCACAATTCCACACAACATACGAGCCGGAAGCATAAAGTGTAAAGCCTGGGGTGCCTA
ATGAGTGAGCTAACTCACATTAATTGCGTTGCGCTCACTGCCCGCTTTCCAGTCGGGAAACCTGTCGTGCCAGCTGCATTAATGAATCGGCCAACG
CGCGGGGAGAGGCGGTTTGCGTATTGGGCGCTCTTCCGCTTCCTCGCTCACTGACTCGCTGCGCTCGGTCGTTCGGCTGCGGCGAGCGGTATCAGC
TCACTCAAAGGCGGTAATACGGTTATCCACAGAATCAGGGGATAACGCAGGAAAGAACATGTGAGCAAAAGGCCAGCAAAAGGCCAGGAACCG
TAAAAAGGCCGCGTTGCTGGCGTTTTTCCATAGGCTCCGCCCCCCTGACGAGCATCACAAAAATCGACGCTCAAGTCAGAGGTGGCGAAACCCGA
CAGGACTATAAAGATACCAGGCGTTTCCCCCTGGAAGCTCCCTCGTGCGCTCTCCTGTTCCGACCCTGCCGCTTACCGGATACCTGTCCGCCTTTCT
CCCTTCGGGAAGCGTGGCGCTTTCTCATAGCTCACGCTGTAGGTATCTCAGTTCGGTGTAGGTCGTTCGCTCCAAGCTGGGCTGTGTGCACGAACC
CCCCGTTCAGCCCGACCGCTGCGCCTTATCCGGTAACTATCGTCTTGAGTCCAACCCGGTAAGACACGACTTATCGCCACTGGCAGCAGCCACTGG
TAACAGGATTAGCAGAGCGAGGTATGTAGGCGGTGCTACAGAGTTCTTGAAGTGGTGGCCTAACTACGGCTACACTAGAAGAACAGTATTTGGTA
TCTGCGCTCTGCTGAAGCCAGTTACCTTCGGAAAAAGAGTTGGTAGCTCTTGATCCGGCAAACAAACCACCGCTGGTAGCGGTGGTTTTTTTGTTT
GCAAGCAGCAGATTACGCGCAGAAAAAAAGGATCTCAAGAAGATCCTTTGATCTTTTCTACGGGGTCTGACGCTCAGTGGAACGAAAACTCACGT
TAAGGGATTTTGGTCATGAGATTATCAAAAAGGATCTTCACCTAGATCCTTTTAAATTAAAAATGAAGTTTTAAATCAATCTAAAGTATATATGAG
TAAACTTGGTCTGACAGTTACCAATGCTTAATCAGTGAGGCACCTATCTCAGCGATCTGTCTATTTCGTTCATCCATAGTTGCCTGACTCCCCGTCG
TGTAGATAACTACGATACGGGAGGGCTTACCATCTGGCCCCAGTGCTGCAATGATACCGCGAGACCCACGCTCACCGGCTCCAGATTTATCAGCA
ATAAACCAGCCAGCCGGAAGGGCCGAGCGCAGAAGTGGTCCTGCAACTTTATCCGCCTCCATCCAGTCTATTAATTGTTGCCGGGAAGCTAGAGT
AAGTAGTTCGCCAGTTAATAGTTTGCGCAACGTTGTTGCCATTGCTACAGGCATCGTGGTGTCACGCTCGTCGTTTGGTATGGCTTCATTCAGCTCC
GGTTCCCAACGATCAAGGCGAGTTACATGATCCCCCATGTTGTGCAAAAAAGCGGTTAGCTCCTTCGGTCCTCCGATCGTTGTCAGAAGTAAGTTG
GCCGCAGTGTTATCACTCATGGTTATGGCAGCACTGCATAATTCTCTTACTGTCATGCCATCCGTAAGATGCTTTTCTGTGACTGGTGAGTACTCAA
CCAAGTCATTCTGAGAATAGTGTATGCGGCGACCGAGTTGCTCTTGCCCGGCGTCAATACGGGATAATACCGCGCCACATAGCAGAACTTTAAAA
GTGCTCATCATTGGAAAACGTTCTTCGGGGCGAAAACTCTCAAGGATCTTACCGCTGTTGAGATCCAGTTCGATGTAACCCACTCGTGCACCCAAC
TGATCTTCAGCATCTTTTACTTTCACCAGCGTTTCTGGGTGAGCAAAAACAGGAAGGCAAAATGCCGCAAAAAAGGGAATAAGGGCGACACGGA
AATGTTGAATACTCATACTCTTCCTTTTTCAATATTATTGAAGCATTTATCAGGGTTATTGTCTCATGAGCGGATACATATTTGAATGTATTTAGAA
AAATAAACAAATAGGGGTTCCGCGCACATTTCCCCGAAAAGTGCCACCTGACGTC

Figure F.2: **Sequence of pDEST40 with T7 mutagenesis.**
Downloaded from SnapGene (version 6.0.6), `https://www.snapgene.com/`.

pDEST40 Cas9wt with T7 mutagenesis

GACGGATCGGGAGATCTCCCGATCCCCTATGGTGCACTCTCAGTACAATCTGCTCTGATGCCGCATAGTTAAGCCAGTATCTGCTCCCTGCTTGTG
TGTTGGAGGTCGCTGAGTAGTGCGCGAGCAAAATTTAAGCTACAACAAGGCAAGGCTTGACCGACAATTGCATGAAGAATCTGCTTAGGGTTAGG
CGTTTTGCGCTGCTTCGCGATGTACGGGCCAGATATACGCGTTGACATTGATTATTGACTAGTTATTAATAGTAATCAATTACGGGGTCATTAGTTC
ATAGCCCATATATGGAGTTCCGCGTTACATAACTTACGGTAAATGGCCCGCCTGGCTGACCGCCCAACGACCCCCGCCCATTGACGTCAATAATGA
CGTATGTTCCCATAGTAACGCCAATAGGGACTTTCCATTGACGTCAATGGGTGGAGTATTTACGGTAAACTGCCCACTTGGCAGTACATCAAGTGT
ATCATATGCCAAGTACGCCCCCTATTGACGTCAATGACGGTAAATGGCCCGCCTGGCATTATGCCCAGTACATGACCTTATGGGACTTTCCTACTT
GGCAGTACATCTACGTATTAGTCATCGCTATTACCATGGTGATGCGGTTTTGGCAGTACATCAATGGGCGTGGATAGCGGTTTGACTCACGGGGAT
TTCCAAGTCTCCACCCCATTGACGTCAATGGGAGTTTGTTTTGGCACCAAAATCAACGGGACTTTCCAAAATGTCGTAACAACTCCGCCCCATTGA
CGCAAATGGGCGGTAGGCGTGTACGGTGGGAGGTCTATATAAGCAGAGCTCTCTGGCTAACTAGAGAACCCACTGCTTACTGGCTTATCGAAATT
AATACGACTCACTATAAGGAGACCCAAGCTGGCTAGTTAAGCTATCAACAAGTTTGTACAAAAAAGCAGGCTTCGCCACCATGAAAAGGCCGGC
GGCCACGAAAAAGGCCGGCCAGGCAAAAAAGAAAAAGGACAAGAAGTACAGCATCGGCCTGGACATCGGCACCAACTCTGTGGGCTGGGCCGT
GATCACCGACGAGTACAAGGTGCCCAGCAAGAAATTCAAGGTGCTGGGCAACACCGACCGGCACAGCATCAAGAAGAACCTGATCGGAGCCCTG
CTGTTCGACAGCGGCGAAACAGCCGAGGCCACCCGGCTGAAGAGAACCGCCAGAAGAAGATACACCAGACGGAAGAACCGGATCTGCTATCTGC
AAGAGATCTTCAGCAACGAGATGGCCAAGGTGGACGACAGCTTCTTCCACAGACTGGAAGAGTCCTTCCTGGTGGAAGAGGATAAGAAGCACGA
GCGGCACCCCATCTTCGGCAACATCGTGGACGAGGTGGCCTACCACGAGAAGTACCCCACCATCTACCACCTGAGAAAGAAACTGGTGGACAGC
ACCGACAAGGCCGACCTGCGGCTGATCTATCTGGCCCTGGCCCACATGATCAAGTTCCGGGGCCACTTCCTGATCGAGGGCGACCTGAACCCCGA
CAACAGCGACGTGGACAAGCTGTTCATCCAGCTGGTGCAGACCTACAACCAGCTGTTCGAGGAAAACCCCATCAACGCCAGCGGCGTGGACGCC
AAGGCCATCCTGTCTGCCAGACTGAGCAAGAGCAGACGGCTGGAAAATCTGATCGCCCAGCTGCCCGGCGAGAAGAAGAATGGCCTGTTCGGCA
ACCTGATTGCCCTGAGCCTGGGCCTGACCCCCAACTTCAAGAGCAACTTCGACCTGGCCGAGGATGCCAAACTGCAGCTGAGCAAGGACACCTAC
GACGACGACCTGGACAACCTGCTGGCCCAGATCGGCGACCAGTACGCCGACCTGTTTCTGGCCGCCAAGAACCTGTCCGACGCCATCCTGCTGAG
CGACATCCTGAGAGTGAACACCGAGATCACCAAGGCCCCCCTGAGCGCCTCTATGATCAAGAGATACGACGAGCACCACCAGGACCTGACCCTGC
TGAAAGCTCTCGTGCGGCAGCAGCTGCCTGAGAAGTACAAAGAGATTTTCTTCGACCAGAGCAAGAACGGCTACGCCGGCTACATTGACGGCGGA
GCCAGCCAGGAAGAGTTCTACAAGTTCATCAAGCCCATCCTGGAAAAGATGGACGGCACCGAGGAACTGCTCGTGAAGCTGAACAGAGAGGACC
TGCTGCGGAAGCAGCGGACCTTCGACAACGGCAGCATCCCCCACCAGATCCACCTGGGAGAGCTGCACGCCATTCTGCGGCGGCAAGGAAGATTTT
TACCCATTCCTGAAGGACAACCGGGAAAAGATCGAGAAGATCCTGACCTTCCGCATCCCCTACTACGTGGGCCCTCTGGCCAGGGGAAACAGCAG
ATTCGCCTGGATGACCAGAAAGAGCGAGGAAACCATCACCCCCTGGAACTTCGAGGAAGTGGTGGACAAGGGCGCTTCCGCCCAGAGCTTCATC
GAGCGGATGACCAACTTCGATAAGAACCTGCCCAACGAGAAGGTGCTGCCCAAGCACAGCCTGCTGTACGAGTACTTCACCGTGTATAACGAGCT
GACCAAAGTGAAATACGTGACCGAGGGAATGAGAAAGCCCGCCTTCCTGAGCGGCGAGCAGAAAAAGGCCATCGTGGACCTGCTGTTCAAGACC
AACCGGAAAGTGACCGTGAAGCAGCTGAAAGAGGACTACTTCAAGAAAATCGAGTGCTTCGACTCCGTGGAAATCTCCGGCGTGGAAGATCGGT
TCAACGCCTCCCTGGGCACATACCACGATCTGCTGAAAATTATCAAGGACAAGGACTTCCTGGACAATGAGGAAAACGAGGACATTCTGGAAGAT
ATCGTGCTGACCCTGACACTGTTTGAGGACAGAGAGATGATCGAGGAACGGCTGAAAACCTATGCCCACCTGTTCGACGACAAAGTGATGAAGCA
GCTGAAGCGGCGGAGATACACCGGCTGGGGCAGGCTGAGCCGGAAGCTGATCAACGGCATCCGGGACAAGCAGTCCGGCAAGACAATCCTGGAT
TTCCTGAAGTCCGACGGCTTCGCCAACAGAAACTTCATGCAGCTGATCCACGACGACAGCCTGACCTTTAAAGAGGACATCCAGAAAGCCCAGGT
GTCCGGCCAGGGCGATAGCCTGCACGAGCACATTGCCAATCTGGCCGGCAGCCCCGCCATTAAGAAGGGCATCCTGCAGACAGTGAAGGTGGTG
GACGAGCTgGTGAAAGTGATGGGCCGGCACAAGCCCGAGAACATCGTGATCGAAATGGCCAGAGAGAACCAGACCACCCAGAAGGGACAGAAG
AACAGCCGCGAGAGAATGAAGCGGATCGAAGAGGGCATCAAAGAGCTGGGCAGCCAGATCCTGAAAGAACACCCCGTGGAAAACACCCAGCTG
CAGAACGAGAAGCTGTACCTGTACTACCTGCAGAATGGGCGGGATATGTACGTGGACCAGGAACTGGACATCAACCGGCTGTCCGACTACGATGT
GGACCACATCGTGCCTCAGAGCTTTCTGAAGGACGACTCCATCGACAACAAGGTGCTGACCAGAAGCGACAAgAACCGGGGCAAGAGCGACAAC
GTGCCCTCCGAAGAGGTCGTGAAGAAGATGAAGAACTACTGGCGGCAGCTGCTGAACGCCAAGCTGATTACCCAGAGAAAGTTCGACAATCTGA
CCAAGGCCGAGAGAGGCGGCCTGAGCGAACTGGATAAGGCCGGCTTCATCAAGAGACAGCTGGTGGAAACCCGGCAGATCACAAAGCACGTGGC
ACAGATCCTGGACTCCCGGATGAACACTAAGTACGACGAGAATGACAAGCTGATCCGGGAAGTGAAAGTGATCACCCTGAAGTCCAAGCTGGTG
TCCGATTTCCGGAAGGATTTCCAGTTTTACAAAGTGCGCGAGATCAACAACTACCACCACGCCCACGACGCCTACCTGAACGCCGTCGTGGGAAC
CGCCCTGATCAAAAAGTACCCTAAGCTGGAAAGCGAGTTCGTGTACGGCGACTACAAGGTGTACGACGTGCGGAAGATGATCGCCAAGAGCGAG
CAGGAAATCGGCAAGGCTACCGCCAAGTACTTCTTCTACAGCAACATCATGAACTTTTTCAAGACCGAGATTACCCTGGCCAACGGCGAGATCCG
GAAGCGGCCTCTGATCGAGACAAACGGCGAAACCGGGGAGATCGTGTGGGATAAGGGCCGGGATTTTGCCACCGTGCGGAAAGTGCTGAGCATG
CCCCAAGTGAATATCGTGAAAAAGACCGAGGTGCAGACAGGCGGCTTCAGCAAAGAGTCTATCCTGCCCAAGAGGAACAGCGATAAGCTGATCG
CCAGAAAGAAGGACTGGGACCCTAAGAAGTACGGCGGCTTCGACAGCCCCACCGTGGCCTATTCTGTGCTGGTGGTGGCCAAAGTGGAAAAGGG
CAAGTCCAAGAAACTGAAGAGTGTGAAAGAGCTGCTGGGGATCACCATCATGGAAAGAAGCAGCTTCGAGAAGAATCCCATCGACTTTCTGGAA
GCCAAGGGCTACAAAGAAGTGAAAAAGGACCTGATCATCAAGCTGCCTAAGTACTCCCTGTTCGAGCTGGAAAACGGCCGGAAGAGAATGCTGG
CCTCTGCCGGCGAACTGCAGAAGGGAAACGAACTGGCCCTGCCCTCCAAATATGTGAACTTCCTGTACCTGGCCAGCCACTATGAGAAGCTGAAG
GGCTCCCCCGAGGATAATGAGCAGAAACAGCTGTTTGTGGAACAGCACAAGCACTACCTGGACGAGATCATCGAGCAGATCAGCGAGTTCTCCA
AGAGAGTGATCCTGGCCGACGCTAATCTGGACAAAGTGCTGTCCGCCTACAACAAGCACCGGGATAAGCCCATCAGAGAGCAGGCCGAGAATAT
CATCCACCTGTTTACCCTGACCAATCTGGGAGCCCCTGCCGCCTTCAAGTACTTTGACACCACCATCGACCGGAAGAGGTACACCAGCACCAAAG
AGGTGCTGGACGCCACCCTGATCCACCAGAGCATCACCGGCCTGTACGAGACACGGATCGACCTGTCTCAGCTGGGAGGCGACagcgctGGAGGAG
GTGGAAGCGGAGGAGGAGGAAGCGGAGGAGGAGGTAGCggacctaagaaaaagaggaaggtgtgaGACCCAGCTTTCTTGTACAAAGTGGTTGATCTAGAGGG
CCCGCGGTTCGAAGGTAAGCCTATCCCTAACCCTCTCCTCGGTCTCGATTCTACGCGTACCGGTCATCATCACCATCACCATTGAGTTTAAACCCGC
TGATCAGCCTCGACTGTGCCTTCTAGTTGCCAGCCATCTGTTGTTTGCCCCTCCCCCGTGCCTTCCTTGACCCTGGAAGGTGCCACTCCCACTGTCC
TTTCCTAATAAAATGAGGAAATTGCATCGCATTGTCTGAGTAGGTGTCATTCTATTCTGGGGGGTGGGGTGGGGCAGGACAGCAAGGGGGAGGAT
TGGGAAGACAATAGCAGGCATGCTGGGGATGCGGTGGGCTCTATGGCTTCTGAGGCGGAAAGAACCAGCTGGGGCTCTAGGGGGTATCCCCACG
CGCCCTGTAGCGGCGCATTAAGCGCGGCGGGTGTGGTGGTTACGCGCAGCGTGACCGCTACACTTGCCAGCGCCCTAGCGCCCGCTCCTTTCGCTT
TCTTCCCTTCCTTTCTCGCCACGTTCGCCGGCTTTCCCCGTCAAGCTCTAAATCGGGGGCTCCCTTTAGGGTTCCGATTTAGTGCTTTACGGCACCTC
GACCCCAAAAAACTTGATTAGGGTGATGGTTCACGTAGTGGGCCATCGCCCTGATAGACGGTTTTTCGCCCTTTGACGTTGGAGTCCACGTTCTTT
AATAGTGGACTCTTGTTCCAAACTGGAACAACACTCAACCCTATCTCGGTCTATTCTTTTGATTTATAAGGGATTTTGCCGATTTCGGCCTATTGGT
TAAAAAATGAGCTGATTTAACAAAAATTTAACGCGAATTAATTCTGTGGAATGTGTGTCAGTTAGGGTGTGGAAAGTCCCCAGGCTCCCCAGCAG
GCAGAAGTATGCAAAGCATGCATCTCAATTAGTCAGCAACCAGGTGTGGAAAGTCCCCAGGCTCCCCAGCAGGCAGAAGTATGCAAAGCATGCA
TCTCAATTAGTCAGCAACCATAGTCCCGCCCCTAACTCCGCCCATCCCGCCCCTAACTCCGCCCAGTTCCGCCCATTCTCCGCCCCATGGCTGACTA
ATTTTTTTTATTTATGCAGAGGCCGAGGCCGCCTCTGCCTCTGAGCTATTCCAGAAGTAGTGAGGAGGCTTTTTTGGAGGCCTAGGCTTTTGCAAA
AAGCTCCCGGGAGCTTGTATATCCATTTTCGGATCTGATCAAGAGACAGGATGAGGATCGTTTCGCATGATTGAACAAGATGGATTGCACGCAGG
TTCTCCGGCCGCTTGGGTGGAGAGGCTATTCGGCTATGACTGGGCACAACAGACAATCGGCTGCTCTGATGCCGCCGTGTTCCGGCTGTCAGCGCA
GGGGCGCCCGGTTCTTTTTGTCAAGACCGACCTGTCCGGTGCCCTGAATGAACTGCAGGACGAGGCAGCGCGGCTATCGTGGCTGGCCACGACGG
GCGTTCCTTGCGCAGCTGTGCTCGACGTTGTCACTGAAGCGGGAAGGGACTGGCTGCTATTGGGCGAAGTGCCGGGGCAGGATCTCCTGTCATCTC
ACCTTGCTCCTGCCGAGAAAGTATCCATCATGGCTGATGCAATGCGGCGGCTGCATACGCTTGATCCGGCTACCTGCCCATTCGACCACCAAGCGA
AACATCGCATCGAGCGAGCACGTACTCGGATGGAAGCCGGTCTTGTCGATCAGGATGATCTGGACGAAGAGCATCAGGGGCTCGCGCCAGCCGA

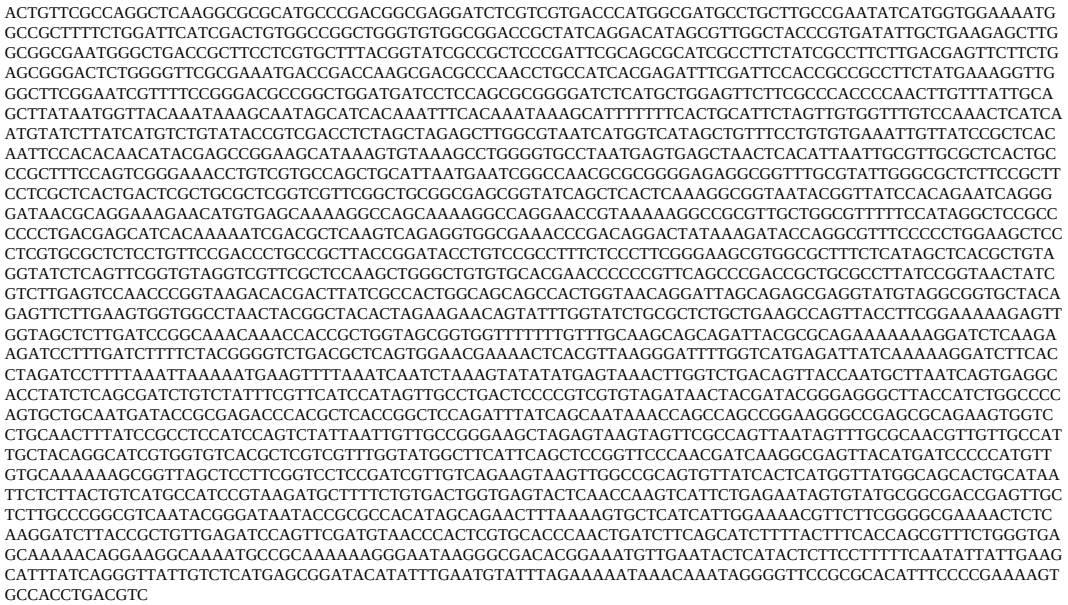

Figure F.3: **Sequence of pDEST40 Cas9wt with T7 mutagenesis.**
Downloaded from SnapGene (version 6.0.6), `https://www.snapgene.com/`.

pDEST40 Cas9-HMGB1 with T7 mutagenesis

GACGGATCGGGAGATCTCCCGATCCCCTATGGTGCACTCTCAGTACAATCTGCTCTGATGCCGCATAGTTAAGCCAGTATCTGCTCCCTGCTTGTG
TGTTGGAGGTCGCTGAGTAGTGCGCGAGCAAAATTTAAGCTACAACAAGGCAAGGCTTGACCGACAATTGCATGAAGAATCTGCTTAGGGTTAGG
CGTTTTGCGCTGCTTCGCGATGTACGGGCCAGATATACGCGTTGACATTGATTATTGACTAGTTATTAATAGTAATCAATTACGGGGTCATTAGTTC
ATAGCCCATATATGGAGTTCCGCGTTACATAACTTACGGTAAATGGCCCGCCTGGCTGACCGCCCAACGACCCCCGCCCATTGACGTCAATAATGA
CGTATGTTCCCATAGTAACGCCAATAGGGACTTTCCATTGACGTCAATGGGTGGAGTATTTACGGTAAACTGCCCACTTGGCAGTACATCAAGTGT
ATCATATGCCAAGTACGCCCCCTATTGACGTCAATGACGGTAAATGGCCCGCCTGGCATTATGCCCAGTACATGACCTTATGGGACTTTCCTACTT
GGCAGTACATCTACGTATTAGTCATCGCTATTACCATGGTGATGCGGTTTTGGCAGTACATCAATGGGCGTGGATAGCGGTTTGACTCACGGGGAT
TTCCAAGTCTCCACCCCATTGACGTCAATGGGAGTTTGTTTTGGCACCAAAATCAACGGGACTTTCCAAAATGTCGTAACAACTCCGCCCCATTGA
CGCAAATGGGCGGTAGGCGTGTACGGTGGGAGGTCTATATAAGCAGAGCTCTCTGGCTAACTAGAGAACCCACTGCTTACTGGCTTATCGAAATT
AATACGACTCACTATAAGGAGACCCAAGCTGGCTAGTTAAGCTATCAACAAGTTTGTACAAAAAAGCAGGCTTCGCCACCATGAAAAGGCCGGC
GGCCACGAAAAAGGCCGGCCAGGCAAAAAAGAAAAAGATGAAAAGGCCGGCGGCCACGAAAAAGGCCGGCCAGGCAAAAAAGAAAAAGGACA
AGAAGTACAGCATCGGCCTGGACATCGGCACCAACTCTGTGGGCTGGGCCGTGATCACCGACGAGTACAAGGTGCCCAGCAAGAAATTCAAGGT
GCTGGGCAACACCGACCGGCACAGCATCAAGAAGAACCTGATCGGAGCCCTGCTGTTCGACAGCGGCGAAACAGCCGAGGCCACCCGGCTGAAG
AGAACCGCCAGAAGAAGATACACCAGACGGAAGAACCGGATCTGCTATCTGCAAGAGATCTTCAGCAACGAGATGGCCAAGGTGGACGACAGCT
TCTTCCACAGACTGGAAGAGTCCTTCCTGGTGGAAGAGGATAAGAAGCACGAGCGGCACCCCATCTTCGGCAACATCGTGGACGAGGTGGCCTAC
CACGAGAAGTACCCCACCATCTACCACCTGAGAAAGAAACTGGTGGACAGCACCGACAAGGCCGACCTGCGGCTGATCTATCTGGCCCTGGCCCA
CATGATCAAGTTCCGGGGCCACTTCCTGATCGAGGGCGACCTGAACCCCGACAACAGCGACGTGGACAAGCTGTTCATCCAGCTGGTGCAGACCT
ACAACCAGCTGTTCGAGGAAAACCCCATCAACGCCAGCGGCGTGGACGCCAAGGCCATCCTGTCTGCCAGACTGAGCAAGAGCAGACGGCTGGA
AAATCTGATCGCCCAGCTGCCCGGCGAGAAGAAGAATGGCCTGTTCGGCAACCTGATTGCCCTGAGCCTGGGCCTGACCCCCAACTTCAAGAGCA
ACTTCGACCTGGCCGAGGATGCCAAACTGCAGCTGAGCAAGGACACCTACGACGACGACCTGGACAACCTGCTGGCCCAGATCGGCGACCAGTA
CGCCGACCTGTTTCTGGCCGCCAAGAACCTGTCCGACGCCATCCTGCTGAGCGACATCCTGAGAGTGAACACCGAGATCACCAAGGCCCCCCTGA
GCGCCTCTATGATCAAGAGATACGACGAGCACCACCAGGACCTGACCCTGCTGAAAGCTCTCGTGCGGCAGCAGCTGCCTGAGAAGTACAAAGA
GATTTTCTTCGACCAGAGCAAGAACGGCTACGCCGGCTACATTGACGGCGGAGCCAGCCAGGAAGAGTTCTACAAGTTCATCAAGCCCATCCTGG
AAAAGATGGACGGCACCGAGGAACTGCTCGTGAAGCTGAACAGAGAGGACCTGCTGCGGAAGCAGCGGACCTTCGACAACGGCAGCATCCCCCA
CCAGATCCACCTGGGAGAGCTGCACGCCATTCTGCGGCGGCAGGAAGATTTTTACCCATTCCTGAAGGACAACCGGGAAAAGATCGAGAAGATCC
TGACCTTCCGCATCCCCTACTACGTGGGCCCTCTGGCCAGGGGAAACAGCAGATTCGCCTGGATGACCAGAAAGAGCGAGGAAACCATCACCCCC
TGGAACTTCGAGGAAGTGGTGGACAAGGGCGCTTCCGCCCAGAGCTTCATCGAGCGGATGACCAACTTCGATAAGAACCTGCCCAACGAGAAGG
TGCTGCCCAAGCACAGCCTGCTGTACGAGTACTTCACCGTGTATAACGAGCTGACCAAAGTGAAATACGTGACCGAGGGAATGAGAAAGCCCGCC
TTCCTGAGCGGCGAGCAGAAAAAGGCCATCGTGGACCTGCTGTTCAAGACCAACCGGAAAGTGACCGTGAAGCAGCTGAAAGAGGACTACTTCA
AGAAAATCGAGTGCTTCGACTCCGTGGAAATCTCCGGCGTGGAAGATCGGTTCAACGCCTCCCTGGGCACATACCACGATCTGCTGAAAATTATC
AAGGACAAGGACTTCCTGGACAATGAGGAAAACGAGGACATTCTGGAAGATATCGTGCTGACCCTGACACTGTTTGAGGACAGAGAGATGATCG
AGGAACGGCTGAAAACCTATGCCCACCTGTTCGACGACAAAGTGATGAAGCAGCTGAAGCGGCGGAGATACACCGGCTGGGGCAGGCTGAGCCG
GAAGCTGATCAACGGCATCCGGGACAAGCAGTCCGGCAAGACAATCCTGGATTTCCTGAAGTCCGACGGCTTCGCCAACAGAAACTTCATGCAGC
TGATCCACGACGACAGCCTGACCTTTAAAGAGGACATCCAGAAAGCCCAGGTGTCCGGCCAGGGCGATAGCCTGCACGAGCACATTGCCAATCTG
GCCGGCAGCCCCGCCATTAAGAAGGGCATCCTGCAGACAGTGAAGGTGGTGGACGAGCTgGTGAAAGTGATGGGCCGGCACAAGCCCGAGAACA
TCGTGATCGAAATGGCCAGAGAGAACCAGACCACCCAGAAGGGACAGAAGAACAGCCGCGAGAGAATGAAGCGGATCGAAGAGGGCATCAAAG
AGCTGGGCAGCCAGATCCTGAAAGAACACCCCGTGGAAAACACCCAGCTGCAGAACGAGAAGCTGTACCTGTACTACCTGCAGAATGGGCGGGA
TATGTACGTGGACCAGGAACTGGACATCAACCGGCTGTCCGACTACGATGTGGACCACATCGTGCCTCAGAGCTTTCTGAAGGACGACTCCATCG
ACAACAAGGTGCTGACCAGAAGCGACAAgAACCGGGGCAAGAGCGACAACGTGCCCTCCGAAGAGGTCGTGAAGAAGATGAAGAACTACTGGC
GGCAGCTGCTGAACGCCAAGCTGATTACCCAGAGAAAGTTCGACAATCTGACCAAGGCCGAGAGAGGCGGCCTGAGCGAACTGGATAAGGCCGG
CTTCATCAAGAGACAGCTGGTGGAAACCCGGCAGATCACAAAGCACGTGGCACAGATCCTGGACTCCCGGATGAACACTAAGTACGACGAGAAT
GACAAGCTGATCCGGGAAGTGAAAGTGATCACCCTGAAGTCCAAGCTGGTGTCCGATTTCCGGAAGGATTTCCAGTTTTACAAAGTGCGCGAGAT
CAACAACTACCACCACGCCCACGACGCCTACCTGAACGCCGTCGTGGGAACCGCCCTGATCAAAAAGTACCCTAAGCTGGAAAGCGAGTTCGTGT
ACGGCGACTACAAGGTGTACGACGTGCGGAAGATGATCGCCAAGAGCGAGCAGGAAATCGGCAAGGCTACCGCCAAGTACTTCTTCTACAGCAA
CATCATGAACTTTTTCAAGACCGAGATTACCCTGGCCAACGGCGAGATCCGGAAGCGGCCTCTGATCGAGACAAACGGCGAAACCGGGGAGATC
GTGTGGGATAAGGGCCGGGATTTTGCCACCGTGCGGAAAGTGCTGAGCATGCCCCAAGTGAATATCGTGAAAAAGACCGAGGTGCAGACAGGCG
GCTTCAGCAAAGAGTCTATCCTGCCCAAGAGGAACAGCGATAAGCTGATCGCCAGAAAGAAGGACTGGGACCCTAAGAAGTACGGCGGCTTCGA
CAGCCCCACCGTGGCCTATTCTGTGCTGGTGGTGGCCAAAGTGGAAAAGGGCAAGTCCAAGAAACTGAAGAGTGTGAAAAGAGCTGCTGGGGATC
ACCATCATGGAAAGAAGCAGCTTCGAGAAGAATCCCATCGACTTTCTGGAAGCCAAGGGCTACAAAGAAGTGAAAAAGGACCTGATCATCAAGC
TGCCTAAGTACTCCCTGTTCGAGCTGGAAAACGGCCGGAAGAGAATGCTGGCCTCTGCCGGCGAACTGCAGAAGGGAAACGAACTGGCCCTGCCC
TCCAAATATGTGAACTTCCTGTACCTGGCCAGCCACTATGAGAAGCTGAAGGGCTCCCCCGAGGATAATGAGCAGAAACAGCTGTTTGTGGAACA
GCACAAGCACTACCTGGACGAGATCATCGAGCAGATCAGCGAGTTCTCCAAGAGAGTGATCCTGGCCGACGCTAATCTGGACAAAGTGCTGTCCG
CCTACAACAAGCACCGGGATAAGCCCATCAGAGAGCAGGCCGAGAATATCATCCACCTGTTTACCCTGACCAATCTGGGAGCCCCTGCCGCCTTC
AAGTACTTTGACACCACCATCGACCGGAAGAGGTACACCAGCACCAAAGAGGTGCTGGACGCCACCCTGATCCACCAGAGCATCACCGGCCTGTA
CGAGACACGGATCGACCTGTCTCAGCTGGGAGGCGACagcgctGGAGGAGGTGGAAGCGGAGGAGGAGGAAGCGGAGGAGGAGGTAGCggacctaagaa
aaagaggaaggtgATGGGCAAAGGAGATCCTAAGAAGCCGAGAGGCAAAATGTCATCATATGCATTTTTTGTGCAAACTTGTCGGGAGGAGCATAAGAA
GAAGCACCCAGATGCTTCAGTCAACTTCTCAGAGTTTTCTAAGAAGTGCTCAGAGAGGTGGAAGACCATGTCTGCTAAAGAGAAAGGAAAATTTG
AAGATATGGCAAAGGCGGACAAGGCCCGTTATGAAAGAGAAATGAAAACCTATATCCCTCCCAAAGGGGAGACAAAAAAGAAGTTCAAGGATC
CCAATGCACCCAAGAGGCCTCCTTCGGCCTTCTTCCTCTTCTGCTCTGAGTATCGCCCAAAAATCAAAGGAGAACATCCTGGCCTGTCCATTGGTG
ATGTTGCGAAGAAACTGGGAGAGATGTGGAATAACACTGCTGCAGATGACAAGCAGCCTTATGAAAAGAAGGCTGCGAAGCTGAAGGAAAAATA
CGAAAAGGATATTGCTGCATATCGAGCTAAAGGAAAGCCTGATGCAGCAAAAAAGGGAGTTGTCAAGGCTGAAAAAAGCAAGAAAAAGAAGGA
AGAGGAGGAAGATGAGGAAGATGAAGAGGATGAGGAGGAGGAAGATGAAGAAGATGAAGATGAAGAAGAAGATGATGATGATGAAgcgct
GGAGGAGGTGGAAGCGGAGGAGGAAGCGGAGGAGGAGGTAGCggacctaagaaaaagaggaaggtgtgaGACCCAGCTTTCTTGTACAAAGTGGTTGATC
TAGAGGGCCCGCGGTTCGAAGGTAAGCCTATCCCTAACCCTCTCCTCGGTCTCGATTCTACGCGTACCGGTCATCATCACCATCACCATTGAGTTT
AAACCCGCTGATCAGCCTCGACTGTGCCTTCTAGTTGCCAGCCATCTGTTGTTTGCCCCTCCCCCGTGCCTTCCTTGACCCTGGAAGGTGCCACTCC
CACTGTCCTTTCCTAATAAAATGAGGAAATTGCATCGCATTGTCTGAGTAGGTGTCATTCTATTCTGGGGGGTGGGGTGGGGCAGGACAGCAAGG
GGGAGGATTGGGAAGACAATAGCAGGCATGCTGGGGATGCGGTGGGCTCTATGGCTTCTGAGGCGGAAAGAACCAGCTGGGGCTCTAGGGGGTA
TCCCCACGCGCCCTGTAGCGGCGCATTAAGCGCGGCGGGTGTGGTGGTTACGCGCAGCGTGACCGCTACACTTGCCAGCGCCCTAGCGCCCGCTC
CTTTCGCTTTCTTCCCTTCCTTTCTCGCCACGTTCGCCGGCTTTCCCCGTCAAGCTCTAAATCGGGGGCTCCCTTTAGGGTTCCGATTTAGTGCTTTA
CGGCACCTCGACCCCAAAAAACTTGATTAGGGTGATGGTTCACGTAGTGGGCCATCGCCCTGATAGACGGTTTTTCGCCCTTTGACGTTGGAGTCC
ACGTTCTTTAATAGTGGACTCTTGTTCCAAACTGGAACAACACTCAACCCTATCTCGGTCTATTCTTTTGATTTATAAGGGATTTTGCCGATTTCGG
CCTATTGGTTAAAAAATGAGCTGATTTAACAAAAATTTAACGCGAATTAATTCTGTGGAATGTGTGTCAGTTAGGGTGTGGAAAGTCCCCAGGCTC
CCCAGCAGGCAGAAGTATGCAAAGCATGCATCTCAATTAGTCAGCAACCAGGTGTGGAAAGTCCCCAGGCTCCCCAGCAGGCAGAAGTATGCAA
AGCATGCATCTCAATTAGTCAGCAACCATAGTCCCGCCCCTAACTCCGCCCATCCCGCCCCTAACTCCGCCCAGTTCCGCCCATTCTCCGCCCCATG
GCTGACTAATTTTTTTTATTTATGCAGAGGCCGAGGCCGCCTCTGCCTCTGAGCTATTCCAGAAGTAGTGAGGAGGCTTTTTTGGAGGCCTAGGCTT

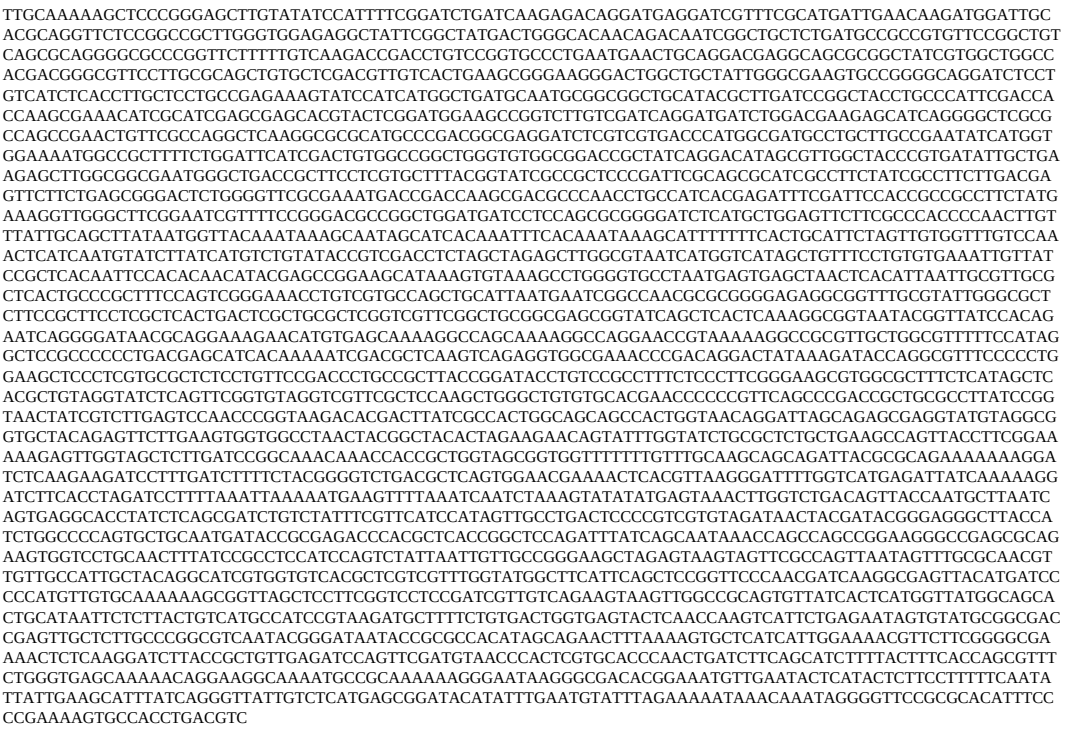

Figure F.4: **Sequence of pDEST40 Cas9-HMGB1 with T7 mutagenesis.** Downloaded from SnapGene (version 6.0.6), `https://www.snapgene.com/`.

G Gating Strategy for HDR and NHEJ

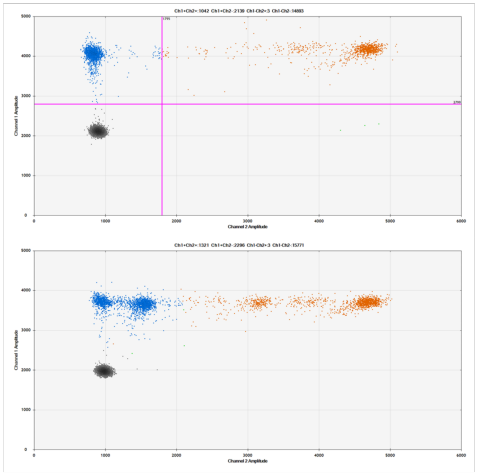

(a) RNPs

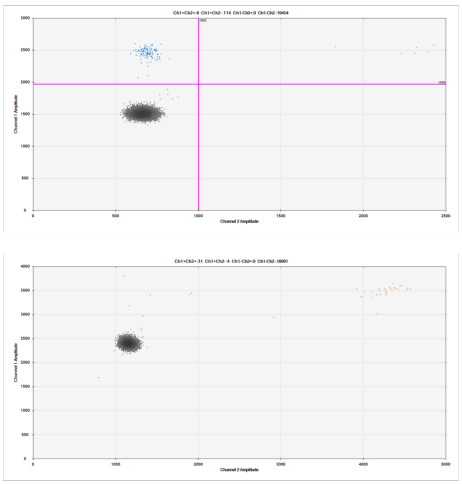

(b) Cas9wt mRNA of fibroblasts

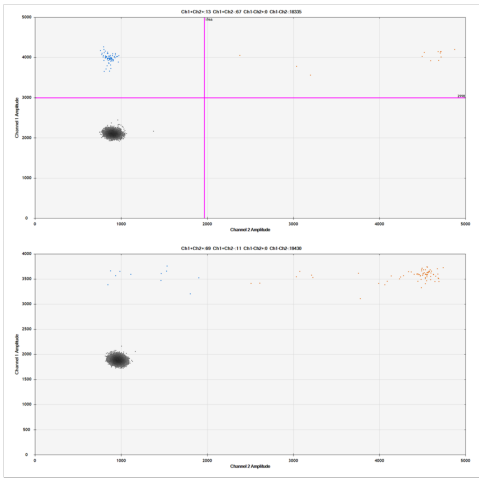

(c) Cas9-HMGB1 mRNA of fibroblasts

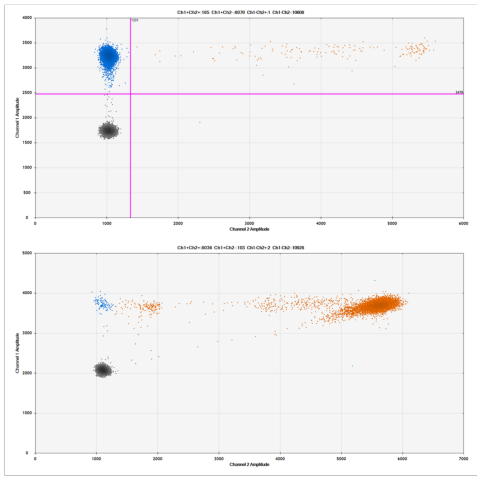

(d) Cas9wt mRNA with repair template

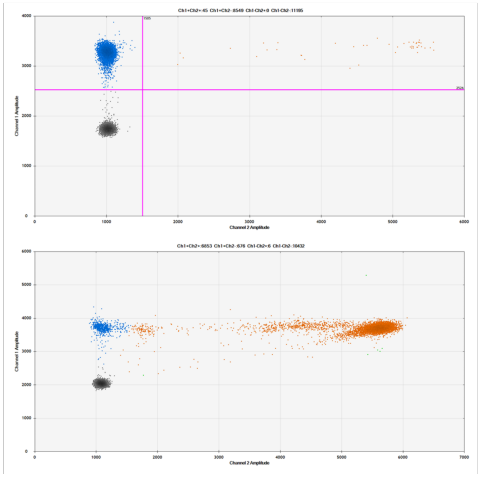

(e) Cas9wt mRNA without repair template

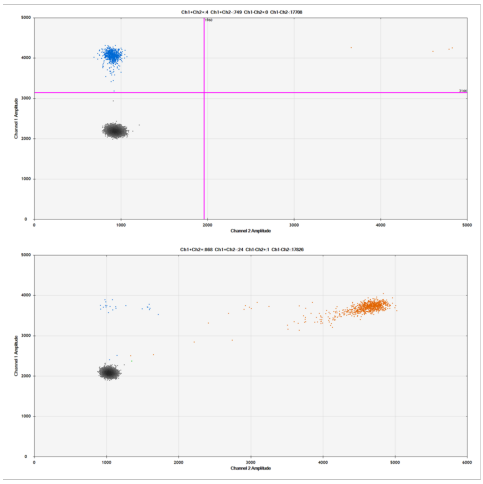

(f) Two-step Electroporation of Cas9wt mRNA

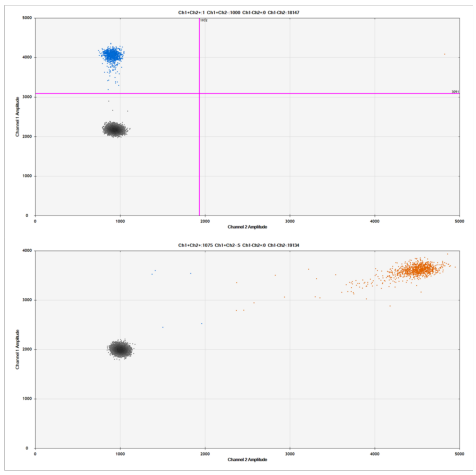

(g) Two-step Electroporation of Cas9-HMGB1 mRNA

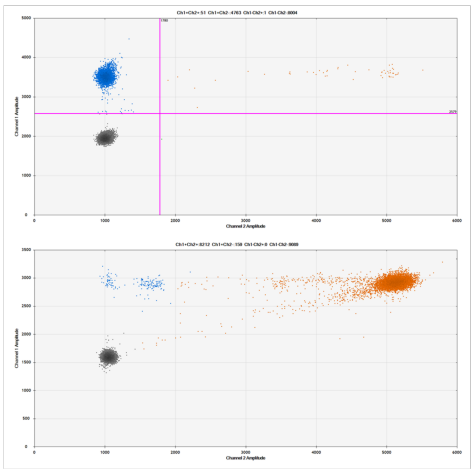

(h) Cas9wt mRNA with urea

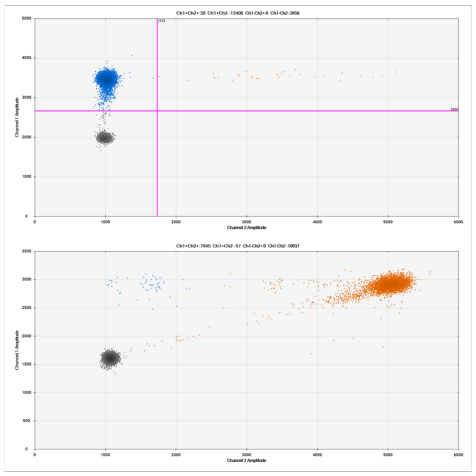

(i) Cas9wt mRNA with extended purification

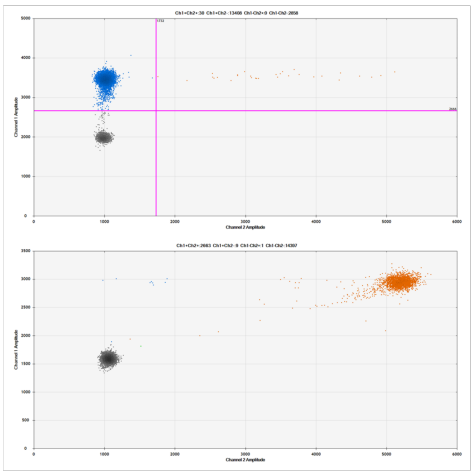

(j) Cas9wt mRNA with urea and extended purification

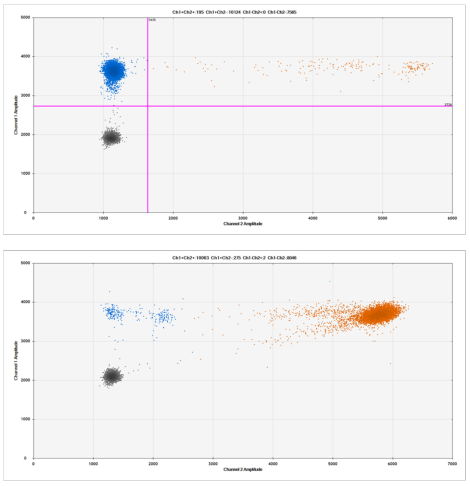

(k) Cas9wt mRNA with RNase Out

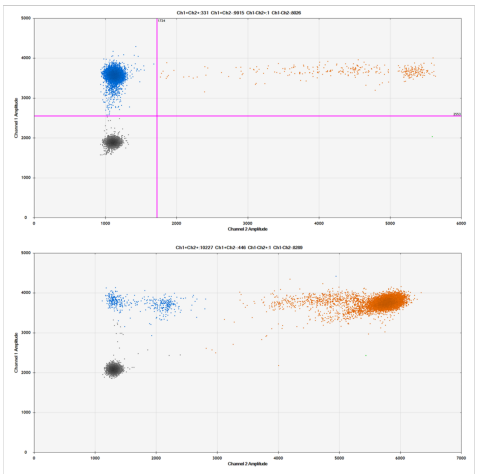

(l) Cas9wt mRNA with RNase Inhibitor

Figure G.1: **Gating strategy of all electroporation experiments for quantifying gene editing with ddPCR.**
The upper panel represents HDR, while lower panel represents NHEJ.The plot demonstrates a two-dimensional cluster in which Channel 1 Amplitude represents the FAM probe and the Channel 2 Amplitude represents the HEX reference probe.

H Cell Pictures

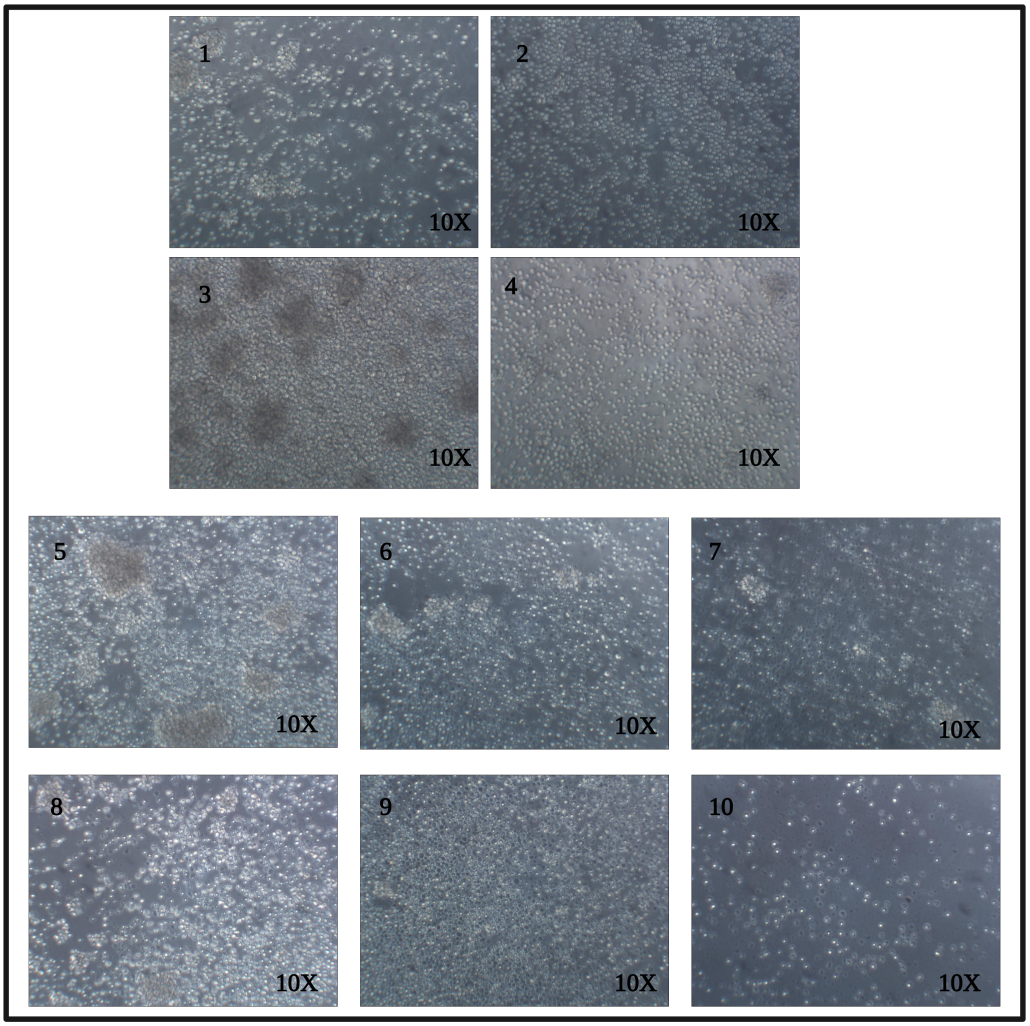

(a) **Picture of PBMCs.** 1. Mock 24 hours post-electroporation, 2. Mock on the day of collection (96 hours post-electroporation), 3. RNPs 24 hours post-electroporation, 4. RNPs on the day of collection (96 hours post-electroporation), 5. Cas9wt 24 hours post-electroporation, 6. Cas9wt 24 hours post Two-step Electroporation, 7. Cas9wt on the day of collection (96 hours post-electroporation), 8. Cas9-HMGB1 24 hours post-electroporation, 9. Cas9-HMGB1 24 hours post Two-step Electroporation, and 10. Cas9-HMGB1 on the day of collection (96 hours post-electroporation).

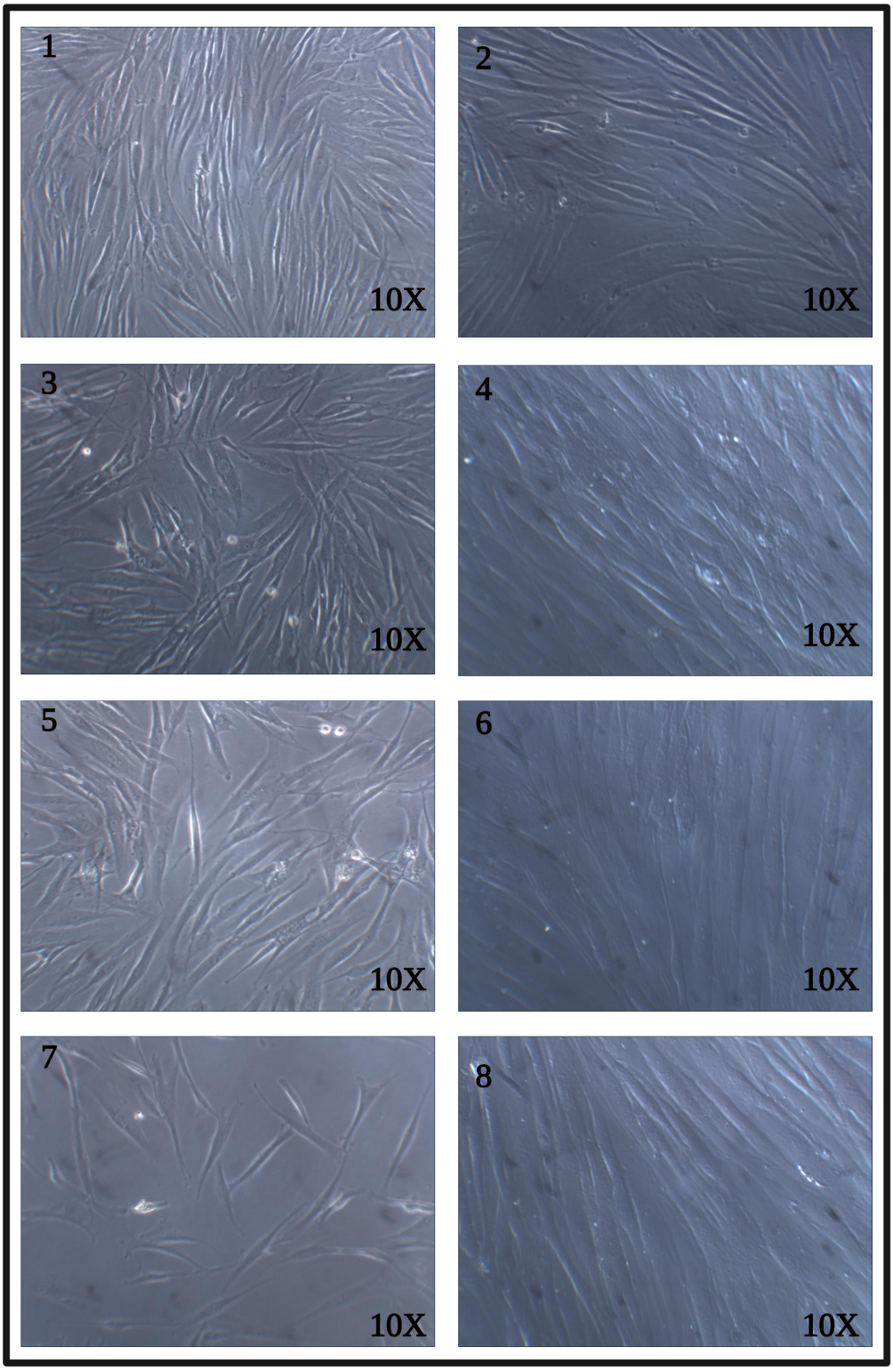

(b) **Picture of fibroblasts.** 1. Cells on the day of transfection, still in the T175 culture flask, 2. Cas9wt 24 hours post-electroporation, 3. Mock 24 hours post-electroporation, 4. Mock on the day of collection (96 hours post-electroporation), 5. RNPs 24 hours post-electroporation, 6. RNPs on the day of collection (96 hours post-electroporation), 7. Cas9-HMGB1 24 hours post-electroporation, and 8. Cas9-HMGB1 on the day of collection (96 hours post-electroporation). Due to the loss of Cas9wt replicates, no picture was taken on the day of collection.

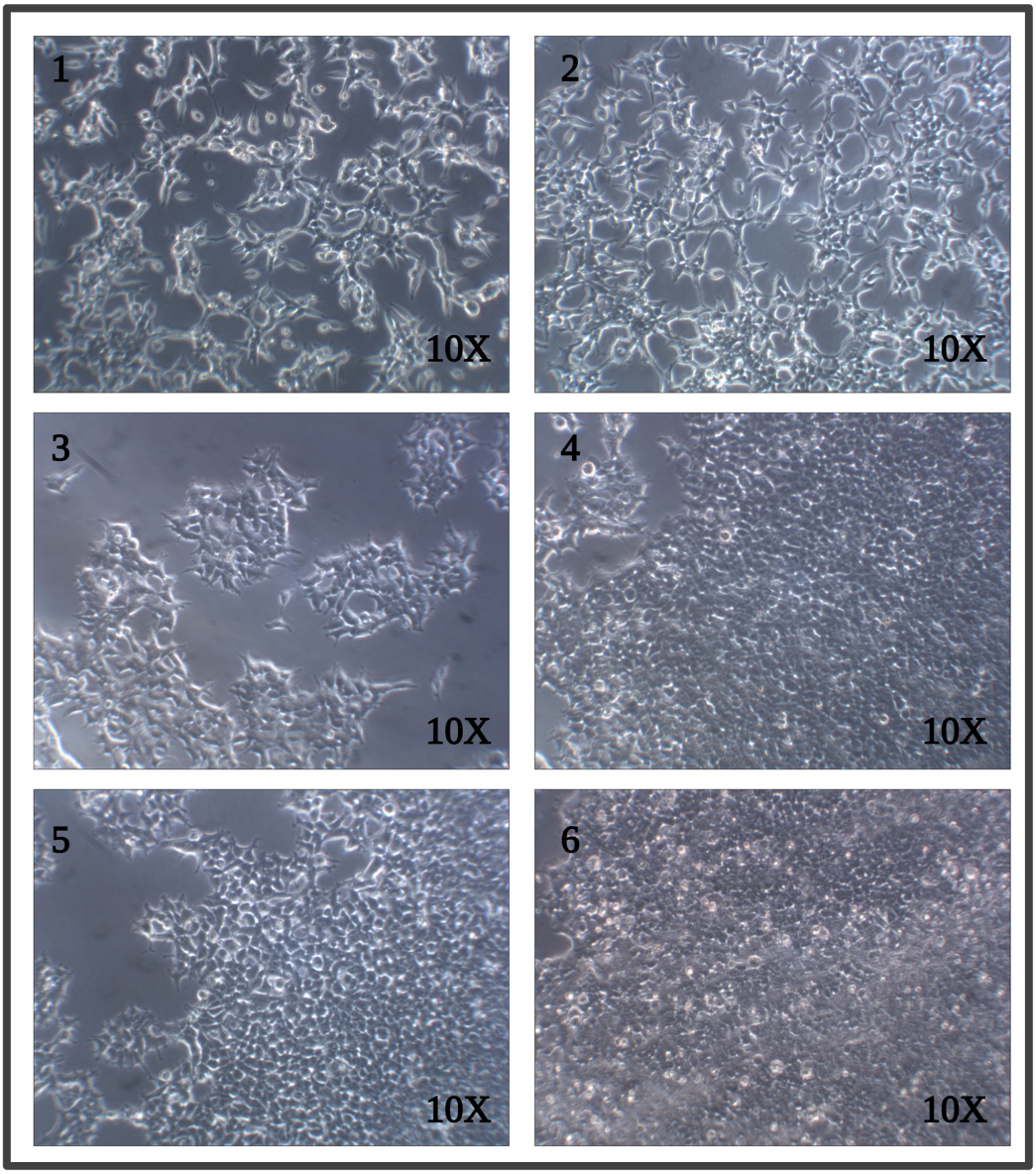

(c) **Picture of HEK293T cells.** 1. and 2. HEK293T cells at 90% confluency, 3. FuGENE transfected Mock, 4. FuGENE transfected Cas9wt plasmid DNA, 5. Lipofectamine transfected Mock, and 6. Lipofectamine transfected Cas9wt plasmid DNA.

Figure H.1: **Pictures of cells at different conditions before and after electroporation**, taken with microscope (Zeiss) at 10X.

I Western Blot Ladder

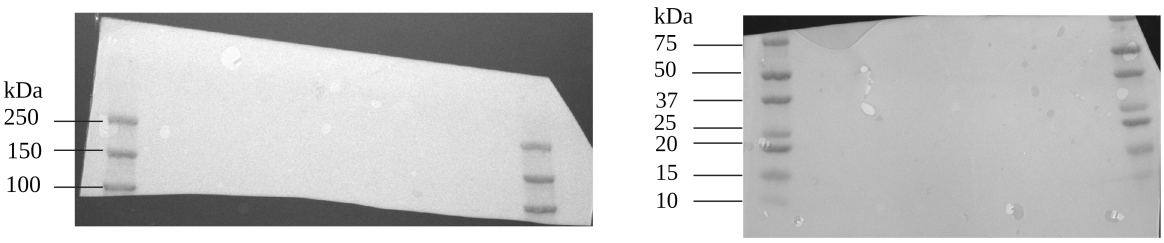

(a) Cas9 (160 kDa) (b) α-tubulin (55 kDa)

Figure I.1: **Western blot ladder colorimetric.**
The membrane is cut between 75 kDa and 100 kDa to obtain one membrane with Cas9 protein and one membrane with control α-tubulin protein.

Norges miljø- og biovitenskapelige universitet
Noregs miljø- og biovitskapelege universitet
Norwegian University of Life Sciences

Postboks 5003
NO-1432 Ås
Norway